GEOLOGIC AND HYDROLOGIC CHARACTERIZATION OF REGIONAL NONGEOTHERMAL GROUNDWATER RESOURCES IN THE COVE FORT AREA, MILLARD AND BEAVER COUNTIES, UTAH

by Stefan Kirby

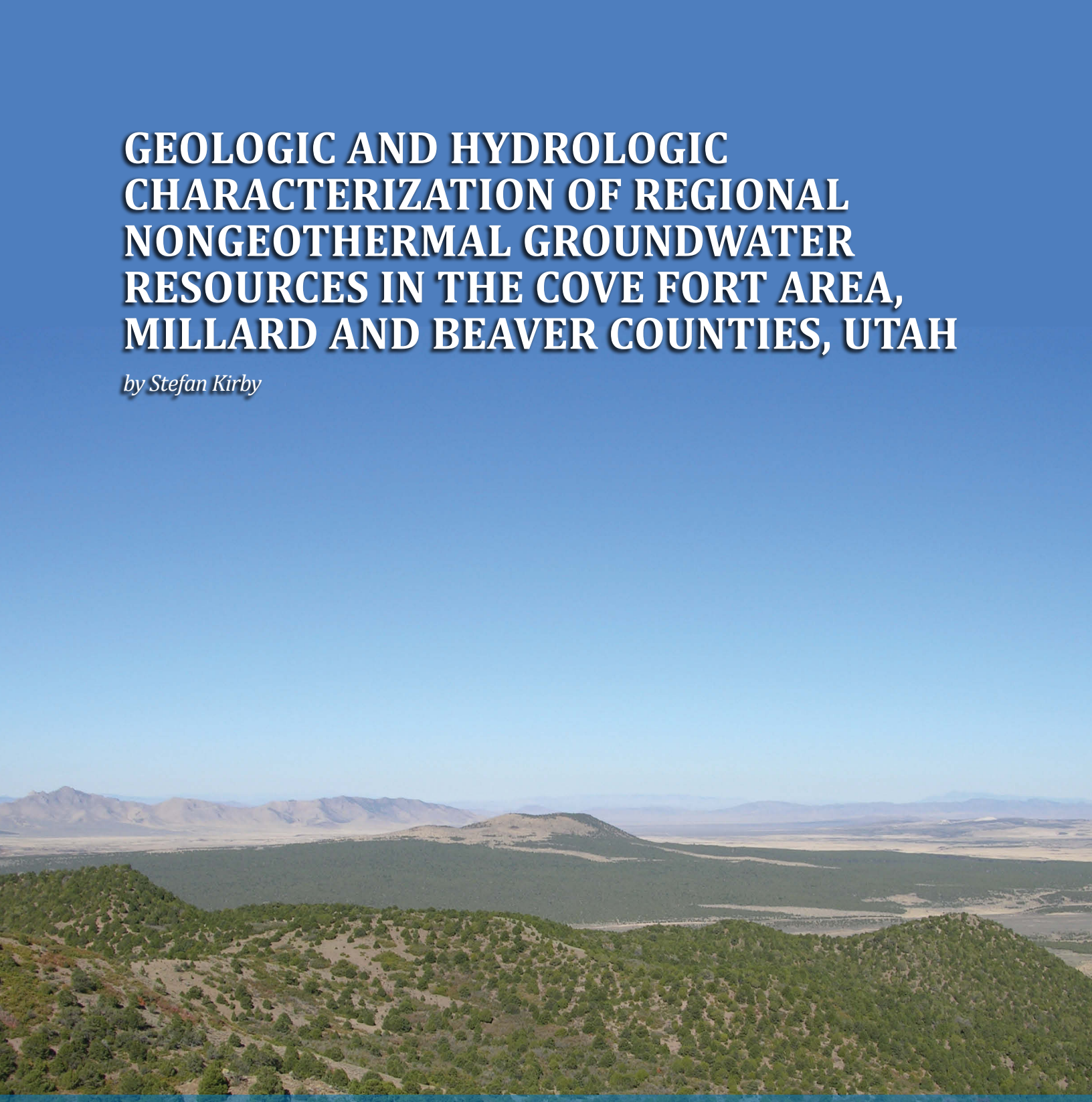

SPECIAL STUDY 140
UTAH GEOLOGICAL SURVEY
a division of
UTAH DEPARTMENT OF NATURAL RESOURCES
2012

GEOLOGIC AND HYDROLOGIC CHARACTERIZATION OF REGIONAL NONGEOTHERMAL GROUNDWATER RESOURCES IN THE COVE FORT AREA, MILLARD AND BEAVER COUNTIES, UTAH

by Stefan Kirby

Cover photo: *View to the west across the Cove Creek basin towards Black Rock and the Mineral Mountains. Groundwater moves from upland areas, near the foreground, to discharge areas in the west near Black Rock.*

ISBN 978-1-55791-854-3

SPECIAL STUDY 140
UTAH GEOLOGICAL SURVEY
a division of
UTAH DEPARTMENT OF NATURAL RESOURCES
2012

STATE OF UTAH
Gary R. Herbert, Governor

DEPARTMENT OF NATURAL RESOURCES
Michael Styler, Executive Director

UTAH GEOLOGICAL SURVEY
Richard G. Allis, Director

PUBLICATIONS
contact
Natural Resources Map & Bookstore
1594 W. North Temple
Salt Lake City, UT 84116
telephone: 801-537-3320
toll-free: 1-888-UTAH MAP
Website: mapstore.utah.gov
email: geostore@utah.gov

UTAH GEOLOGICAL SURVEY
contact
1594 W. North Temple, Suite 3110
Salt Lake City, UT 84116
telephone: 801-537-3300
Website: geology.utah.gov

CONTENTS

FIGURES

TABLES

PLATES

GEOLOGIC AND HYDROLOGIC CHARACTERIZATION OF REGIONAL NONGEOTHERMAL GROUNDWATER RESOURCES IN THE COVE FORT AREA, MILLARD AND BEAVER COUNTIES, UTAH

by Stefan Kirby

ABSTRACT

This report describes the nongeothermal hydrogeologic system of the Cove Creek basin and an adjoining part of the Beaver River basin north of Milford, in Millard and Beaver Counties, Utah. The groundwater system in the study area hosts two commercial geothermal reservoirs, provides the entire agricultural and culinary water supply, and may be connected with groundwater in adjoining basins.

The principal aquifer consists of basin-fill deposits and interbedded volcanics, in lowland portions of the study area, bounded by mountain ranges consisting of relatively impermeable Tertiary volcanic and intrusive rocks and Neoproterozoic through Mesozoic bedrock. Impermeable geologic units and high groundwater levels along mountainous parts of the drainage basin boundary preclude interbasin flow. Elsewhere, interbasin flow may occur across parts of the northern boundary of the study area and across study area boundaries spanned by interconnected basin fill along the Beaver River.

Groundwater in the principal aquifer moves from areas of high elevation and recharge near the bases of the Mineral, Tushar, and San Francisco Mountains, toward areas of low elevation and discharge along the Beaver River, and possibly to the north of the study area in Pahvant Valley. Depth to groundwater along ephemeral portions of the Cove Creek channel is commonly greater than 100 feet (30 m). Depth to groundwater is generally less than 50 feet (15 m) across much of the Beaver River valley. Long-term groundwater-level data are spatially isolated and do not show significant fluctuations in groundwater level or storage across the study area.

Groundwater quality is good in the Cove Fort area with total dissolved solids (TDS) values of less than 1000 mg/L and lower in quality (greater than 2000 mg/L [TDS]) near Roosevelt Hot Springs and along the Beaver River. High TDS correlates with higher groundwater temperature. Varying amounts of surficial recharge and deeper inflow associated with the geothermal systems near Cove Fort and Roosevelt Hot Springs likely control the chemical composition and temperature of groundwater in the principal aquifer. Stable isotope ratios in groundwater in the Cove Creek basin are consistent with recharge of the principal aquifer by infiltration of cool-season precipitation along the uppermost parts of the principal aquifer near Cove Fort and Interstate 15. Isotopes of tritium and carbon-14 indicate groundwater recharge since or just prior to 1950 for upper parts of the principal aquifer near Cove Fort and along Interstate 15. Elsewhere in the study area, isotopic data indicate limited modern recharge and at least several areas where groundwater recharge occurred thousands of years ago.

Recharge to the principal aquifer occurs from infiltration of cool-season precipitation and surface water. Discharge from the principal aquifer is dominated by evapotranspiration along the Beaver River valley. Spring flow and consumptive well withdrawal account for the remainder of discharge from the principal aquifer. Water budgets for three basins within the study area yield excess recharge only for the Cove Creek basin. Recharge in the San Francisco and Mineral basins is generally balanced with discharge by evapotranspiration, leaving little water available for subsurface outflow from these basins. Groundwater in the Cove Creek basin not consumed by evapotranspiration, spring flow, or well withdrawals, may leave the study area by northward subsurface flow or contribute to adjoining parts of the San Francisco or Mineral basins along areas of interconnected basin fill. The regional water budget is largely unaffected by current rates of pumping and is instead likely driven by changes in recharge and discharge due to climatic flux. A significant increase of groundwater consumption along the upper reaches of the principal aquifer in the Cove Creek basin will alter the water budget and may lead to declines in spring flow near Black Rock and a reduction of potential interbasin flow to Pahvant Valley to the north and the San Francisco and Mineral basins.

INTRODUCTION

This report describes the results of a hydrogeologic framework study of the Cove Creek basin and an adjoining part of the Beaver River basin north of the town of Milford. Groundwater in the study area hosts two commercial geothermal reservoirs, the Cove Fort Known Geothermal Resource Area (KGRA) and the Roosevelt Hot Springs KGRA (figure 1) (Utah Division of Water Resources, 1995; Blackett and Wakefield, 2004). Low-temperature groundwater provides the entire culinary water supply for residents and nearly all of the water used for irrigation and stock watering within the study area. Water budgets for the prinicipal aquifer are unknown and the potential for groundwater in the study area to contribute flow to surrounding basins is significant.

Previous work in the study area consists of modeling and framework studies of cool groundwater resources near Milford and in Pahvant Valley (Mower, 1965; Mower and Cordova, 1974; Mower, 1978; Holmes and Thiros, 1991; Mason, 1998), and a variety of geologic, geophysical, and hydrologic investigations of the high-temperature geothermal resources associated with the Cove Fort and Roosevelt Hot Springs KGRAs (see Mabey and Budding, 1987; Blackett and Wakefield, 2004; and references therein). None of these studies cover the entire area addressed by this study and no significant work has been

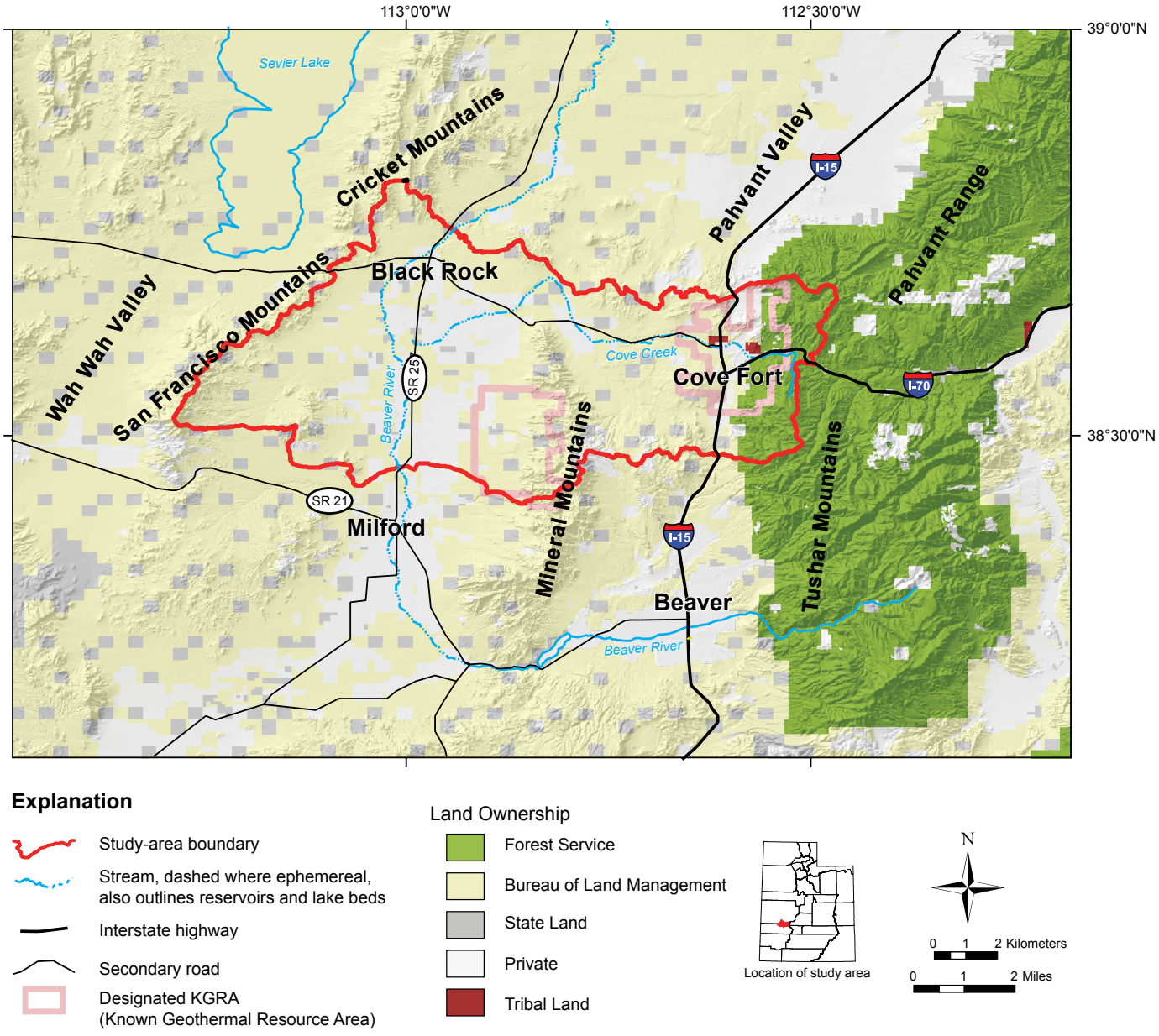

Figure 1. *Cove Fort study area overview. The Cove Fort–Sulphurdale KGRA is located in the eastern part of the study area; to the west is the Roosevelt Hot Springs KGRA.*

done on low-temperature groundwater resources in the Cove Creek drainage.

Previous workers have assumed subsurface outflow of groundwater from the study area to adjoining basins to the north and south (Pahvant Valley and Milford areas, respectively) (Holmes and Thiros, 1991; Mason, 1998). Large quantities of groundwater are consumed for irrigation and stock watering in both of these areas (Mower, 1965; Mower and Cordova, 1974; Holmes and Thiros, 1991; Utah Division of Water Resources, 1995; Mason, 1998). Existing groundwater models and water budgets for Pahvant Valley and Milford assume inflow of groundwater from the Cove Creek basin (Mower, 1965; Mower and Cordova, 1974; Holmes and Thiros, 1991; Mason, 1998), yet none of the previous workers have estimated water budgets and interbasin flow for the area including the Cove Creek drainage or attempted to directly quantify recharge. This study therefore provides the first regional assessment of low-temperature groundwater resources between Pahvant Valley and the Milford area. Detailed discussion of current and potential thermal groundwater resources is beyond the scope of this study. However, discussion of the geologic framework, regional water budget, and rates of recharge may be directly applicable to current and future geothermal production and exploration.

Results of this study include (1) characterization of the geologic framework in which groundwater resides, (2) definition of large-scale flow paths for the principal aquifer, (3) estimation of recharge and discharge to the groundwater system, and (4) estimation of potential interbasin groundwater flow from the Cove Fort study area to adjoining basins.

GEOGRAPHIC SETTING

Geography

The Cove Fort study area lies in central Utah and includes parts of southern Millard and northern Beaver Counties. The study area includes the Cove Creek drainage and the portion of the Beaver River drainage between Milford and Black Rock (figure 1). The northern Tushar Mountains and southern Pahvant Range form the eastern study-area boundary. The western boundary includes parts of the San Francisco and Cricket Mountains. The southern margin of the study area follows the east-west hydrologic divide along Gillies Hill extending west across the Mineral Mountains and the Beaver River valley, north of Milford, to the San Francisco Mountains. The northern margin follows the hydrologic divide separating the Cove Creek drainage from the Pahvant Valley to the north.

Within the study area elevations range from over 10,000 feet (3050 m) in the Tushar Mountains to less than 4900 feet (1490 m) along the Beaver River channel north of Black Rock. Approximately one-quarter of the study area is mountainous. The remainder consists of intervening basins and lower hills (figure 2). In subsequent text the term *upland* describes mountainous portions of the study area above approximately 6000 feet (1830 m) while *lowland* describes all areas below approximately 6000 feet (1830 m).

The study area may be divided into three smaller hydrographic basins based on 1:24,000-scale watershed boundaries available from the Utah Automated Geographic Reference Center (figure 2). The hydrographic boundaries follow major ridgelines and stream channels, except along the Beaver River channel where generally flat topography produces a slight mismatch between the mapped channel and the basin boundaries. In the east, the Cove Creek basin encompasses the entire Cove Creek watershed from its upland topographic divide westward to near the Beaver River channel and covers an area of 199,080 acres (80,570 ha). The remainder of the study area west of the Cove Creek drainage is part of the larger Beaver River basin between Milford and Pahvant Valley. This area is divided into two parts referred to as the Mineral and San Francisco basins. The Mineral basin comprises the west-facing slopes of the Mineral Mountains and parts of the adjoining basin that lie east of the Beaver River channel and covers an area of 90,770 acres (36,730 ha). The San Francisco basin encompasses 125,230 acres (50,680 ha) and the remainder of the study area west of the Beaver River channel.

The study area is entirely rural with only a few permanent residents centered primarily near Cove Fort in the eastern portion of the study area and at several ranches to the west near the Beaver River and Black Rock (figure 2). Consequently, many of the existing water wells are located near Cove Fort. Other wells are widely scattered across the study area with several located to the west near the Beaver River (Utah Division of Water Rights, 2006). Most of the study area is administered by federal and state agencies including the U.S. Bureau of Land Management, U.S. Forest Service, and the Utah School and Institutional Trust Lands Administration (figure 1). Private land exists along the Beaver River drainage and near Cove Fort; these two areas of private land are the most likely areas for future increases in groundwater use. Because of limited surface-water resources, groundwater is and will continue to be the primary source of both irrigation and domestic water in most of the study area.

Surface Water and Springs

Perennial surface water in the study area is limited to upland stretches of several streams that drain the Tushar Mountains along the eastern margin of the study

area (figure 2). Prior to construction of an upstream dam above Minersville, the Beaver River flowed north through the western part of the study area (Mason, 1998). Currently the Beaver River channel in the study area contains flowing water only during rare high-runoff events (Mason, 1998). Numerous smaller intermittent channels and washes drain upland areas of the Mineral, San Francisco, and Cricket Mountains (Mower and Cordova, 1974). Both upland and lowland portions of these channels and washes are commonly dry, with flowing water only occasionally during snowmelt and brief high-intensity rainfall events (Mower and Cordova, 1974).

Several spring systems provide important sources of perennial water in low-elevation portions of the study area. These include the Black Rock spring system, Antelope Spring, Coyote spring system, Black Spring, and Twin Peaks Spring (figure 2). Other minor seeps and springs exist upstream of Antelope Spring along Cove Creek near the Cove Creek well and along parts of the Beaver River near Black Rock. These smaller springs and seepage areas do not provide for perennial flow beyond their immediate discharge areas. Isolated upland springs are also present in the mountainous parts of the study area above 6000 to 7000 feet (1830–2130 m). These springs provide perennial flow in small drainages in the bounding mountain ranges. All of the smaller drainages in the mountain ranges cease to flow at or just above the interface with the adjacent basins.

Climate

Climate places fundamental constraints on recharge and discharge relations within a groundwater system. Long-term climatic records exist for lowland portions of the study area both near Cove Fort and to the west near Black Rock (Western Regional Climate Center, 2007). Mean annual precipitation at Cove Fort is 13 inches (33 cm) and mean temperature is 9°C (48°F) (Western Regional Cli-

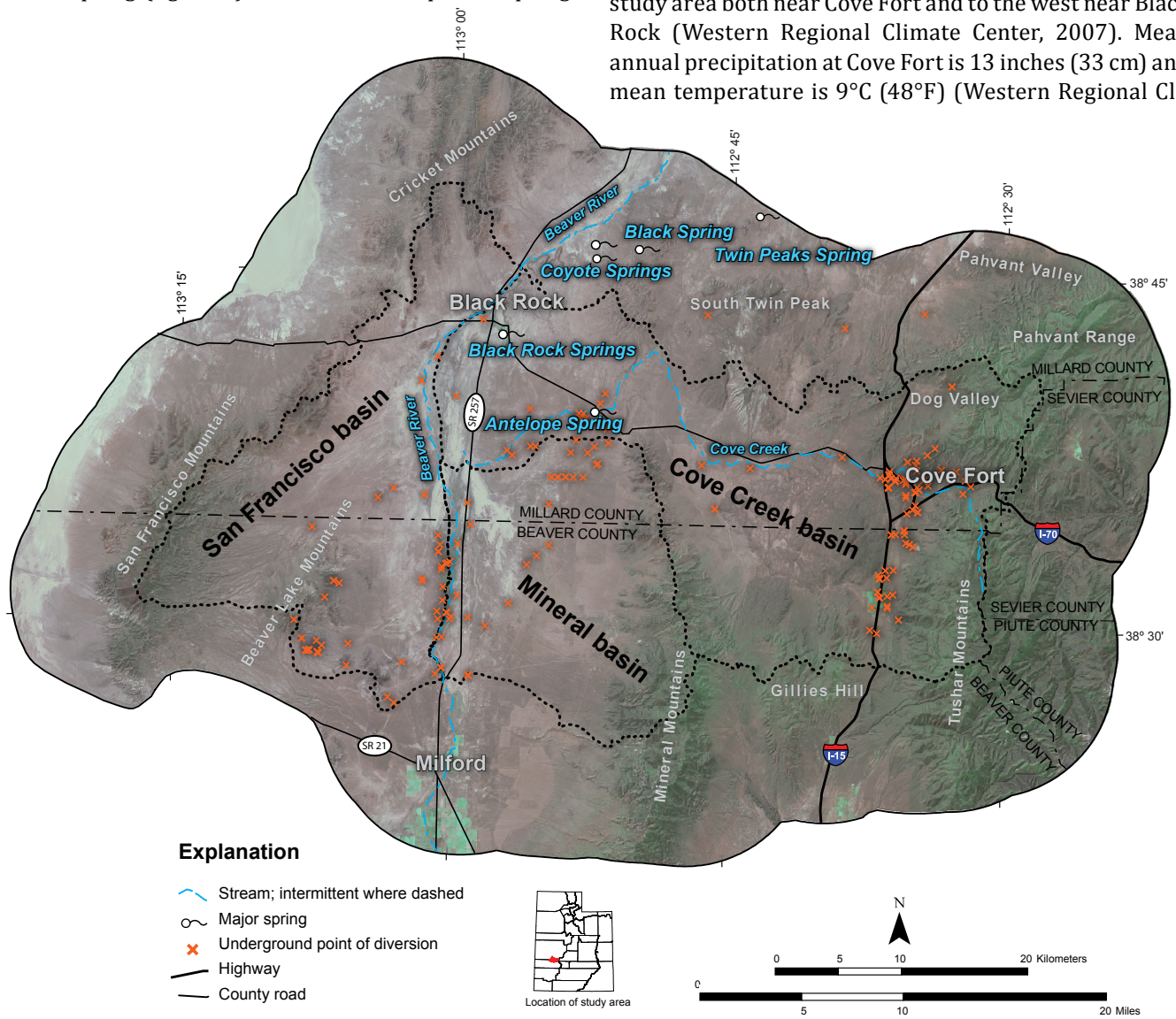

Figure 2. *Landsat image of the Cove Fort study area showing three hydrographic basins and major springs. Image date is 6/21/2001, data available from Intermountain Region Digital Image Archive Center (2007). Underground points of diversion from the Utah Division of Water Rights (2006).*

mate Center, 2007). To the west, mean annual precipitation is 9 inches (23 cm) and mean annual temperature is 10°C (49°F) at the Black Rock weather station (Western Regional Climate Center, 2007). No data exist for upland areas within the study area but are assumed consistent with nearby stations in adjoining portions of the Tushar Mountains (Natural Resources Conservation Service, 2007; Western Regional Climate Center, 2007). Parts of the Tushar Mountains along the eastern boundary of the study area likely receive annual precipitation of more than 35 inches (89 cm) (Natural Resources Conservation Service, 2007), primarily in the form of winter-season snowfall. Other upland mountain ranges—the San Francisco and Mineral Mountains, southern Pahvant Range, and Gillies Hill—also receive important but smaller amounts of winter snowfall. This upland snowfall likely represents the bulk of annual precipitation across the entire study area and is therefore a major source of potential recharge.

GEOLOGIC AND HYDROGEOLOGIC SETTING

Introduction

The geologic units in the study area both harbor and convey groundwater and are of primary concern when considering regional groundwater resources. This section presents geologic, geophysical, and well data that better define the extent and characteristics of the principal aquifers and aquitards in the study area. Regional hydrostatigraphy is generalized from a geologic map and unit descriptions (plates 1 and 2; appendix B).

I compiled a 1:100,000-scale geologic map of the study area (plate 1) from existing digital geologic maps of the Richfield (Hintze and others, 2003), Wah Wah Mountains North (Hintze and Davis, 2002), and Beaver (Rowley and others, 2005) 30′x 60′ quadrangles and a paper map of the 1:48,000-scale Milford and Frisco quadrangles (Best and others, 1989). I examined oil- and water-well logs for the study area to constrain the subsurface extent of hydrostratigraphic units (tables A.1 and A.2). Existing geophysical data, including an isostatic gravity map (Bankey and others, 1998) and modeled basin depth map (Saltus and Jachens, 1995), provide additional constraints on the extent of potential aquifers and aquitards in the subsurface. I combined data from the geologic map, well logs, and geophysical sources to create a series of simplified cross sections that depict the subsurface extent of the hydrostratigraphic units (plate 2).

Geologic Background

The study area lies within the transition zone between the tectonically stable and relatively undeformed rocks of the Colorado Plateau to the east from the tectonically active and relatively deformed rocks of the eastern Great Basin to the west (Smith and others, 1989; Wannamaker and others, 2001). Important rock units include Neoproterozoic metamorphic rocks, Neoproterozoic through early Tertiary sedimentary rocks, Tertiary through Quaternary volcanic rocks, and Tertiary through Quaternary basin-fill deposits (Best and others, 1989; Hintze and Davis, 2002, 2003; Hintze and others, 2003; Rowley and others, 2005). Within the study area these units are exposed in upland mountain ranges consisting of Tertiary igneous rocks and various thrust-faulted Neoproterozoic through Mesozoic sedimentary rocks, and intervening lowland basins filled with interlayered sediments and volcanics of Tertiary and Quaternary age (figure 3). Rocks exposed within the study area record a series of major tectonic events including (1) Neoproterozoic through early Mesozoic deposition along a subsiding continental margin, followed by (2) east-directed thrusting and folding of the Sevier fold and thrust belt from the middle Mesozoic through early Tertiary, and (3) subsequent regional volcanism, basin formation, and extension that continues to the present (Hintze and Davis, 2003).

Neoproterozoic through early Mesozoic sedimentary rocks record cyclic deposition along a continental margin subject to various marine transgressions and regressions and changes in regional sediment supply and subsidence rates (Hintze and Davis, 2003). This sedimentary sequence includes a thick lower section of quartzite and minor argillite, overlain by carbonates that were deposited throughout much of the Paleozoic era (Hintze and Davis, 2003). Permanent marine regression occurred during the early Mesozoic and subsequent strata record continental clastic deposition dominated by sandstone with lesser mudstone, claystone, and carbonates (plates 1 and 2; figure 3) (Hintze and Davis, 2003).

After deposition of the Neoproterozoic through middle Mesozoic sedimentary section, large sheets of these strata were imbricated and folded along east-directed thrust faults of the Sevier fold and thrust belt (Armstrong, 1968; DeCelles and Coogan, 2006, and references therein). Sevier thrusting closely juxtaposed rocks of greatly different ages and lithologies and locally thickened the crust by tens of kilometers (DeCelles and Coogan, 2006). Significant portions of the thrust belt are exposed in the San Francisco and Cricket Mountains in the west and along the Pahvant Range in the east as well as the northern tip of the Mineral Mountains (figure 3). After cessation of Sevier thrusting in the late Eocene or early Oligocene, major regional extension and volcanism began (DeCelles and Coogan, 2006).

Igneous rocks of Oligocene through Miocene age are exposed in the Tushar and Mineral Mountains, southern San Francisco Mountains, and along Gillies Hill. These

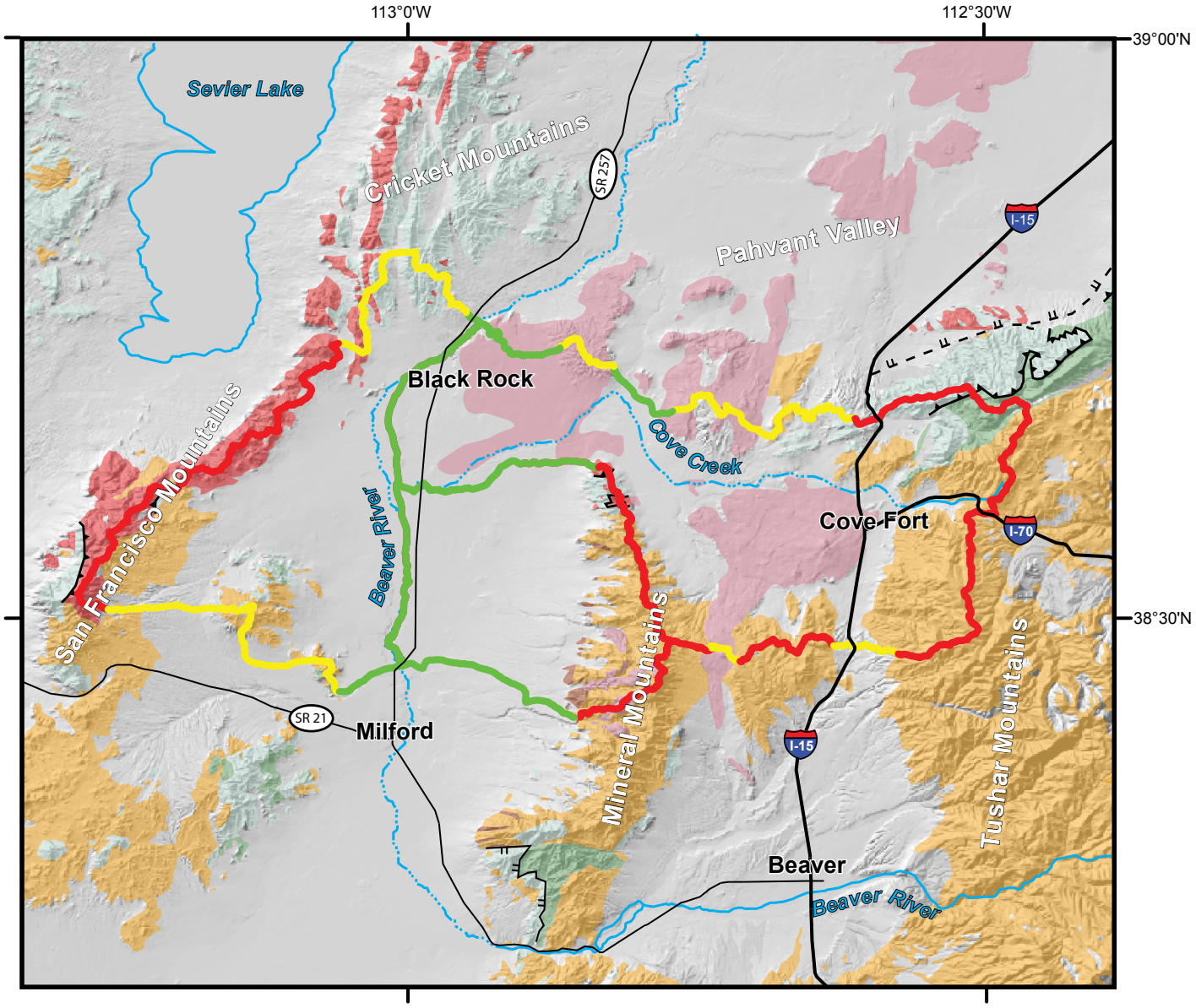

Explanation

- Major stream; dashed where ephemeral
- Major thrust fault
- Major low-angle extensional fault
- Impermeable basin boundary, transverse groundwater flow unlikely
- Moderately permeable basin boundary, transverse groundwater flow possible
- Permeable basin boundary, transverse groundwater flow likely

Geologic Units

- Quaternary basin fill and unconsolidated deposits
- Quaternary volcanic rocks
- Tertiary igneous rocks
- Tertiary sedimentary rocks
- Mesozoic sedimentary rocks
- Paleozoic carbonates
- Precambrian and Cambrian quartzites
- Precambrian metamorphic rocks

Figure 3. *Simplified geology of the Cove Fort study area. Important aquifers include interlayered Quaternary basin fill and volcanics and Paleozoic carbonates. Important aquitards include Tertiary igneous rocks and Precambrian and Cambrian quartzites. The relative potential for groundwater flow across basin boundaries is shown. See text for further explanation. Geology is generalized from Hintze and Davis (2002, 2003), Hintze and others (2003), and Rowley and others (2005).*

rocks range from plutonic rocks exposed in the Mineral Mountains to a suite of calderic rocks of the Marysvale volcanic field, including tuffaceous sedimentary rocks, exposed in the Tushar Mountains (Nielson and others, 1986; Coleman and others, 1997; Rowley and others, 2002, 2005). Between these mountain ranges, in the Cove Creek basin, Pliocene and Quaternary volcanic rocks ranging from basalt to rhyolite constitute an important part of the basin fill (Nash, 1981; Steven and Morris, 1983; Hintze and others, 2003).

Significant east-west extension began in the Oligocene and accelerated in the Miocene concurrent with emplacement of the Mineral Mountain intrusives (Coleman and others, 1997). Extension continues to the present day and has created the modern basin and range topography of uplifted bedrock mountain ranges separated by intervening basins filled with variously lithified sediments and volcanic rocks (Zoback and Anderson, 1983; Smith and Bruhn, 1984; Smith and others, 1989; Hintze and Davis, 2003). Extensional deformation is ongoing within the study area and notable Quaternary fault scarps that cut both Quaternary volcanics and unconsolidated basin fill exist near Cove Fort (Anderson and Bucknam, 1979; Nash, 1981; Steven and Morris, 1983). Further detailed descriptions of the tectonic and geologic history of the study area are available from several previous sources (primarily Hintze and Davis, 2003, and references therein).

Hydrostratigraphy

Introduction

The relative geologic complexity, scale of the study area, and potential for groundwater to reside and travel through multiple geologic units necessitates broad generalization of aquifer systems. For this study geologic units are divided into four hydrogeologic groups based on relative permeability and importance to basin-wide groundwater flow. Geologic units may be broadly divided into permeable and impermeable groups based on general lithology. Regionally important impermeable units include a thick section of late Neoproterozoic through Early Cambrian sedimentary strata consisting mostly of orthoquartzite, and Tertiary intrusive and volcanic units. Important permeable units include Paleozoic strata dominated by carbonates, and basin fill that includes Tertiary through Quaternary sedimentary deposits and various volcanics.

The impermeable units likely form important barriers to groundwater movement in the subsurface at several locations in the study area and may generally have poor yield to wells. By contrast the permeable units, particularly the contiguous basin-fill deposits, facilitate groundwater movement and may readily yield water to wells. Within each of these hydrogeologic groups significant local variability exists due to structural and lithologic factors. These groupings provide an accurate depiction of regional-scale aquifers and aquitards that control groundwater movement and availability across the study area.

Impermeable Units

The impermeable late Neoproterozoic and Early Cambrian strata are dominated by a thick, relatively continuous section of quartzite interlayered with argillite and shale. These rocks exist primarily along the western margin of the study area, extending north from the San Francisco Mountains to the southern Cricket Mountains (figures 3 and 4). Geologic units in this group include the Pocatello Formation, the argillaceous Blackrock Canyon Limestone, Caddy Canyon Quartzite, Inkom Formation, Mutual Formation, Prospect Mountain Quartzite, and Pioche Formation (plate 2; appendix B) (Hintze and Kowallis, 2009). These units form an aggregate thickness of nearly 9000 feet (2700 m) along the western margin of the study area (Hintze and Davis, 2002). These rocks may also be locally important where present in the subsurface, such as northwest of the Mineral Mountains where they may form an important barrier to deep regional flow (see cross section B–B′ on plate 2).

Igneous plutonic and volcanic rocks of Tertiary age comprise the second broad category of impermeable units. This hydrostratigraphic unit includes rocks related to the Marysvale volcanic field and igneous rocks of the Mineral Mountains. Rocks of the Marysvale volcanic field are exposed in the Tushar Mountains, along Gillies Hill, and south of the San Francisco Mountains (Rowley and others, 2002, 2005). The Tushar Mountains and nearby Gillies Hill are largely underlain by the Bullion Canyon and Mount Belknap volcanic rocks and associated units that include various welded tuffs, lava flows, and intrusive rocks (Rowley and others, 2002). Individual rock types include welded tuffs and many types of intrusive rocks that are generally impermeable (Domenico and Schwartz, 1997), and the complex interlayering of these units in the Tushar Mountains likely serves to further reduce regional-scale permeability. South of the San Francisco Mountains the Horn Silver andesite and associated volcanic rocks comprise other impermeable volcanics in the southwest quadrant of the study area (Best and others, 1989; Hintze and Davis, 2002; Rowley and others, 2005). Impermeable igneous rocks in the Mineral Mountains consist primarily of Oligocene to Miocene plutonic rocks. Numerical flow modeling of the groundwater system within intrusive rocks of the Mineral Mountains and adjoining Roosevelt Hot Springs KGRA indicates that horizontal permeability in these rocks is insufficient to support significant regional flow across the Mineral Mountains (Faulder, 1991). All of these volcanic and

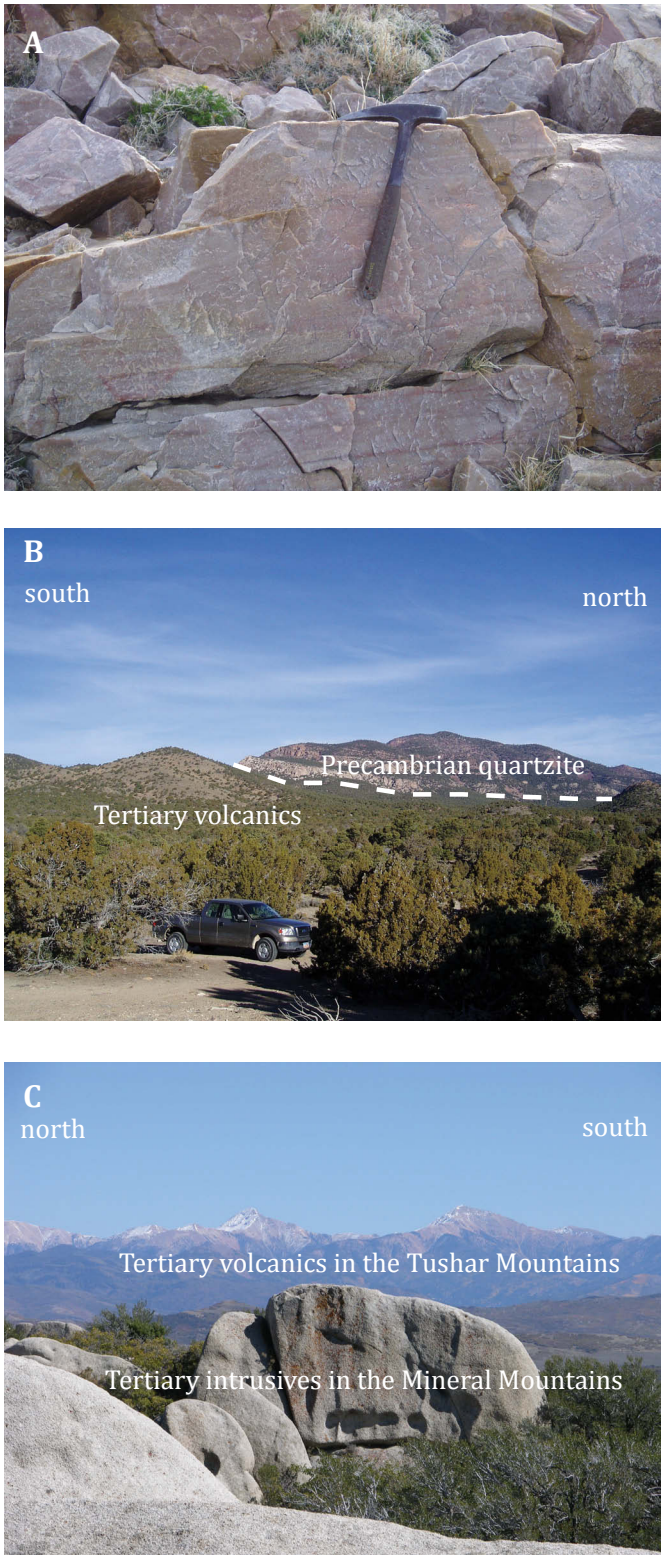

Figure 4. *Examples of impermeable units, including A) Precambrian and lower Cambrian quartzites, pictured is the compact orthoquartzite of the Prospect Mountain Formation, B) Tertiary volcanics and Precambrian quartzite exposed in the San Francisco Mountains, and C) Tertiary intrusive rocks of the Mineral Mountains in the foreground with Tertiary volcanics of the Tushar Mountains in the background.*

intrusive rocks may be locally permeable with sufficient fracturing, most notably at the Cove Fort and Roosevelt Hot Springs KGRAs where these rocks host commercial geothermal resources (Moore and Nielsen, 1994; Moore and others, 2000).

Permeable Rocks

The permeable Paleozoic units are dominated by carbonate units (limestone or less commonly dolomite) and include numerous Cambrian formations above the Pioche Formation, as well as the Pogonip Group, Laketown and Fishhaven Dolomites, Sevy and Simonson Dolomites, Guilmette Formation, Redwall Limestone, Callville Limestone, Pakoon Dolomite, and Kaibab Limestone (Hintze and others, 2003; Hintze and Davis, 2003; Hintze and Kowallis, 2009). Within this carbonate section several zones of sandstone and quartzite exist that may locally yield water including the Eureka Quartzite, Cove Fort Quartzite, and Queantoweap Sandstone. Permeable Paleozoic-age rocks are present mostly in areas north of Cove Fort, including Dog Valley and areas just to the west along the southernmost Pahvant Range, and in the Cricket Mountains along the northwestern margin of the study area (figures 3 and 4). Whereas these rocks are likely permeable, few water wells are completed in these units. This results from the limited spatial extent of these rocks and is not indicative of their relative yield to wells.

Permeable basin fill covers much of the study area and represents the single largest and most important hydrogeologic group. It also contains the greatest variety of rock types and lithologies, ranging from consolidated Eocene-age conglomerates of the Flagstaff Formation that directly overlie older bedrock to surficial unconsolidated deposits of Holocene age (Hintze and Davis, 2002, 2003; Hintze and others, 2003; Rowley and others, 2005). Sedimentary basin fill also contains important sections of lithified and carbonate-dominated rocks that include the Miocene to Pliocene-age Sevier River Formation (Oviatt, 1991; Hintze and others, 2003). Interbedded with these sedimentary deposits, particulary in the Cove Creek basin, is a wide range of volcanic rocks ranging from Quaternary basalt, andesitic flows and cinder cones near Cove Fort (figures 3 and 5) (Nash, 1981; Steven and Morris, 1983) to Oligocene tuffaceous and volcaniclastic deposits that likely exist in deep subsurface parts of the basin along the Beaver River (Hintze and Davis, 2003). Volcanic basin fill is likely less spatially continuous than sedimentary basin fill, but where present, particularly in the Cove Creek basin, may contain significant amounts of groundwater. Groundwater in the basin-fill aquifer exists under confined and unconfined conditions depending on local geology. Along the Beaver River, north of Milford and south of Black Rock, groundwater in the upper basin fill exists in a mix of confined and unconfined conditions

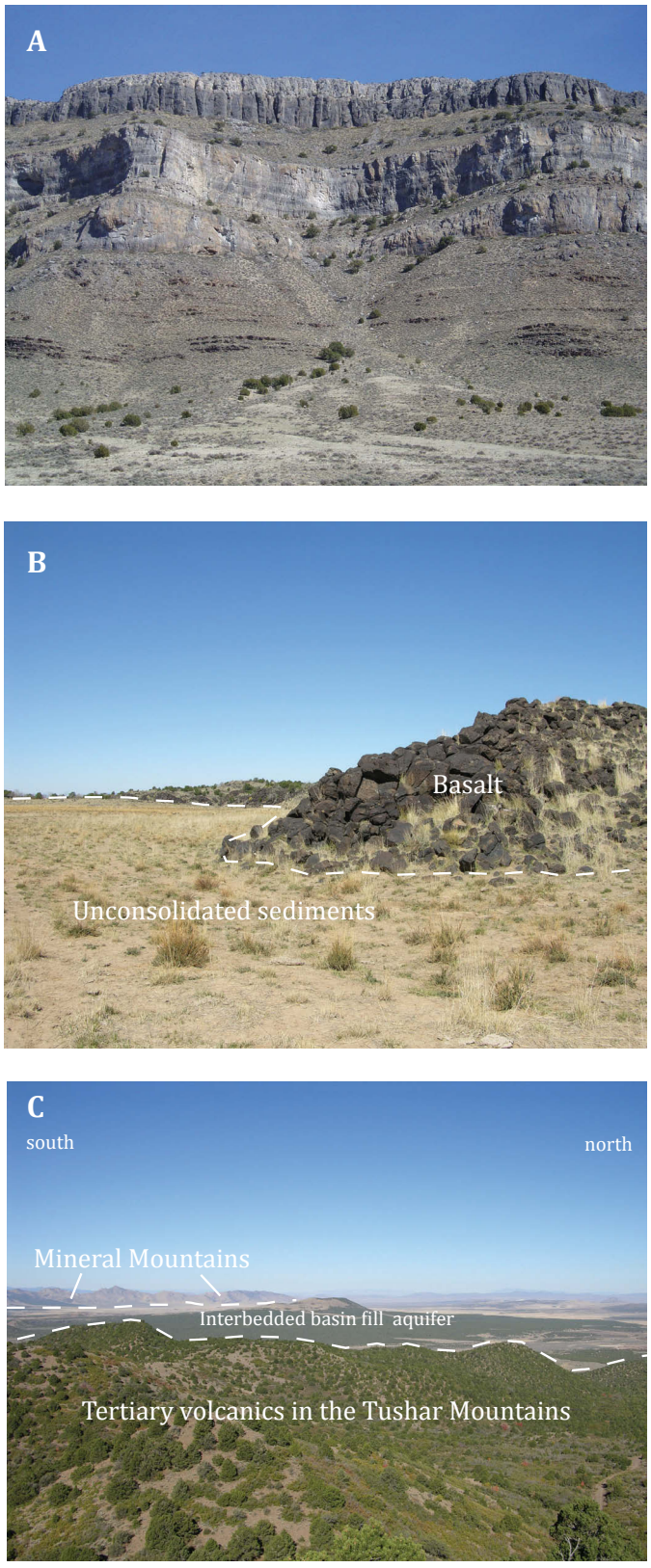

Figure 5. *Examples of permeable units, including A) Paleozoic carbonates, pictured are Middle Cambrian limestones in the Cricket Mountains near the base of the important carbonate section, B) interbedded Quaternary volcanics and unconsolidated sediments typical of the basin-fill aquifer in the Cove Creek basin, C) overview of the basin-fill aquifer in the Cove Creek basin inset between lower permeability rocks in the Tushar and Mineral Mountains.*

(Mower and Cordova, 1974). Perched aquifers may also be locally important but are difficult to characterize based on existing well data. Available data for the principal aquifer in the Cove Creek basin suggest much of the aquifer is unconfined.

The discussion above covers the majority of the permeable rock units in the study area. Other rock units may also be locally important as aquifers; chief among these is a sequence of Mesozoic sedimentary rocks that includes the Jurassic Navajo Sandstone and Triassic Chinle Formation (Best and others, 1989; Hintze and others, 2003; Hintze and Kowallis, 2009). The extent of these units is limited, but they may form a relevant localized aquifer system in the southern part of the Pahvant Range and to the west in the Beaver Lake Mountains. Within and near the southern Pahvant Range a series of early Tertiary sedimentary rocks overlies these Mesozoic sedimentary rocks and may also be an important local aquifer (Hintze and others, 2003).

Structural Control of Permeability

Geologic structures of various scale, including faults, fractures and folds, likely also alter groundwater movement in the study area. A variety of faults and fractures are ubiquitous in consolidated rocks across the study area. Faults range from shallowly dipping thrust faults and steeply dipping strike slip faults of the Sevier fold and thrust belt, to steeply or shallowly dipping normal faults related to Tertiary and more recent extension.

The ultimate hydrogeologic effect of any fault or group of faults is complex, localized, and generally beyond the scope of this study. However, map scale faults, like those shown on plate 1, likely have low-permeability fault cores that reduce fluid flow perpendicular to the strike of these faults and near-fault fracturing that may increase fluid flow parallel to the strike of these faults. The hydrogeologic effect of folding is more complex but generally fracturing parallels fold axes and fluid flow may be increased parallel to fold axes and reduced perpendicular to fold axes.

Hydrogeologic Boundary Conditions

The distribution of permeable and impermeable hydrogeologic groups control groundwater flow between basins. Where hydrographic boundaries of the Cove Creek, Mineral, and San Francisco basins lie along impermeable units, such as igneous rocks in the Mineral Mountains (figure 3), regional-scale transverse groundwater flow is unlikely. Where basin boundaries coincide with zones of contiguous, permeable basin fill, such as along the Beaver River drainage north of Milford (figure 3), regional-scale transverse groundwater flow is likely. A third boundary type consists of moderate-

permeability rocks, such as surficial volcanic rocks along the northern boundary of the Cove Creek basin, across which transverse groundwater flow is possible but less likely than in adjoining areas of unconsolidated basin fill. Faults and fractures may locally alter these boundary conditions, increasing or decreasing groundwater flow depending on fault characteristics and location.

In the Cove Creek basin impermeable boundaries exist along the Mineral Mountains, across Gillies Hill, and through the Tushar Mountains, where impermeable igneous rocks occur. Along the northern boundary of the Cove Creek basin a mix of permeable and moderately permeable basin boundaries allow for transverse groundwater flow to the north. The western boundary of the Cove Creek basin consists of permeable basin fill and allows transverse groundwater flow between the Cove Creek basin and the San Francisco and Mineral basins. The western boundary of the San Francisco basin consists of impermeable quartzites, precluding regional-scale groundwater flow to the west. Moderately permeable boundaries occur along the northwest margin of the San Francisco basin in the Cricket Mountains and transverse groundwater flow is possible there.

High topography and associated elevated groundwater levels also exert important controls on hydrogeologic boundaries and the potential for cross-boundary groundwater flow and may be considered in addition to the discussion of hydrogeologic boundary conditions presented above. Elevated groundwater levels likely occur in areas of regionally significant topography and precipitation (Domenico and Schwartz, 1997) including the Tushar and San Francisco Mountains and along Gillies Hill and the Mineral Mountains. Groundwater highs and consequent divergent flow paths further reduce the possibility of regional transverse flow in these areas. Lower elevation areas, including the southern Cricket Mountains and the northern margin of the Cove Creek basin, likely lack groundwater highs and therefore allow transverse groundwater flow.

Well Data

Overview

I examined all available water and oil well logs to better constrain the subsurface geology and extent of aquifers and aquitards across the study area. A summary of water and oil well logs having sufficient data are presented in tables A.1 and A.2. Basic lithology and completion information is noted for water well logs, including total depth, basin-fill thickness, generalized bottom-hole lithology, depth to water at time of completion, screened interval, and presence of impermeable clay layers greater than 20 feet thick. For oil well logs basic lithology is noted, including basin-fill thickness, total depth, and generalized bottom-hole lithology. Location and summary information of water well and oil boreholes is shown in figure 6.

Water wells completed in the basin fill penetrate either unconsolidated sedimentary deposits or interbedded volcanics in the upper several hundred feet of the aquifer. Most of the water wells completed in basin fill in the Cove Creek basin penetrate at least one volcanic interval. Volcanic intervals include basalt or mixed-composition rocks that likely correlate with nearby surficial volcanics. Several water wells in the Cove Creek basin penetrate Tertiary-age limestone that is considered part of the larger basin-fill aquifer. Similar Tertiary limestone sequences in the basin-fill aquifer occur in several water wells southwest of Black Rock. Water wells completed in basin fill in the San Francisco and Mineral basins commonly penetrate only unconsolidated sand and clay of the basin fill. Several oil wells penetrate Paleozoic bedrock near Dog Valley where these units crop out or are shallowly buried (Utah Division of Oil, Gas, and Mining, 2006). Few water wells are completed in Paleozoic-age carbonates or igneous rocks not related to the basin fill. Several oil wells south of Black Rock penetrate significant thicknesses of lithified basin fill that likely form much of the deepest basin-fill deposits. Well logs constrain depth to bedrock north of Cove Fort and at a deep oil-well west of the Mineral Mountains (Utah Division of Oil, Gas and Mining, 2006; Utah Division of Water Rights, 2006) (figure 6). However, most well logs do not penetrate a complete section of basin fill and therefore constrain only minimum basin-fill thickness.

Recharge Type Mapping

The presence or absence of extensive thick, fine-grained clay layers and relative groundwater levels based on well logs may be used to delineate recharge and discharge type for basin-fill aquifers according to the methods of Anderson and others (1994). Recharge type mapping can be an important tool for land managers to control potential contamination of basin-fill aquifers and may also show the extent of potential confining layers and diffuse areas of groundwater discharge within these aquifers. Primary recharge consists of areas having clay layers less than 20 feet (6 m) thick and a downward groundwater gradient. Secondary recharge occurs in areas having clay layers thicker than 20 feet (6 m) and a downward groundwater gradient (groundwater levels at or below thick clay layers). Discharge areas are mapped in areas of upward groundwater gradients (at or above thick confining layers) and clay layers greater than 20 feet (6 m) thick (Anderson and others, 1994).

As shown on figure 7, basin fill across the study area is subdivided into primary recharge, secondary recharge, and discharge zones using well-log data (table A.1). In the upper part of the basin-fill aquifer, confining layers of clay are uncommon and most well logs indicate unconfined

and primary recharge conditions. Significant confining layers along the Beaver River define areas of secondary recharge and discharge. Previous workers have noted laterally continuous confining layers along the Beaver River that partition the upper basin fill into two aquifers south of the study area and may be contiguous with those to the north (Mower and Cordova, 1974; Mason, 1998). Confining layers are largely absent in wells in the Cove Creek basin and most of the basin fill is mapped as primary recharge. A small zone of secondary recharge is mapped south of Cove Fort and in Dog Valley. Based on the recharge type mapping much of the upper part of the principal aquifer in the study area is unconfined. Confined conditions may exist locally in areas mapped as secondary recharge or discharge and may also exist at depths greater than that penetrated by available well logs.

Geophysical Data

Introduction

Complex geology and a relative lack of well control warrant additional examination of geophysical data sets to better determine the extent and geometry of the basin

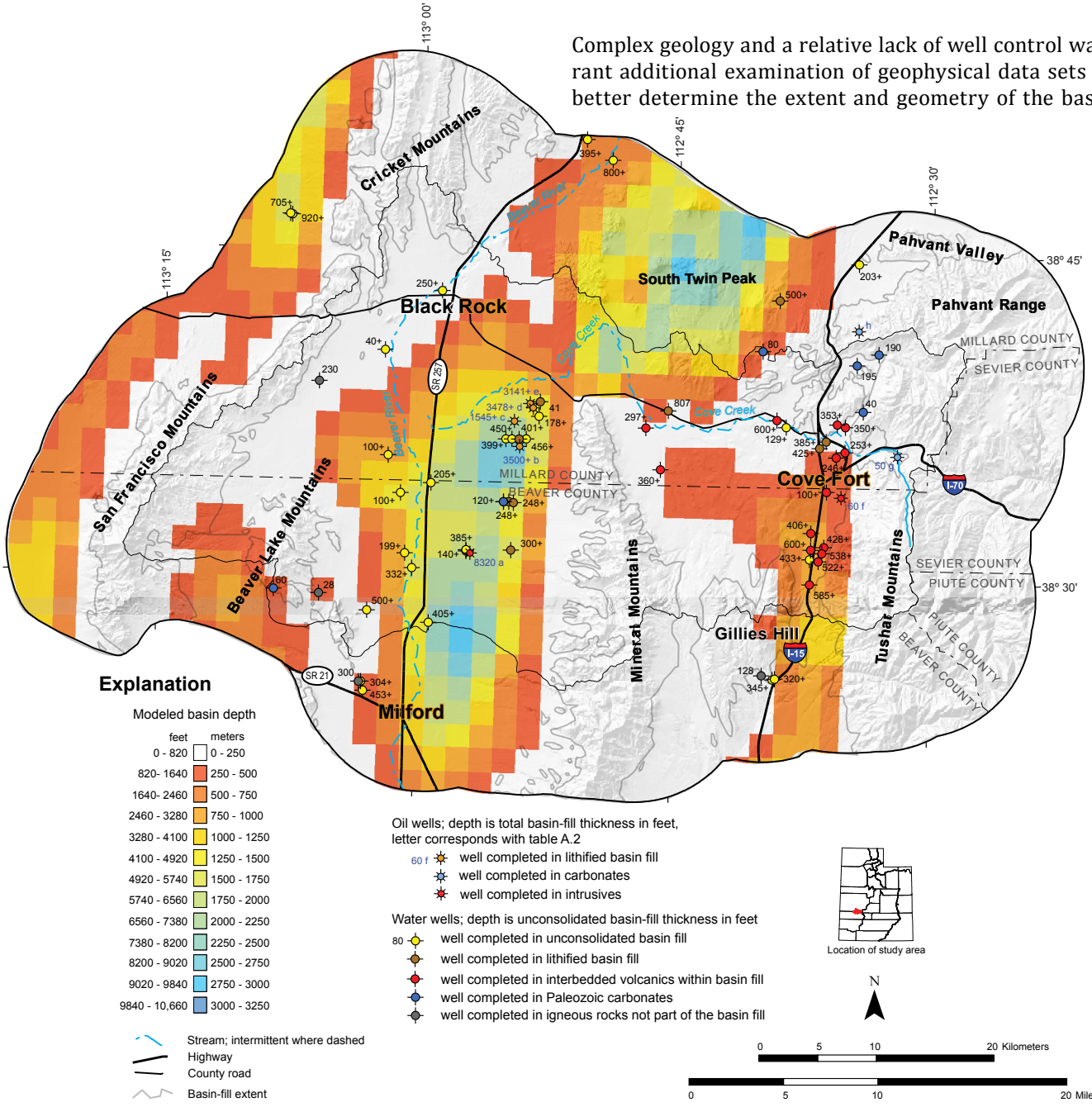

Figure 6. *Modeled basin depth and well-log data for oil and water wells in the study area. Modeled basin depth is modified from Saltus and Jachens (1995). Well data are from the Utah Division of Oil, Gas, and Mining (2006) and the Utah Division of Water Rights (2006). Water-well log identifiers are shown on figure 7. See text and tables A.1 and A.2 for details and well log information.*

fill in the study area. The basin-depth modeling of Saltus and Jachens (1995), together with the well data presented above, provide the best estimate of basin-fill thickness across the study area. Discussion of recently available isostatic gravity anomaly data for the study area is presented to further support modeled basin depth and provide additional detail for subsurface basin geometry.

Isostatic Gravity Anomaly

Isostatic gravity anomalies represent the local density distribution of middle and upper crustal rocks and unconsolidated deposits after accounting for elevation, terrain, deep crustal density, and regional effects (Simpson and others, 1986; Saltus and Jachens, 1995). These data provide a useful tool to evaluate subsurface basin geometry and its correlation with surficial geology. This is particularly useful in areas of poor well control that typify much of the study area. Recently available gravity data for the study area were extracted from the statewide isostatic gravity anomaly map (figure 8) (Bankey and others, 1998). Anomalies are presented as discretely valued grid data with a cell size of 4 kilometers (2.5 mi) on a side.

As shown in figure 8, isostatic gravity anomalies within the basin fill range from 26 to -30 mGal in the study area. A prominent north-south oblong gravity low defines the deepest part of the basin along the Beaver River south of Black Rock. Flanking this low are gravity highs that correlate with bedrock exposures in the Mineral, San Francisco, and Beaver Lake Mountains. Areas of Paleozoic-age sedimentary rocks in the Cricket and San Francisco Mountains and the Pahvant Range cor-

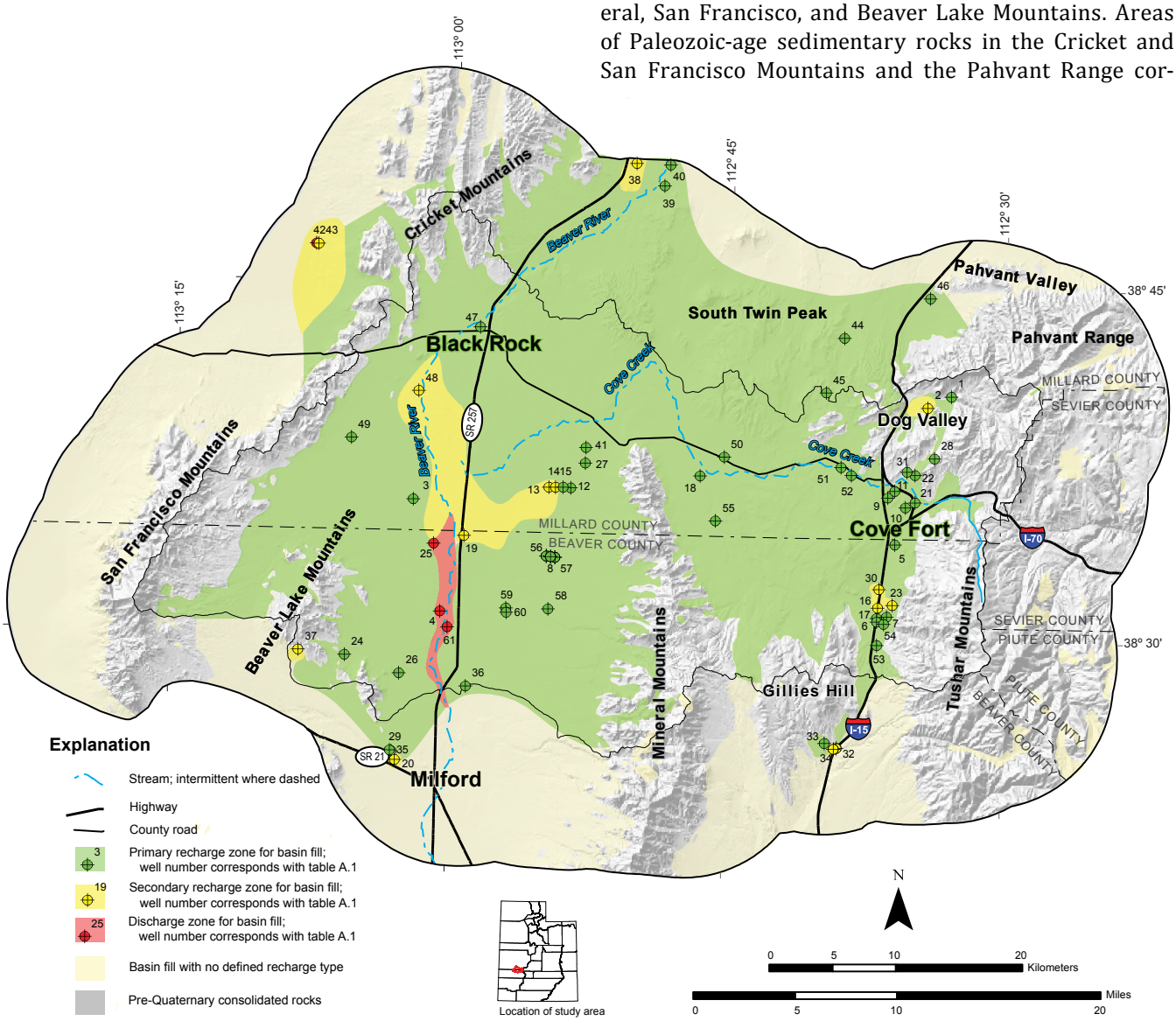

Figure 7. *Recharge and discharge type for the study area. All boundaries between recharge and discharge types are approximate. Well-log information used to construct figure is presented in appendix table A.1. Primary recharge zones are mapped in areas of basin fill that do not have clay layers greater than 20 feet thick. Secondary recharge zones are mapped in areas of basin fill that have clay layers thicker than 20 feet and a downward groundwater gradient. Discharge areas are mapped where basin fill has clay layers thicker than 20 feet and an upward groundwater gradient. See text for further description.*

relate with the highest isostatic gravity values. A narrow southeast-trending gravity high extends from the Cricket Mountains, beneath the Black Rock area, towards the northernmost Mineral Mountains and likely represents a southeastward-deepening prow of buried Paleozoic rocks (Carrier and Chapman, 1981). In the east two parallel, north-south-trending gravity gradients extend from the town of Cove Fort south to the Beaver Basin and define the Cove Fort graben (Carrier and Chapman, 1981; Mabey and Budding, 1987). To the west and north of the Cove Fort graben, a broad west-southwest-trending gravity saddle extends from exposures of Paleozoic bedrock near Dog Valley to the northern Mineral Mountains and likely represents a relative bedrock high between the Cove Fort graben and Pahvant Valley to the north. Elsewhere, volcanic rocks near Gillies Hill and in the Tushar and Mineral Mountains and nearby subsurface areas give lower isostatic gravity values relative to exposures of Paleozoic bedrock in nearby mountain ranges. Steep gravity gradients, particularly along the western flank of the Mineral Mountains, likely represent large basin-forming extensional faults (Thangsuphanich, 1976; Carrier and Chapman, 1981; Barker, 1986).

Modeled Basin Depth

Using isostatic gravity data similar to those described above, and select regional geology, deep well logs, and depth versus density data, Saltus and Jachens (1995) modeled depth to basement for many basins in western Utah.

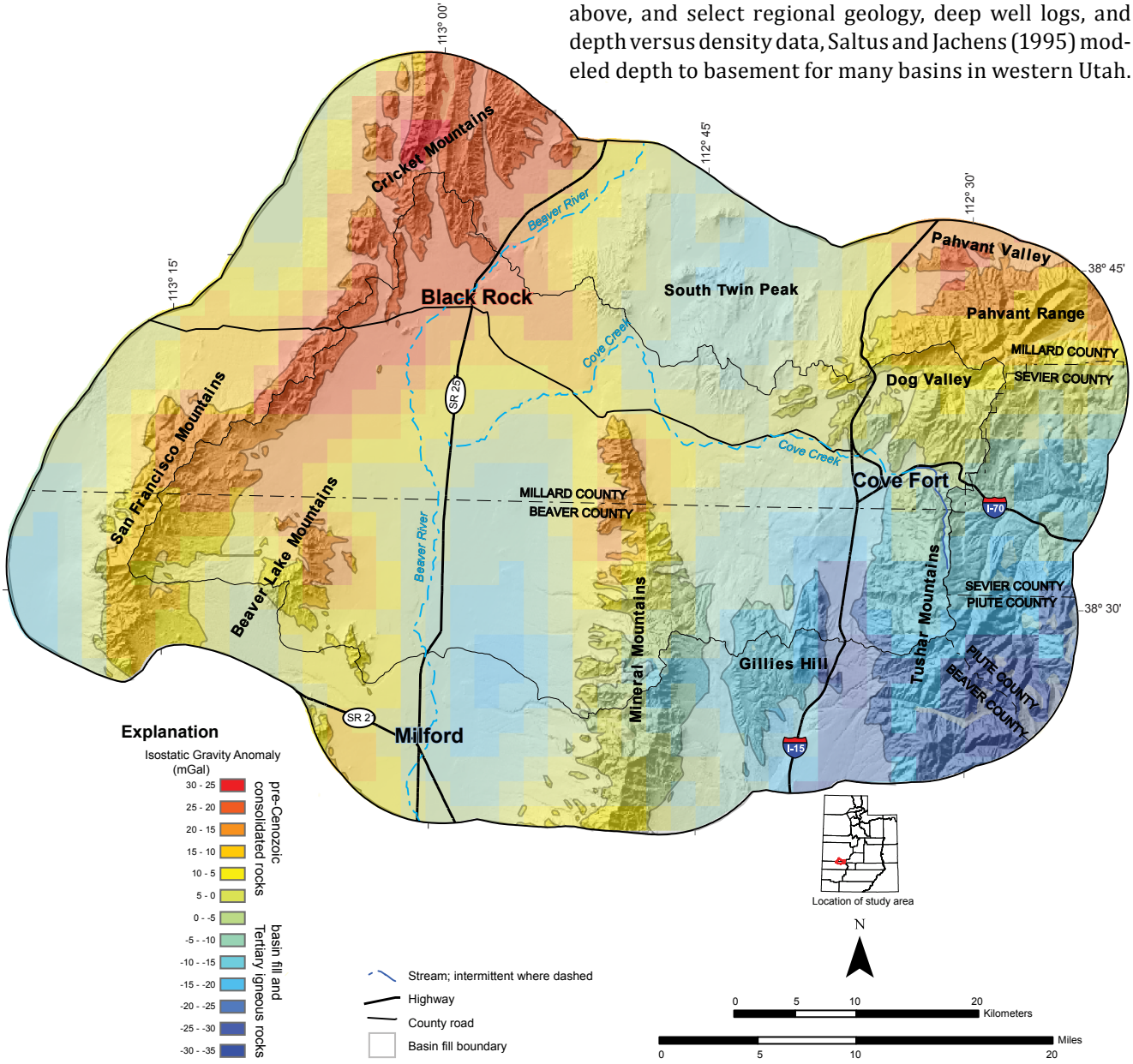

Figure 8. *Isostatic gravity map of the study area. Data are from Bankey and others (1998). Gravity highs correspond to exposures of pre-Cenozoic consolidated rocks and areas where these rocks lie in the shallow subsurface. Gravity lows correspond to areas of deep basin fill and exposures of Tertiary igneous rocks. See text for further description.*

Modeled basin-fill thickness in the study area ranges from 0 to 9000 feet (0–3000 m). The area of greatest basin-fill thickness corresponds with the prominent gravity low located north of Milford along the southern study area boundary (figures 6 and 8). Two relatively deep pockets of basin fill, greater than 8500 feet (2600 m), exist in this large depression beneath the Beaver River north of Milford. Existing isostatic gravity data do not define two separate deep basins in this area, and the modeled result may instead reflect changes in lateral density distribution due to the presence of relatively dense lower Paleozoic rocks in the northern Mineral Mountains and in the nearby subsurface. Along the eastern margin of the San Francisco Mountains a shallowly buried shelf, likely consisting of impermeable quartzites of the adjacent mountain range, may further reduce the potential for significant east-to-west transverse groundwater flow. Modeled depth to bedrock decreases over a southeast-plunging bedrock high extending from the Cricket Mountains to the northernmost Mineral Mountains. To the northeast, basin fill thickens to 7500 to 9000 feet (2300–2750 m) beneath Pahvant Valley. A north-south-trending trough of basin fill, with depth to bedrock greater than 1000 feet (300 m) and as much as 4000 feet (1200 m), defines the Cove Fort graben in the southeastern quadrant of the study area. An east-northeast-trending shelf of shallow basin fill, less than 1200 feet (400 m) deep, separates deep basin fill in the Cove Fort graben from deep basin fill to the northwest beneath South Twin Peaks and Pahvant Valley.

Based on observed patterns in modeled basin-fill thickness, the deepest portions of basin fill are separated from one another by intervening subsurface bedrock highs. Permeability contrasts between basin fill and bedrock in these areas may reduce or preclude groundwater flow. Deep basin fill may therefore be hydrologically isolated beneath the Beaver River from deep basin fill to the north beneath Pahvant Valley (figure 6). The deepest portions of the Cove Fort graben are similarly hydrologically isolated from deeper basin fill to the north beneath Pahvant Valley and from deep basin fill beneath the Beaver River valley to the west (figure 6). Within the Cove Creek basin, basin-fill thickness patterns have the effect of limiting significant regional groundwater flow to the upper 1200 feet (370 m) of basin fill.

Direct comparison of the modeled basin-fill depth with existing well data is possible only at a few locations because of the paucity of wells that intersect bedrock (figure 6). Modeled depth to bedrock, near a deep oil well that intersects bedrock west of the Mineral Mountains (well a in table A.2 and figure 6), is within 10 percent of the actual depth based on the well log. Shallow modeled basin-fill depths correspond well with well logs north of Cove Fort, further suggesting that modeled basin-fill thickness provides a useful constraint on basin depth across the study area.

Cross Sections

Plate 2 shows five simplified cross sections based on the compiled geologic map, hydrostratigraphy, well logs, and geophysical data presented in this report. These cross sections provide simplified views of the subsurface extent of the aquifers and aquitards on a regional scale, and are not meant to be balanced geologic cross sections capable of depicting the complex structural relationships at the scale of the compiled map.

Cross section A–A′ runs southeast to northwest and shows imbricated thrust plates of the Sevier fold and thrust belt in the southern Pahvant Range overlain by a thickening section of basin fill to the northwest. To the north the contact between these two units has been interpreteted as the Sevier Desert detachment, a regionally extensive low-angle normal fault that has accommodated several kilometers of extension (Davis, 1983; George, 1985; DeCelles and Coogan, 2006). Basin fill above this contact is regionally contiguous but cut by many smaller normal faults that may have important local effects on groundwater flow. Cross section B–B′ extends from the Mineral Mountains north and northwest to the southern Cricket Mountains. This section depicts the impermeable intrusive rocks that make up the core of the Mineral Mountains and a structurally attenuated section of Neoproterozoic and Lower Cambrian impermeable quartzites that occur on the northern tip of the Mineral Mountains and extend into the subsurface as a shallow bedrock high connecting with the Cricket Mountains to the northwest (Hintze, 1984). Cross section C–C′ runs east to west and depicts thrust-faulted Paleozoic rocks likely separated from relatively thick basin fill by a southern extension of the Sevier Desert detachment. To the west, basin fill thins markedly over a buried bedrock high near Black Rock and the intersection with cross section B–B′ before carbonate rocks are again encountered in the Cricket Mountains. Cross section D–D′ runs east to west across the Tushar Mountains and the Cove Fort area to the San Francisco Mountains. This cross section shows the relatively thick basin fill and underlying isolated Paleozoic carbonates of the Cove Fort graben inset in a variety of relatively impermeable volcanic rocks of the Tushar Mountains and the deeper subsurface of the upper Cove Creek basin. To the west, impermeable intrusives in the Mineral Mountains and quartzites in the San Francisco Mountains bound thick basin fill beneath the Beaver River valley. Finally cross section E–E′ depicts the north-to-south changes in basin-fill thickness along the Beaver River valley.

GROUNDWATER LEVELS

Groundwater Elevation

Elevation of the groundwater surface of the basin-fill aquifer system is defined by existing springs and seeps, U.S. Geological Survey (2007) long-term monitoring wells, and new water-level measurements obtained during this study (figure 9). These water levels are assumed to represent unconfined or water table conditions that are apparently typical of the upper part of the principal aquifer across most of the study area (see figure 7 and discussion in Recharge-Type Mapping section). Areas of confined conditions are likely localized and not differentiated based on available water-level measurements. The groundwater surface was contoured using ArcGIS, and then modified in areas of poor fit, based on water-level and spring location and elevation data (table 1) obtained during March and June of 2007. Dashed lines on figure 9 show areas of estimated groundwater elevation, where well or spring data are lacking and groundwater elevations are assumed based on nearby measured values and geology. Error in areas of estimated groundwater elevation may be significant and is propagated in subsequent calculations that are based on the potentiometric surface (figures 9, 10, and 11). Groundwater elevation is best constrained in the Cove Creek basin and least constrained near the San Francisco Mountains.

As shown on figure 9, groundwater in the eastern part of the study area flows to the north and north-northwest away from regional areas of high topography and high precipitation in the southeastern part of the Cove Creek basin. Farther to the west near Black Rock, groundwater flows to the west in the Cove Creek basin. Near South Twin Peak and elsewhere along the northern boundary of the study area, groundwater flows to the northwest into

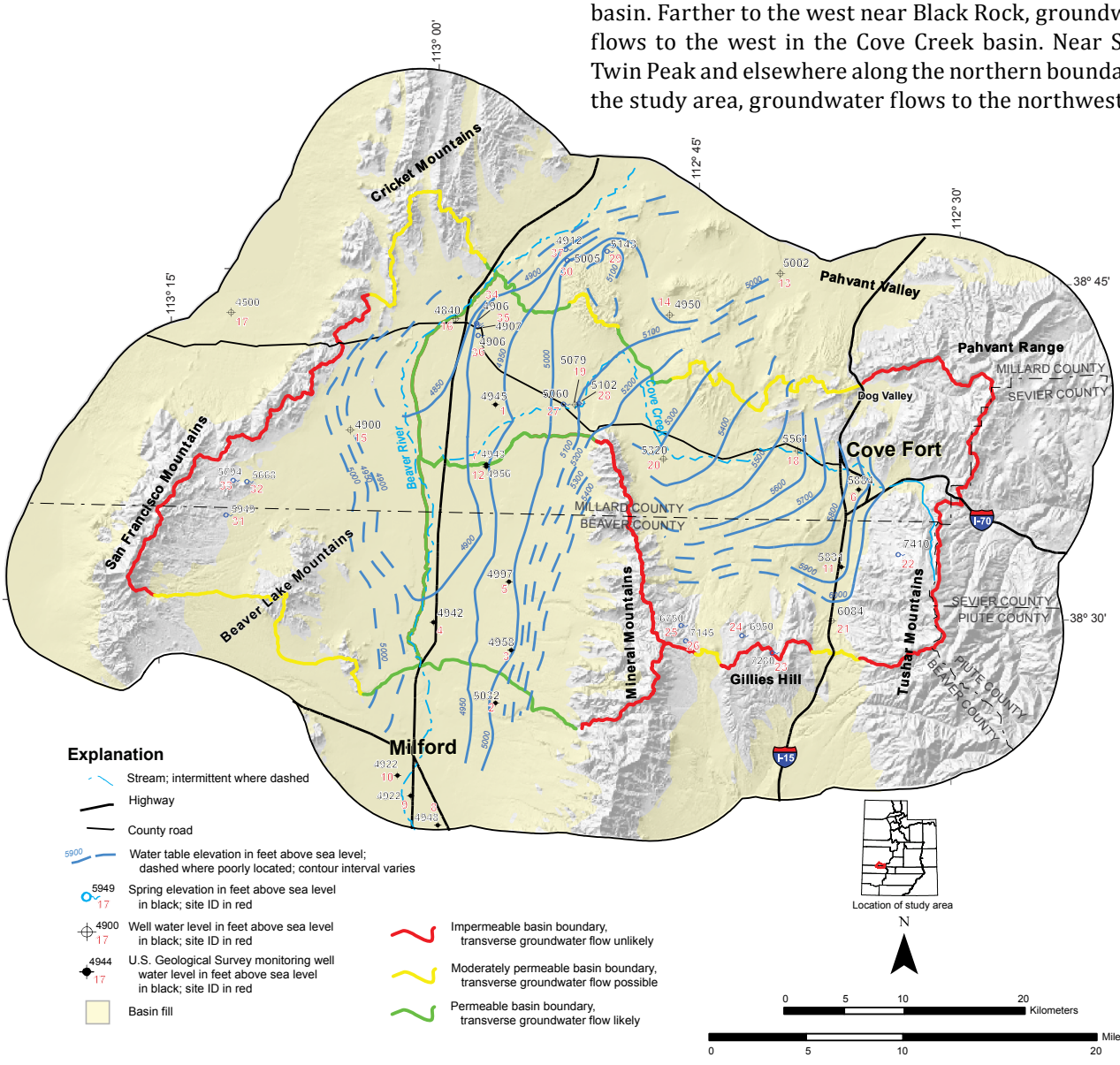

Figure 9. *Groundwater elevation in spring 2007 for the basin fill in the Cove Fort study area. Well and spring ID corresponds to data in table 1.*

Table 1. *Water-level sites used to construct potentiometric surface on figure 9.*

ID	East[1]	North	Water Elevation[2]	Date	Description[3]
1	331409	4280084	4945	03/26/07	USGS well 383912112561201
2	331398	4255381	5032	03/26/07	USGS well 382551112555101
3	332702	4259764	4958	03/26/07	USGS well 382814112550101
4	326254	4262060	4942	03/22/07	USGS well 382924112592901
5	332505	4265412	4997	03/26/07	USGS well 383117112551401
6	361441	4273031	5884	03/14/07	USGS well 383555112354802
7	330627	4275135	4943	03/26/07	USGS well 383631112564001
8	326620	4245275	4948	03/22/07	USGS well 382020112585901
9	324390	4247729	4922	03/22/07	USGS well 382138113003303
10	323285	4249387	4922	03/22/07	USGS well 382231113012001
11	359999	4266643	5831	03/14/07	USGS well 383214112362001
12	330623	4274950	4956	03/26/07	USGS well 383625112564003
13	354970	4290929	5002	03/12/07	well
14	345813	4287499	4950	03/12/07	well
15	319377	4277994	4900	03/14/07	well
16	328087	4287183	4840	03/14/07	well
17	309518	4287715	4500	03/15/07	well
18	356410	4276272	5561	03/16/07	well
19	338312	4280088	5079	03/12/07	well
20	345298	4275602	5320	03/15/07	well
21	359205	4262192	6084+	03/12/07	well
22	364908	4267673	7410	03/15/07	spring/seep
23	354495	4259567	7280	03/15/07	spring/seep
24	351976	4260970	6950	03/15/07	spring/seep
25	346935	4261823	6750	03/16/07	spring/seep
26	347314	4260539	7145	03/16/07	spring/seep
27	337205	4280122	5060	03/16/07	spring/seep
28	338486	4280172	5102	03/16/07	spring/seep
29	340830	4292779	5143	03/16/07	spring/seep
30	337526	4292043	5005	03/15/07	spring/seep
31	309303	4270949	5949	03/13/07	spring/seep
32	311014	4273741	5668	03/13/07	spring/seep
33	309880	4273839	5794	03/13/07	spring/seep
34	330013	4286823	4906	03/14/07	spring/seep
35	330080	4286642	4907	03/15/07	spring/seep
36	330151	4285815	4906	03/15/07	spring/seep
37	337383	4292926	4912	03/16/07	spring/seep

[1]Easting, northing coordinates are in NAD 27 UTM zone 12 N
[2]Feet above sea level
[3]USGS number corresponds to the NWIS database at http://waterdata.usgs.gov

Pahvant Valley. Along the Beaver River drainage south of Black Rock, groundwater elevations vary by only tens of feet (several meters). These areas coincide with areas of shallow groundwater and phreatophyte communities discussed in subsequent sections of this report. Water elevation at Well 4 on figure 9 indicates a saddle south of which groundwater flows towards Milford and north of which groundwater moves toward Black Rock and Pahvant Valley. Groundwater flows westward toward the Beaver River from the Mineral Mountains and eastward from the San Francisco Mountains.

Near Sevier Lake, groundwater elevations are several hundred feet lower than along the Beaver River near Black Rock. Previous work by Mason (1998), based on groundwater levels near Sevier Lake and several wells east of the northernmost San Francisco Mountains, suggested groundwater west of Black Rock moves west beneath portions of the northernmost San Francisco Mountains toward Wah Wah Valley and Sevier Lake. However, I found no evidence for westward groundwater movement, based on extensive field checking of well sites presented by Mason (1998), along the eastern flank of the northern San Francisco Mountains. I have instead inferred eastward groundwater flow in this area because of a lack of direct observation of decreasing groundwater elevation east to west across the Beaver River valley south of Black Rock, and the presence of low-permeability rocks along the western boundary of the study area in this area.

Figure 10 shows a detailed depiction of groundwater

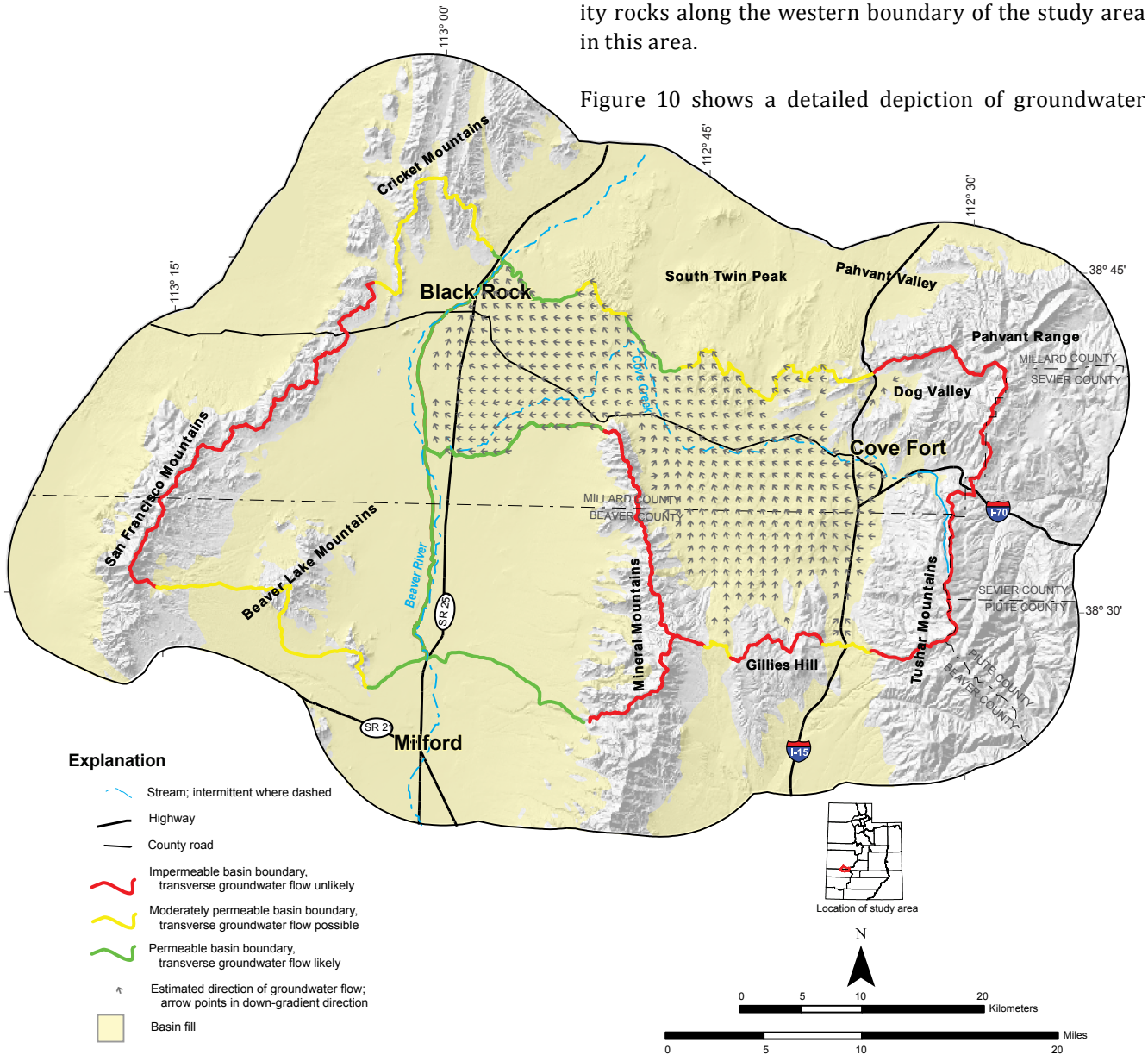

Figure 10. *Estimated direction of groundwater flow in spring 2007 for the basin-fill aquifer in the Cove Creek basin. Flow direction is based on the potentiometric surface shown on figure 9. Flow direction was calculated using ArcGIS and represents only the direction of the potentiometric slope at various points. Flow direction was not estimated for the remainder of the study area because of the relative lack of water-level data and potential for error. See text for further explanation.*

flow in basin fill of the Cove Creek basin. Direction of groundwater flow was calculated from potentiometric surface using the ArcGIS groundwater toolset. This toolset calculates flow direction at discrete intervals across a continuous potentiometric surface. This is not a directly modeled solution and does not account for potential changes in lateral transmissivity or localized upward or downward groundwater gradients that may occur in the principal aquifer. Groundwater flow direction is not shown for the San Francisco or Mineral basins due to a lack of data. These derived flow directions provide a simplistic overview of groundwater flow between any two points within the basin fill of the Cove Creek basin. The flow directions indicates groundwater flow away from areas of high topography near Gillies Hill and the Mineral and Tushar Mountains, and then generally northwest toward the Black Rock area. Modeled flow directions in much of the northern part of the basin converge along the Cove Creek drainage northwest of the Mineral Mountains and groundwater may flow into Pahvant Valley. Along the Beaver River channel south of Black Rock, groundwater flow is to the north.

Depth to Groundwater

Depth to groundwater in the study area (figure 11) was determined by the difference between grids of groundwater elevation (based on measured water levels) and a 5-meter (16 ft) elevation dataset (Automated Geographic Reference Center [AGRC], 2007). Pixel size of the resulting raster is 200 meters (660 ft). Error in this estimate of depth to water is at least that associated with the water table surface (figure 9) from which it was derived, and

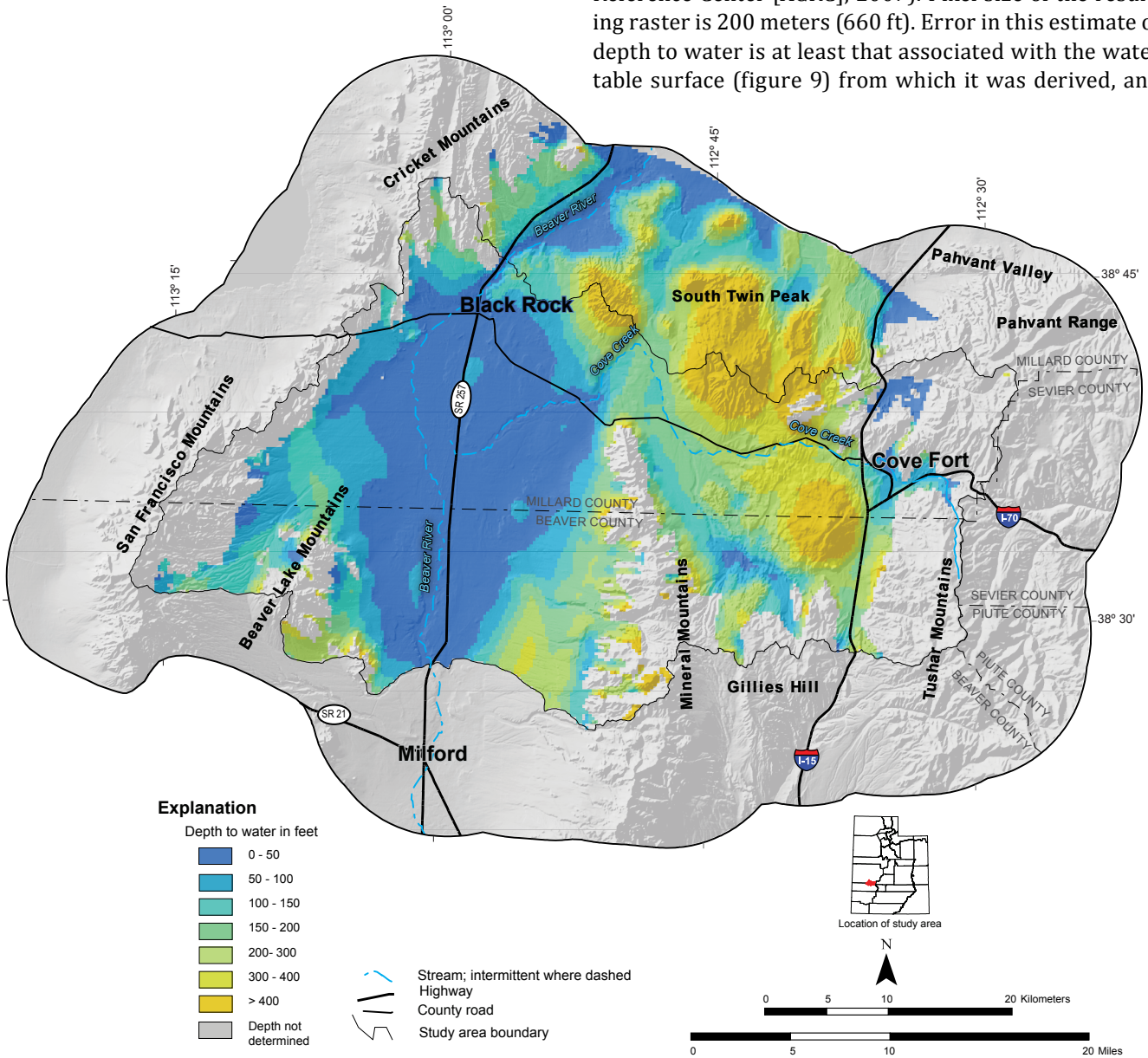

Figure 11. *Depth to water for the basin-fill aquifer in the study area and potentially hydrologically connected areas to the north, calculated as the difference between a 5-meter elevation dataset (AGRC, 2008) and the groundwater elevation derived from the potentiometric surface in figure 9. Along much of the Cove Creek drainage depth to water exceeds 100 feet (30 m). Potential error is significant and may be greater than 50 feet (15 m) in many areas.*

in some areas may be greater than 50 feet (15 m). This estimate of depth to water does not account for localized perched aquifers and error may be greatest in areas of significant topography within the basin-fill aquifer. Depth to water does not account for seasonal changes in water elevation and represents conditions in the spring of 2007. Despite the potential for significant error, the method provides a gross estimate of depth to water across the study area.

As shown on figure 11, depth to groundwater along much of the ephemeral portions of the lower Cove Creek channel is greater than 100 feet (30 m). Perennial flow along the Cove Creek channel is therefore unlikely without groundwater level increases of greater than 100 feet (30 m) along much of this channel. To the west along the Beaver River and the lower reaches of Cove Creek, groundwater is shallow, generally within 50 feet (15 m) of the land surface. The greatest calculated depth to water, greater than 400 feet (120 m), occur near areas of high topography in the basin-fill aquifer, such as near South Twin Peak.

Long-Term Groundwater Levels

Water levels from wells completed in the basin-fill aquifer have been periodically measured by the U.S. Geological Survey. Seven sites (sites 1 through 7 in table 1, locations shown on figure 9) with annual water-level data for at least the previous 20 years are examined in greater detail to evaluate changes in water level in the basin-fill aquifer. Two of the sites (sites 1 and 6) are located within the Cove Creek basin; site 1 is west of Antelope Springs and site 6 is near Cove Fort. Sites 3, 4, 5, and 7 are located between the Beaver River channel and the Mineral Mountains within the western Mineral basin. Site 2 is located just south of the study area and records water-level change northeast of Milford. Spatial distribution of the long-term monitoring wells with respect to the total area of the prinicipal aquifer is poor and water-level changes in these wells may therefore not reflect overall changes in storage in the principal aquifer. Instead, data presented here show local trends in groundwater level based on the available data.

Water-level data are presented as feet of change at a given site relative to the initial water-level measurement at that site (figure 12). Positive values therefore represent relative water-level rise and negative values represent relative water-level decline. Long-term groundwater levels measured by the U.S. Geological Survey (2007) have fluctuated with time. All sites show varying periods of increasing and decreasing water levels. Water levels at four of the seven monitoring sites (sites 1, 2, 3, and 7) show relatively little variation compared with the other sites and have a cumulative increase or decrease of less than 3 to 4 feet (1–1.2 m) across the period of record. The remaining three monitoring sites (sites 4, 5, and 6) show greater variability with cumulative water-level fluctuations greater than 5 feet (1.5 m) and year-to-year fluctuations of several feet or more. This high variability may result from a relatively high component of recent recharge from surficial runoff at these sites. In spring 2007 only site 5 had cumulative fluctuation greater than 5 feet (1.5 m). Site 1 is located in the western part of the Cove Creek basin and shows an increase in water level of less than 3 feet (1 m) across the period of record. Site 2, located just south of the study area north of Milford, shows a net decline of 4 feet (1.2 m).

Water-level data available for the study area show systematic, volumetrically limited and spatially isolated, change in storage in the principal aquifer. The actual spatial extent of water-level change is unconstrained because of limited well coverage, and the overall magnitude of these changes is minimal at most sites, less than 5 feet (1.5 m). Therefore, water-level change and change in storage in the principal aquifer are not considered in subsequent water-budget calculations.

Available Groundwater in Storage

The hydrologic framework data presented above is used to calculate a total volume of groundwater that could be withdrawn from the principal aquifer. Total available groundwater in storage is defined as the volume of groundwater potentially available for withdrawal from the principal aquifer. This estimate is limited to the active groundwater system in the Cove Creek basin above the elevation of the major springs at Black Rock. No estimates are presented for the remainder of the study area due either to a lack of data or probable reduced water quality in the case of the deeper part of the Cove Creek basin below the elevation of the Black Rock springs. Any annual withdrawal of groundwater in storage greater than the estimated annual recharge discussed in subsequent sections of this report will lead to permanent water-level declines and will reduce or eliminate discharge at major springs within the principal aquifer.

Total available groundwater in storage is the product of the saturated volume and the effective pore space. Saturated volume in the principal aquifer is the difference between the potentiometric surface shown on figure 9 and the basin depth model shown on figure 6. This volume is limited to elevations above the outflow of Black Rock Springs (4906 feet [1495 m]), yielding a saturated volume of 42.7 million acre-feet (52,700 hm^3). Error in the saturated volume estimate is assumed to be plus or minus 10 percent. Based on data for deposits similar to those that characterize the principal aquifer, effective porosity is assumed to be between 20 and 30 percent with a preferred value of 25 percent (Domenico and Schwartz, 1997). These variables yield between 7.7 and 14.2 million

acre-feet (9500–17,500 hm^3) of available groundwater in storage. Available groundwater in storage in the upper part of the principal aquifer in the Cove Creek basin based on preferred values of saturated volume and effective porosity is 10.7 million acre-feet (13,100 hm^3).

GROUNDWATER CHEMISTRY AND ISOTOPIC DATA

Introduction

Ground and surface waters have distinct chemical and isotopic characteristics that can be used to better understand groundwater flow and its relation to surface water and areas of groundwater recharge and discharge. For this study I collected water samples from 14 locations and combined analysis results with existing data from the National Water Information System database (U.S. Geological Survey, 2007) and reports that focused on the geothermal systems within the study area (Bowman and Rohrs, 1981; Vuataz and Goff, 1987). Sample sites from previous studies are primarily located in the San Francisco and Mineral basins, with the remainder located in the Cove Creek basin and at several locations beyond the study area boundary. Preexisting geochemical data include field parameters of pH and temperature and concentrations of dissolved anions (chloride, bicarbonate, sulfate) and cations (calcium, magnesium, sodium, potassium) with a charge balance of less than plus or minus 5 percent (Vautaz and Goff, 1987; U.S. Geological Survey, 2007) (table A.3). Additional stable isotopic data for a series of upland springs and other wells are taken from Bowman and Rohrs (1981) and compared with data gathered during this study. Data presented by Bowman and Rohrs (1981) used an older less accurate method for measurement of stable isotopic ratios but nonetheless

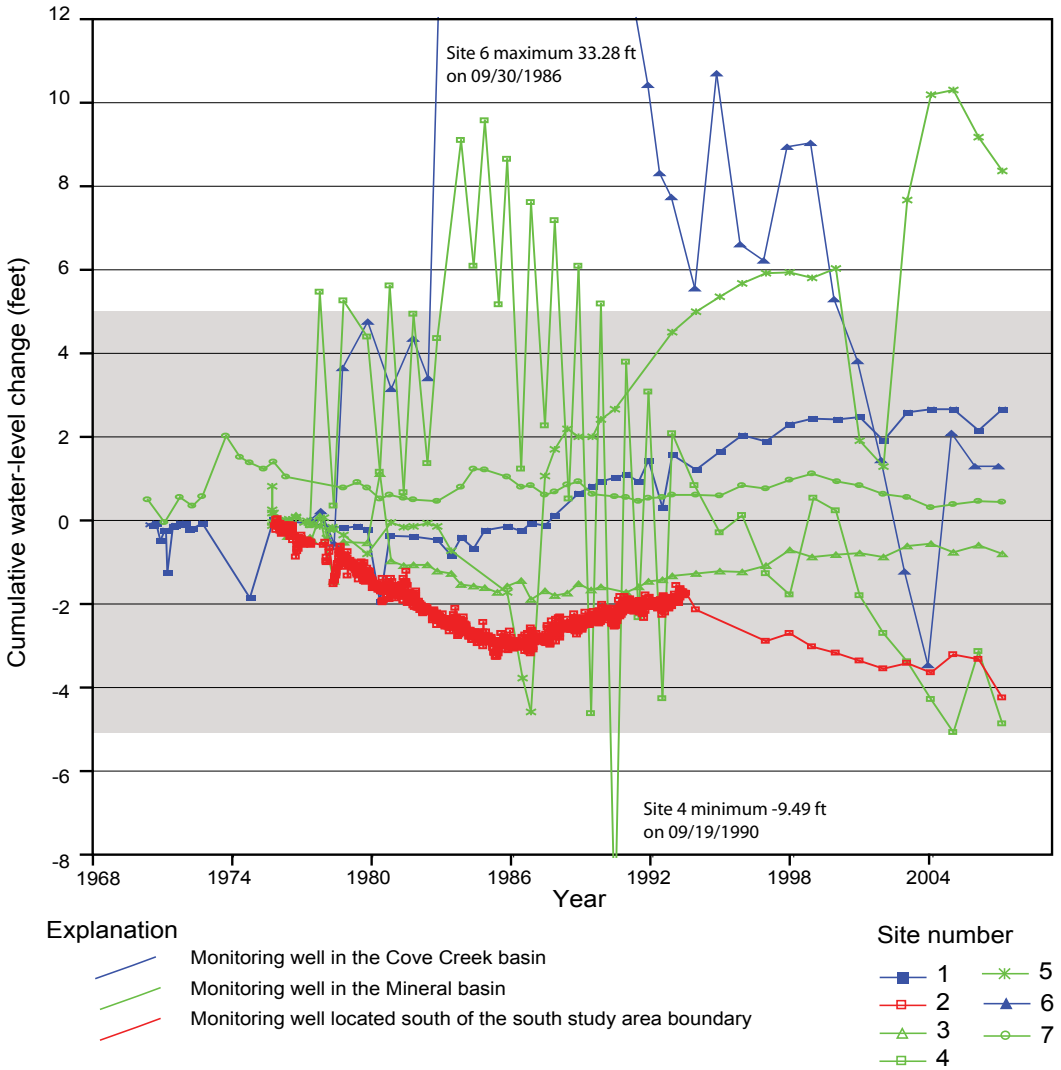

Figure 12. *Long-term water-level change for seven wells in the principal aquifer. Six of the seven sites have cumulative water-level change of less than 5 feet (2 m) as of 2007. Well ID corresponds with those in table 1 and figure 9. Data are from the U.S. Geological Survey (2007) National Water Information Database.*

provide important qualitative comparisons with data collected during this study.

New groundwater sampling focused on the Cove Creek basin and included several springs and wells just north of the Cove Creek basin. Sample sites were chosen based on access and relevance to potential interbasin flow from the Cove Creek basin. Sample collection followed techniques presented by Wilde and others (1998). All 14 samples collected for this study were analyzed for major solute chemistry and stable isotopes. Concentrations of major dissolved anions and cations were determined at the Brigham Young University Hydrogeology Laboratory using standard techniques presented in Fishman and Friedman (1989) and Fishman (1993). These data are presented in table A.3. Isotopic data for these sites is presented in table 2. Eight of the 14 new samples were analyzed for carbon isotopes and 11 samples were analyzed for tritium concentration. The geochemical data and discussion presented below are limited to summary data of the most relevant features and those that may best aid in understanding the basin-fill groundwater system.

Most sample sites, new and compiled, are from the wells or springs that are part of the large basin-fill aquifer. Sampled wells are commonly completed in the upper 300 feet (100 m) of the basin-fill aquifer (U.S. Geological Survey, 2007). The data set also includes a series of upland springs that issue from bedrock (U.S. Geological Survey, 2007) (figure 13; table A.3). Most samples can be assumed to represent the shallow upper portion of the basin-fill aquifer or bedrock aquifers within 300 feet (100 m) of the land surface. All interpolated data presented below were created in ArcGIS using a natural neighbor interpolation and a 200-meter (600 ft) pixel size.

Groundwater Chemistry

A plot of Stiff diagrams for new and compiled sample data is presented on figure 13. The Stiff diagrams are divided into groups of chloride concentration less than 10 meq/L and those of 10 meq/L or greater. Most sites having chloride concentration of 10 meq/L and greater have water temperatures above 25°C (77°F) (Vuataz and Goff, 1987) (table A.3) and may contain a large component of water discharging from deep geothermal flow paths. Other potential sources of high chloride concentration may include evaporative enrichment in areas of significant evapotranspiration and dissolution of salts from units that make up the basin-fill aquifer. The chemical composition of sites having chloride concentration less than 10 meq/L is more complex and indicates patterns that are likely the result of local aquifer characteristics and circulation patterns.

Groundwater type ranges from calcium or sodium-bicarbonate type, typical of upland portions of the study area, to sodium-chloride type more commonly associated with low-elevation thermal waters and areas of discharge (table A.3; figures13 and 14) (Vuataz and Goff, 1987). Most groundwater sampled in the Cove Creek basin is dominated by calcium and bicarbonate ions, and there is little apparent difference in chemical composi-

Table 2. *Summary of stable and radiogenic isotope results for sampling sites in the Cove Fort area collected during this study. Dashed entries represent no data.*

Site ID	Site name	Sample type	δ^2H[1]	$\delta^{18}O$[2]	Recharge elevation[3]	Tritium[4]	$\delta^{13}C$[5]	pmc[6]
1	South Twin well	well	-121.2	-16.37	6600	0.7±0.4	-8.14	33.4±0.5
2	Cedars of Lebanon well	well	-127.5	-16.74	7320	0.9±0.3	-5.94	2±0.3
3	Black Spring	spring	-119.5	-21.35	--	0.2±0.3	--	--
4	Kaufman spring	spring	-118.1	-15.76	6250	0.5±0.3	-8.71	54.0±0.2
5	Kaufman windmill	well	-116.2	-15.69	6030	0.6±0.4	-9.69	54.9±0.2
6	Upper Coyote spring	spring	-117.8	-15.6	6210	0.7±0.4	-7.96	50.7±0.2
7	Lower Coyote spring	spring	-117.1	-16.43	--	0.8±0.3	--	--
8	Black Rock well	well	-114.7	-15.38	5860	0.3±0.3	-10.94	54.1±0.7
9	Antelope Spring	spring	-116.9	-15.67	6110	--	--	--
10	Cove Fort well 1	well	-117.4	-15.09	6170	0.8±0.3	-10.85	83.0±0.3
11	Yardley well	well	-117.3	-14.89	6160	7.1±0.5	-11.38	111.5±0.4
12	Fourmile spring	spring	-115.3	-16.93	--	--	--	--
13	Twin Peaks Spring	spring	-121.9	-15.69	6340	0.2±0.4	--	--
14	Cove Creek	creek	-117.5	-15.75	--	--	--	--

[1]Error for all samples is ±1.0; [2]Error for all samples is ±0.20; [3]Mean recharge elevation in feet; see text for discussion of methods; [4]Units are tritium units; [5]$\delta^{13}C_{(PDB)}$ values were calculated using standard methods described by Coplen (1996); [6]pmc is percent modern carbon.

tion between sites 10, 11, and down-gradient sites 5, 9, and 4. Elsewhere, geochemical patterns based on the Stiff diagrams are more complex. Groundwater with high chloride concentration occurs near the Roosevelt Hot Springs KGRA, west of the Mineral Mountains (sites 20, 23, 37, 39, 40), and several sites (8, 13, and 34) to the north (figure 13). High chloride concentration near Roosevelt Hot Springs likely results from flow from underlying geothermal aquifers into shallow parts of the basin-fill aquifer. Discharge of deep-seated geothermal waters may also occur over isolated areas corresponding with the remaining high-chloride samples to the north.

Sample sites are further grouped by geography and sample set in a trilinear (Piper) diagram to better delineate chemical relations (figure 14). Samples collected during this study generally lie along a trend of increasing relative concentrations of chloride, sodium, and potassium between end-member waters of sodium-chloride and calcium-bicarbonate type. Groundwater samples from the San Francisco basin show a contrasting trend of increasing magnesium and sulfate. The total spread of solute compositions across the remainder of the data set is large and many of the geographic and sample set fields overlap. Geochemical overlap among the geographic locations likely results from equilibration with similar aquifer materials for sites that may not be directly upgradient or downgradient of one another.

Total dissolved solids (TDS) concentration calculated from new and compiled solute data ranges from 58 to 8100 mg/L (figure 15). Across much of the study area TDS concentration is between 200 and 2000 mg/L, with an average value of 600 mg/L. Large parts of the shallow aquifer in the Cove Creek basin have TDS values of less than 1000 mg/L. Based on TDS, groundwater in the Cove

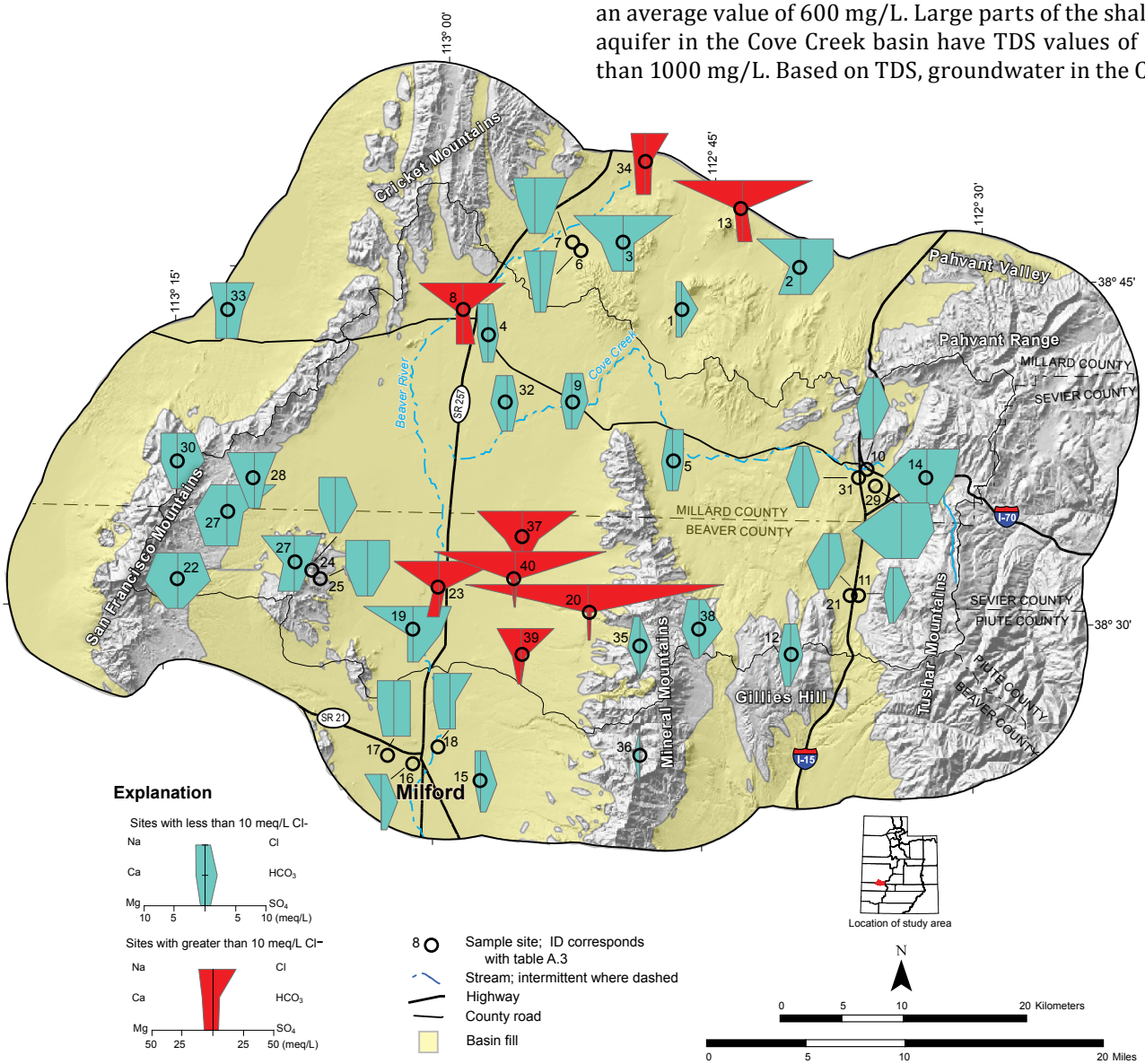

Figure 13. *Stiff diagrams for groundwater in the study area. Sites are divided into two groups based on chloride concentration. Sample numbers correspond with those in table A.3. Sample sites 1 through 14 were collected during this study; other sites are compiled from previous work. See text for further discussion.*

Creek basin is of relative high quality when compared to other parts of the study area. Higher TDS values are apparent in the Mineral and San Francisco basins and at sites north of the study area. The highest TDS values correspond to geothermal waters having temperatures above 25°C (77°F), whereas low TDS is commonly associated with temperatures below 25°C (77°F) (figures 15 and 16; table A.3).

Groundwater Temperature

Water temperature can provide important basic information about groundwater flow paths, aquifer characteristics, and crustal heat flow (Domenico and Schwartz, 1997; Anderson, 2005). Groundwater temperature during recharge is generally considered equal to the local average annual temperature. Following recharge groundwater temperature generally increases, depending on crustal heat flow and residence time, in the principal aquifer. Consequently, temperature may be an important indicator of depth of groundwater circulation and heat flux; i.e., higher temperatures may be assumed to result from groundwater with deeper flow paths and/or areas with higher heat flux. Cooler temperatures result from near-surface shallow flow paths, recent recharge, and/or areas of low background heat flux (Domenico and Schwartz, 1997; Anderson, 2005).

Water temperature measured in shallow wells and springs varies significantly across the study area (figure 16; table A.3). Within the study area two known commercial high-temperature geothermal reservoirs exist at the Cove Fort and Roosevelt KGRAs. Temperatures sufficient for geothermal power generation are commonly associated with groundwater at considerable depths (Mabey and Budding, 1987), significantly deeper than most wells

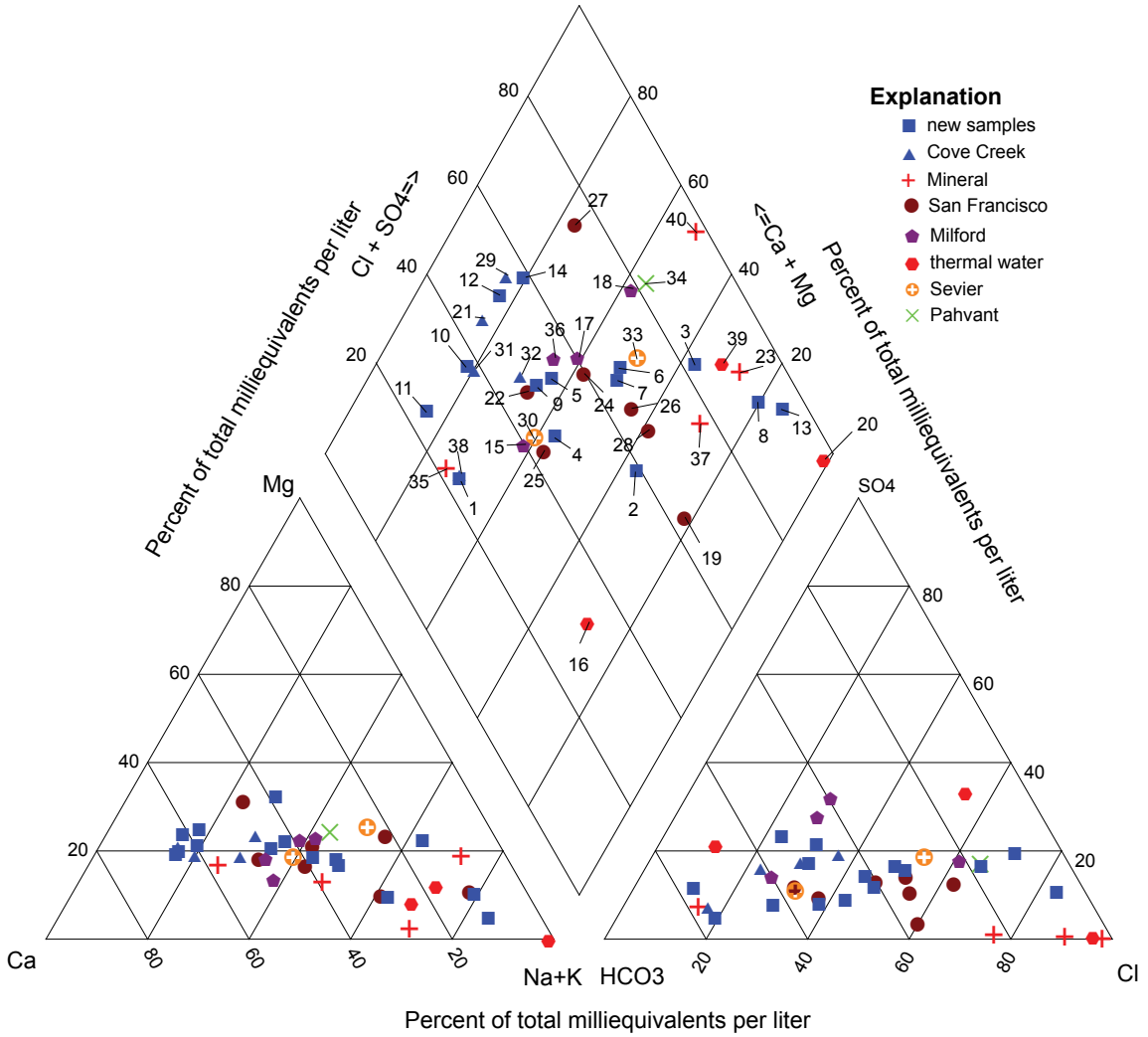

Figure 14. *Trilinear Piper diagram of groundwater samples for the Cove Fort area. Sample groupings include new samples collected during this study and a range of preexisting samples from various geographic areas. Cove Creek, Mineral, and San Francisco sample sites are located within their respective basins. Milford sample sites are located south of the study area. Pahvant sample sites are located north of the study area, and Sevier sample sites are located west of the study area. Thermal water sites are those with measured temperatures greater than 25°C. Sample locations and data are presented on figure 13 and in table A.3.*

examined in this study. High groundwater temperatures in the shallow aquifers near these areas likely result from discharge and heat flow from deeper geothermal systems. Elsewhere, shallow groundwater temperatures are lower, generally less than 20°C (68°F). Across much of the Cove Creek basin, groundwater temperatures in the uppermost part of the principal aquifer are less than 20°C (68°F), with notably cool groundwater in areas of likely recharge near sites 10 and 11 and to the west in areas of likely groundwater discharge at sites 4 and 8 (figure 16). Water temperature also is strongly correlated with water quality (TDS; figure 15) and is therefore a useful indicator of water quality.

Stable Isotopes

Sources of recharge to an aquifer may be determined by analyzing the composition of stable isotopes of oxygen and hydrogen in groundwater. Measured isotopic ratios of oxygen (^{16}O and ^{18}O) and hydrogen (^{1}H and ^{2}H) in precipitation vary systematically with topography, temperature, and distance from the ocean (Craig, 1961; Dansgard, 1964; Clark and Fritz, 1997; Bowen and Revenaugh, 2003). Isotopic ratios in near-surface water may be altered by evaporation following precipitation, but after recharge generally remain unchanged in groundwater if no mixing occurs and therefore record the isotopic signature of meteoric or surface waters at the time of recharge (Clark and Fritz, 1997).

Water samples collected during this study (tables 2 and A.3) were analyzed for the stable-isotopic ratios

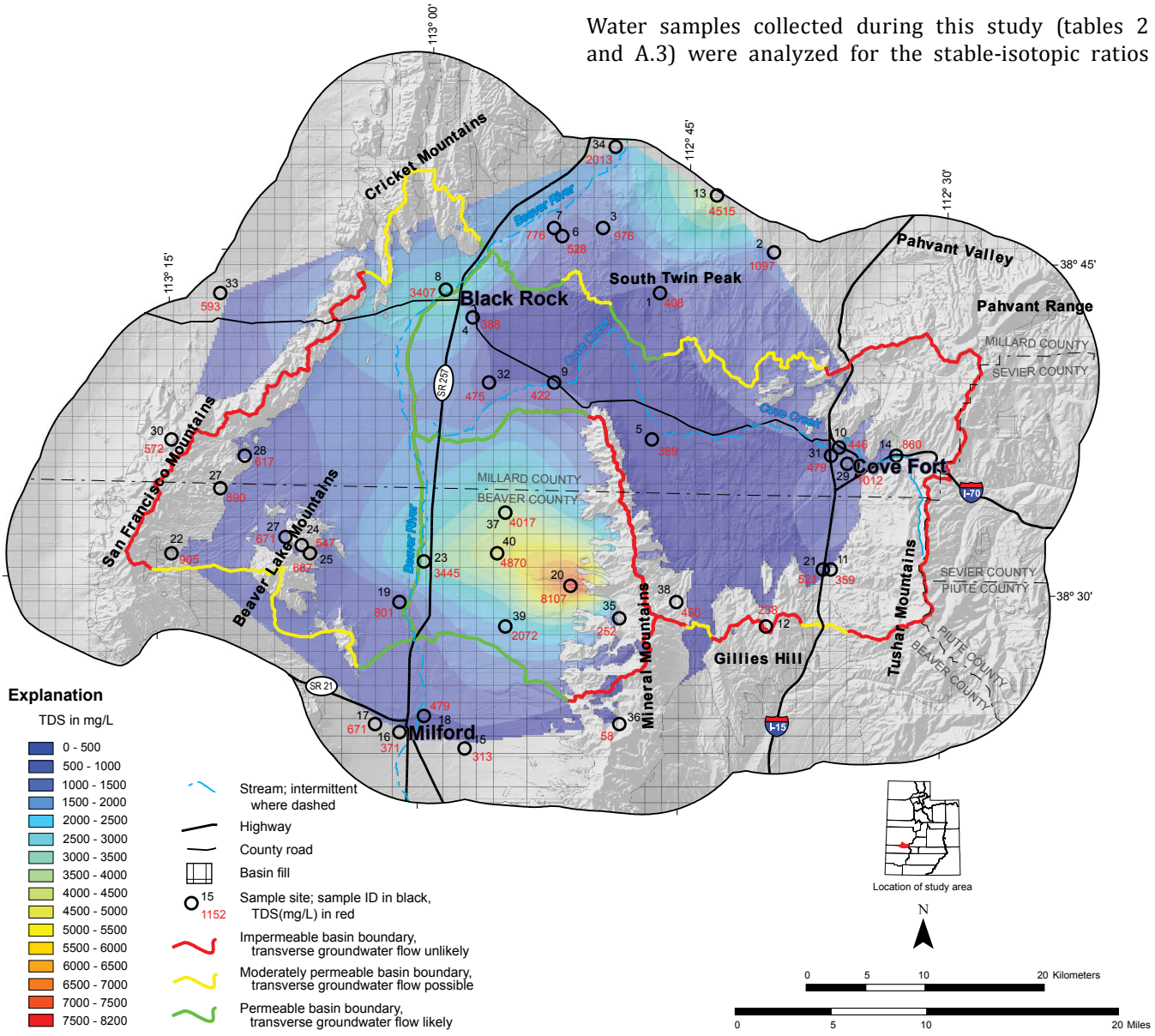

Figure 15. *Total dissolved solids (TDS) concentration for groundwater in the study area. TDS is less than 500 mg/L across much of the Cove Creek basin. High TDS values exist in the Mineral basin near the Roosevelt Hot Springs KGRA. Sample numbers correspond with those in table A.3. Samples 1 through 14 were collected for this study, other sites are compiled from previous work. See text for further discussion.*

of hydrogen (δD) and oxygen ($\delta^{18}O$). The stable-isotope ratios were measured at the Brigham Young University Hydrogeology Laboratory with a Finnigan Delta^{plus} isotope ratio mass spectrometer, and were normalized to the VSMOW/SLAP scale following the procedures of Coplen (1996) and Nelson (2000).

Isotopic ratios of hydrogen ($^{2}H/^{1}H$) and oxygen ($^{18}O/^{16}O$) are reported as delta (δ) values in units of parts per thousand (per mil, or ‰) relative to a reference standard (Standard Mean Ocean Water) (Craig, 1961) via the following equation:

$$\delta x = \left(\frac{Rsample}{Rstandard} - 1\right) \cdot 1000 \qquad (1)$$

where:

δx = delta ^{18}O or ^{2}H (‰)

Rsample = $^{18}O/^{16}O$ or $^{2}H/^{1}H$ in the sampled water

Rstandard = $^{18}O/^{16}O$ or $^{2}H/^{1}H$ in the reference standard

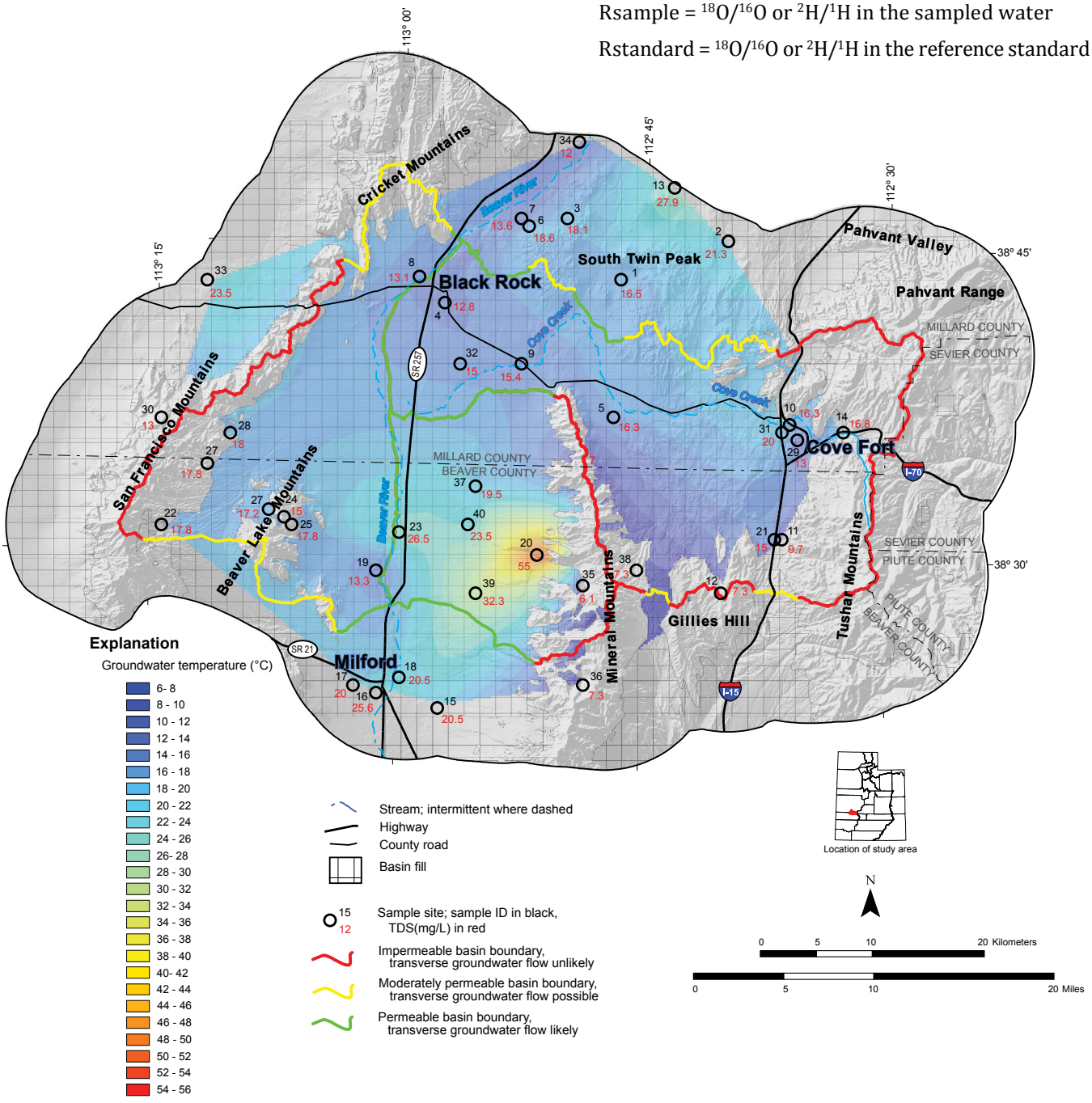

Figure 16. *Temperature for groundwater in the study area. All samples are assumed to represent temperature within the upper 300 feet (90 m) of the groundwater system. High temperature values exist in the Mineral basin near the Roosevelt Hot Springs KGRA. Lower temperatures near 15°C are typical of the Cove Creek basin. Sample numbers correspond with those in table A.3. Samples 1 through 14 were collected for this study, other sites are compiled from previous work. See text for further discussion.*

Figure 17 shows the new stable isotope data plotted along with preexisting data (Bowman and Rohrs, 1981) for areas near the study area. Most data plot below and roughly parallel to the global meteoric water line of Craig (1961). Similar trends are typical of arid areas where evaporation commonly occurs before or during recharge (Clark and Fritz, 1997). Much of the new sample data (sites 4, 6, 8, 9, 10, 11, and 14) plots within a compositional range similar to that of samples from the Tushar Mountain and Gillies Hill springs. Two sites, 5 and 8, plot within the compositional range of springs in the Mineral Mountains. The remaining sites (1, 2, 3, 7, 12, and 13) plot beyond the range of preexisting data and may indicate distinct precipitation events and/or localized recharge not characterized by previous work on upland spring systems. Three sites (3, 7, and 12) plot well above the meteoric water line, possibly due to relatively depleted $\delta^{18}O$ values and/or enriched δD values. Relative depletion of $\delta^{18}O$ may result from fractionation in the saturated part of the aquifer due to mineral exchange or precipitation among oxygen-bearing mineral species at temperatures greater than 50°C (112°F) (Clark and Fritz, 1997). Enrichment of δD relative to $\delta^{18}O$ is more difficult to explain and may be the result of laboratory error. Because of this unconstrained isotopic shift, sites 3, 7, and 12 are excluded from subsequent calculations. All other sites are assumed to retain an isotopic composition indicative of the time of recharge and are examined in greater detail to estimate timing and location of recharge.

Comparison of the stable isotopic composition of groundwater with that of precipitation can yield detailed information concerning the spatial and temporal distribution of recharge (Clark and Fritz, 1997). However, no direct measurements of the stable isotopic composition of precipitation exist within the study area. Measured values for groundwater are instead compared with (1) modeled isotopic values for precipitation in the study area (Bowen and Revenaugh, 2003) to constrain the temporal distribution of recharge and (2) regional measured values for precipitation (Friedman and others, 2002) to constrain the spatial distribution of recharge.

Figure 18 shows the temporal relationship of sampled groundwater and modeled monthly deuterium values for precipitation in the study area. The range of modeled monthly deuterium values is divided into upland areas (above 6000 feet [1830 m]) and lowland areas (below 6000 feet [1830 m]). The measured deuterium values for all sites intersect the modeled curves of deuterium in precipitation between the months of November and March, implying that much of the groundwater sampled results from cool winter precipitation. Many samples may also consist of a mix of cool-season precipitation from both upland and lowland sources. Based on the data shown on figure 18, little evidence exists for significant recharge

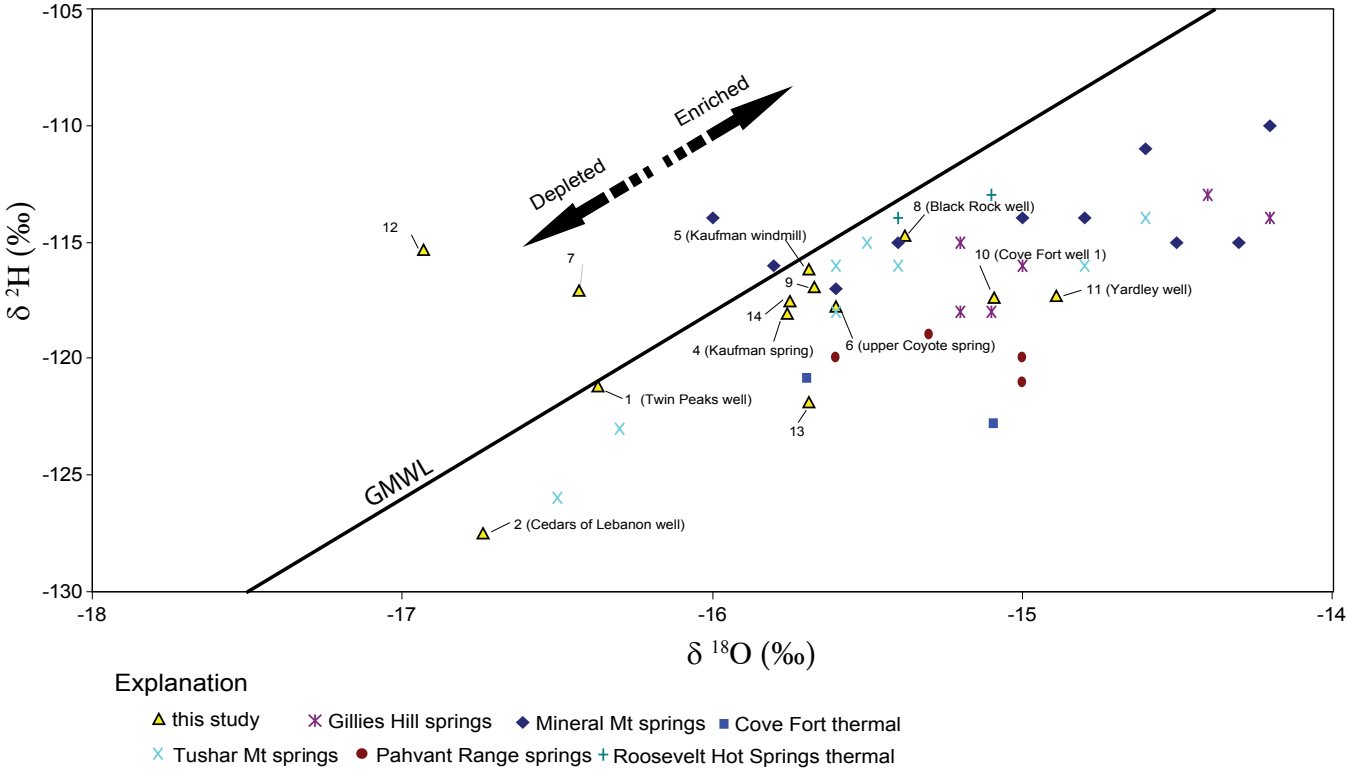

Figure 17. *Stable-isotopic composition of groundwater in the Cove Fort area. Site ID numbers correspond with those in table 2. Site 3 plots beyond the extent of this figure. All other data are compiled from Bowman and Rohrs (1981). Compiled data are grouped by geographic location; data from Roosevelt Hot Springs and Cove Fort are for wells, all other sites are springs. GMWL is the global meteoric water line of Craig (1961).*

from warm-season precipitation, and subsequent estimates of elevation of recharge are calculated only for cool-season precipitation.

Stable isotopes in groundwater may also be used to determine the elevation at which recharge occurs. The elevation of recharge of groundwater samples collected during this study was determined via a comparison with recent measurements of the stable isotopic composition of precipitation collected at sites of varying elevation in the Great Basin (Friedman and others, 2002, see their table 7). For this comparison the data of Friedman and others (2002) is used to calculate a simple linear equation, using a least squares regression that relates measured deuterium concentration in precipitation to elevation (table 2; figure 19). Assuming precipitation infiltrates near the elevation at which it falls, this equation may be used to calculate elevation of recharge for groundwater samples. This inherently simplified calculation assumes that changes in δD measured in groundwater is the result of a simple change in recharge elevation and does not consider potential changes in temperature of precipitation, evaporation, or other processes that may occur during recharge or residence in the principal aquifer. For this analysis it is also assumed that climate and stable isotopic patterns in precipitation have remained constant relative to recent measured conditions taken from Friedman and others (2002). Subsequent sections of this report show that most samples consist of groundwater likely recharged during the Holocene, in climatic conditions broadly similar to modern conditions. Only site 2, which may contain water recharged during the Pleistocene, was likely recharged during very different climatic conditions.

Elevation of recharge, from figure 19, is between 5900 and 7300 feet (1800–2230 m); most sites have an estimated elevation of recharge between 6000 and 7000 feet (1830–2130 m). Based on this methodology, most sites have elevations of recharge that correspond closely with the uppermost reaches of the principal aquifer in the Cove Creek basin, near sampling sites 10 or 11 (figure 20).

Tritium

Tritium-count data provide qualitative evidence for the presence of modern water recharged since 1950. Tritium concentrations greater than 2.0 Tritium Units (TU) indicate that a given sample consists of a significant fraction of water recharged since 1950. Tritium concentrations between 2.0 and 0.5 TU indicate at least a part of the sample consists of modern water recharged since the 1950s (Clark and Fritz, 1997). Tritium concentrations less than 0.5 TU likely represent water recharged prior

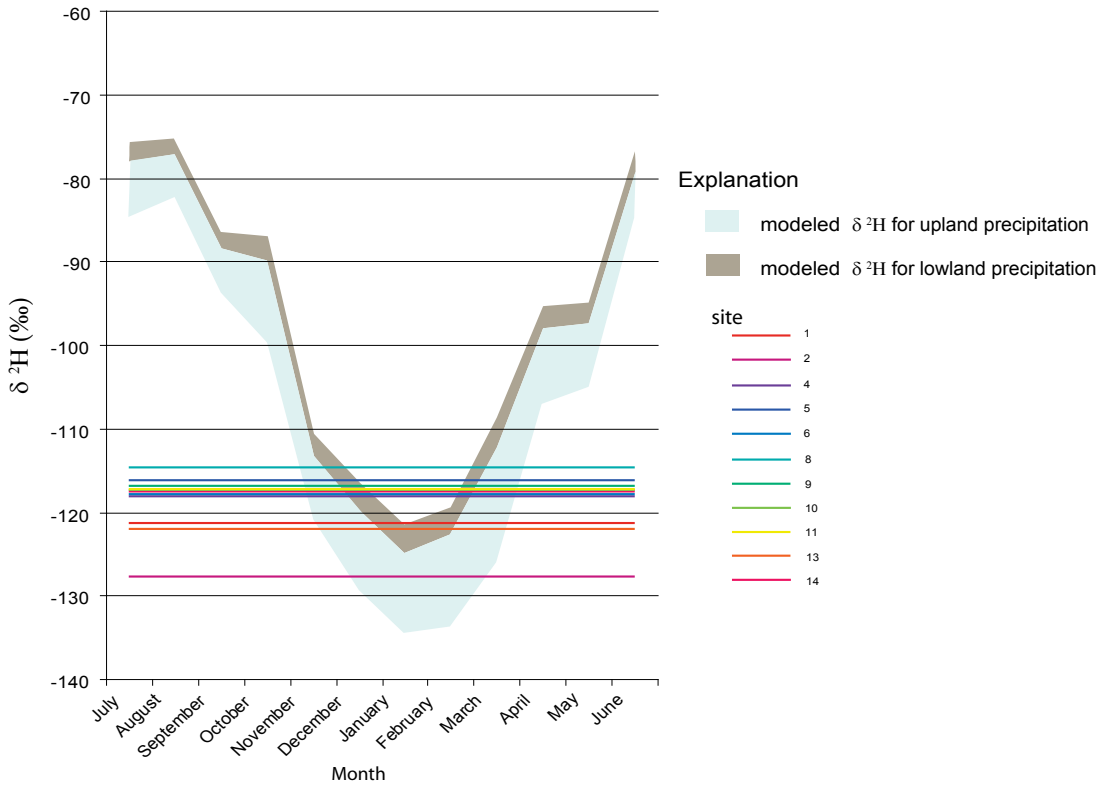

Figure 18. *Modeled monthly range of deuterium composition of precipitation (from Bowen and Revenaugh, 2003). Upland precipitation is broadly assumed to represent areas above 6000 feet (1830 m), whereas lowland precipitation applies to areas below 6000 feet (1830 m) elevation. Most sites may consist of mixtures of lowland and upland recharge. Site locations and data correspond with table 2 and figure 13. See text for details.*

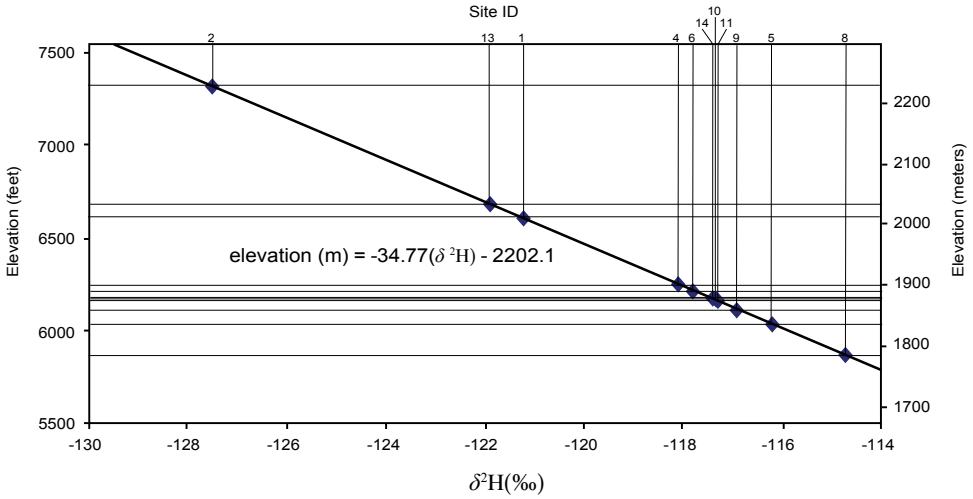

Figure 19. *Estimated elevation of recharge for selected samples based on δ^2H. Equation and regression line were calculated in this study based on the measured stable isotopic concentration of precipitation in the Great Basin from Friedman and others (2002). See text for details. Error in these elevation estimates is potentially significant because of the assumption of local isotopic concentration of precipitation and the potential for isotopic fractionation both during recharge and residence of groundwater in the principal aquifer. Most sites have mean elevations of recharge between 7000 feet (2130 m) and 6000 feet (1830 m).*

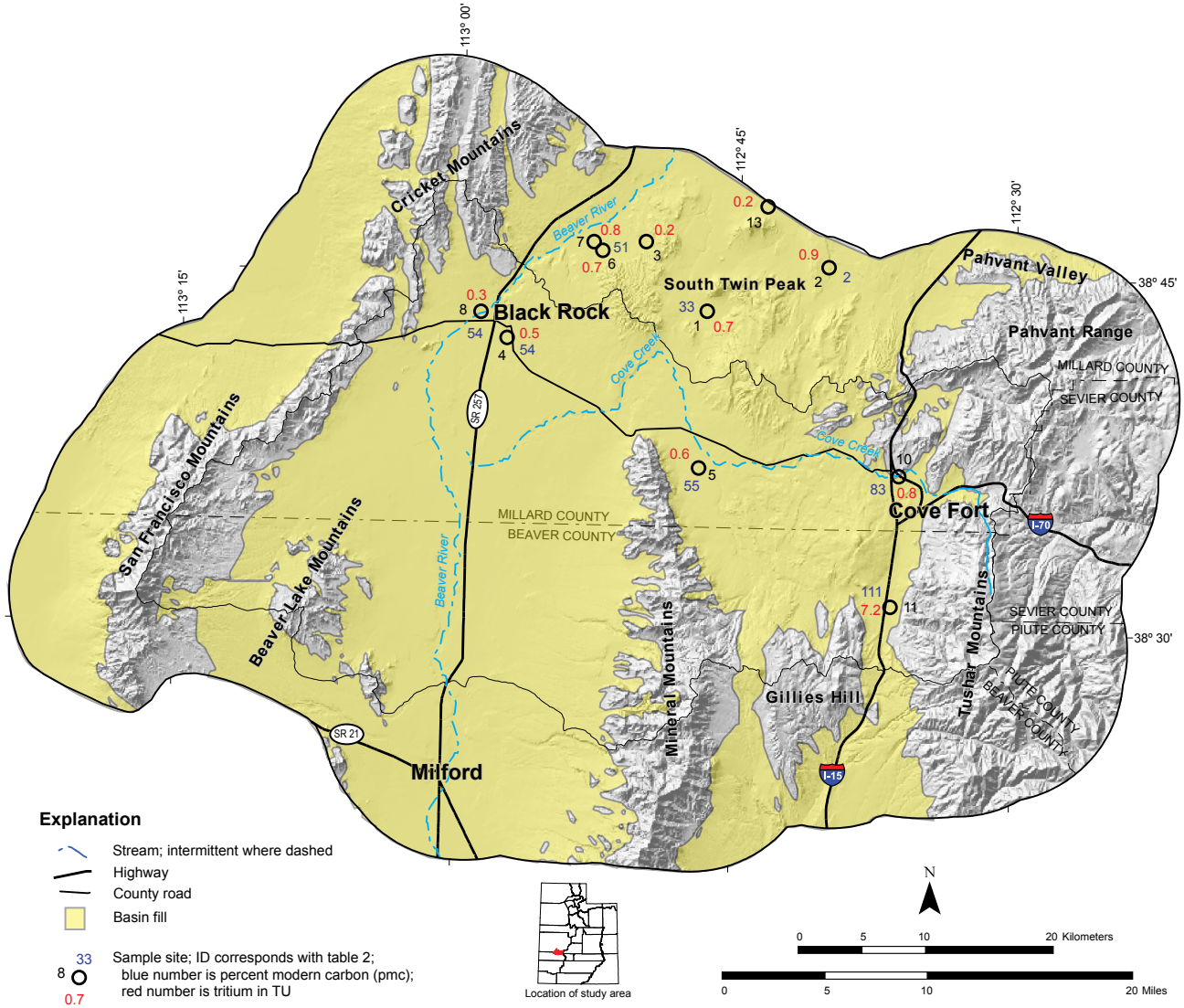

Figure 20. *Summary of new sampling for tritium and carbon isotopes in the study area. Sites 10 and 11 are up-gradient of all other sites and are indicative of recharge to the principal aquifer in the Cove Creek basin. Isotope data are presented in table 2. See text for further discussion.*

to 1950 (Alan Mayo, Brigham Young University, written communication, 2010).

Eleven of the samples collected during this study were analyzed for tritium concentration (figure 20). Tritium samples were distilled and electrolytically enriched to increase tritium concentration by a factor of at least 10. Analysis was done using a Perkin Elmer Quantulus 1220 ultra low-level liquid scintillation counter. Samples were evaluated against blanks and an NIST traceable standard (SRM 4361C) (David Tingey, Brigham Young University, written communication, 2008).

Only site 11 has a tritium concentration greater than 1 TU, all other sites have tritium concentrations between 0.9 and 0.2 TU (table 2). Error values for these measurements vary from 0.3 to 0.5 TU. For sites with tritium values less than 1 TU, the error represents a significant fraction of the measured values and only two sites have tritium concentrations greater than 0.5 TU when error is considered. Based on tritium concentration, the sample from site 11 consists primarily of water recharged since 1950. Other sites including 1, 2, 4, 5, 6, 7, and 10 may contain a small component of water recharged since 1950 but generally consist of older groundwater recharged prior to 1950. Sites 3, 8, and 13 have tritium concentrations less than 0.5 TU and therefore likely consist entirely of groundwater recharged before 1950.

Carbon Isotope Data

The isotopes of carbon dissolved in groundwater, ^{13}C and ^{14}C, provide quantitative information about residence time, recharge rates, flow paths, and the geochemical evolution of the aqueous and mineral phases of a groundwater system (Plummer and others, 1994; Clark and Fritz, 1997). The radiogenic isotope ^{14}C has a known half-life, and assuming geochemical sources and sinks for this isotope in the groundwater system allows estimation of residence time in the principal aquifer (Plummer and others, 1994) and the carbon isotopic fractionation and evolution in the aqueous system is recorded by the stable isotope ^{13}C (Clark and Fritz, 1997). Relatively enriched $\delta\ ^{13}C$ (higher values) corresponds with increased residence time and carbon mass transfer (Clark and Fritz, 1997). Relatively depleted $\delta\ ^{13}C$ (lower values) represents carbon isotope systems that are less evolved and have undergone less aquifer matrix and groundwater interaction (Plummer and others, 1994).

Carbon isotopes of ^{13}C and ^{14}C were analyzed for eight sites across the study area (table 2, figure 20). Samples were collected in polycarbonate bottles and sealed in the field with a minimum of headspace. All samples for carbon isotope analysis were processed to concentrate at the Brigham Young University Hydrogeology Laboratory. Five samples were analyzed at Brigham Young University using an ICP-MS machine. Three samples were shipped to the University of Georgia Center for Applied Isotope Studies and analyzed by accelerator mass spectrometry. Samples were analyzed for ^{13}C and ^{14}C using a National Electrostatics Corporation Model 1.5SDH-1 AMS. Values of $\delta\ ^{13}C$ were calculated relative to the Pee Dee Belemnite (PDB) standard using methods described by Coplen (1996). The concentration of the radiogenic isotope ^{14}C is expressed as percent modern carbon (pmc) by comparing measured ^{14}C activities against the activity of a National Bureau of Standards oxalic acid reference solution (David Tingey, Brigham Young University, written communication, 2008).

Percent modern carbon for the sample sites ranges from 2 to 111 percent (figure 20, table 2). Values of pmc greater than 60 (sites 10 and 11) generally reflect recent recharge, since or just before ~1950 (Clark and Fritz, 1997). Considering dissolution of carbonate minerals and cement with groundwater, pmc values as low as ~50 may be possible for recently recharged water (Alan Mayo, Brigham Young University, written communication, 2011). Based on these assumptions all sites except sites 1 and 2 contain at least some water recharged within the last several hundred years. Sites 1 and 2 consist of water that is substantially older and groundwater at these sites may have been recharged at least several thousand years ago. Well sites 10 and 11, located in the assumed recharge zone for the principal aquifer in the Cove Creek basin, have respective pmc values of 83 and 111 and likely consist primarily of groundwater recharged since 1950. Four sites (sites 4, 5, 6, and 8) have similar pmc values that range between 50 and 55. These four sites may be a mixture of young and much older groundwater as evidenced by their low tritium values and low pmc value relative to sites 10 and 11, or alternatively they may have recharged near or just prior to 1950.

A graph of $\delta\ ^{13}C$ versus pmc (figure 21) shows a simple correlation of lower pmc values (increased residence time) and enriched $\delta\ ^{13}C$ values (increased isotopic evolution). Values of $\delta\ ^{13}C$ range from -5.94 to -11.38 (table 2). Site 8 represents an outlier to this correlation with a lower pmc and a depleted $\delta\ ^{13}C$ value (figure 21). This may result from partial re-equilibration of low-pmc and enriched-$\delta\ ^{13}C$ groundwater with more modern (i.e., depleted) $\delta\ ^{13}C$ carbon isotopic content of the shallow aquifer or other isotopic fractionation reactions within the aquifer. Other sites, including 4, 5, and 6, have relatively high pmc values between 50 and 60 and may also represent older, low-pmc water that has partially re-equilibrated with near-surface conditions. Combined tritium and pmc data further support these qualitative age interpretations (figure 22). Only site 11 has both tritium greater than 2 TU and pmc greater than 60 that should be indicative of recent recharge. Site 10 has pmc greater than 60 but low tritium values indicative of groundwater recharged just over 50

years ago. The remaining sites all have pmc (less than 60 percent and tritium (less than 2 TU) indicative of older groundwater that has resided in the principal aquifer for more than several hundred years.

WATER BUDGET

Introduction

An annual water budget represents the balance of groundwater recharge and discharge plus or minus any change in storage in the principal aquifer (Freeze and Cherry, 1979). The principal sources of groundwater recharge are direct infiltration of precipitation or infiltration of surface water. Components of discharge include evapotranspiration, consumptive well withdrawals, springflow and seepage, and subsurface outflow.

Components of recharge and discharge are estimated separately for each of the three basins within the study area (see figure 2). No delineation of recharge and discharge is made based on aquifer type or hydrogeologic group; instead estimates are made for the groundwater system as a whole in each of the three basins. Because of

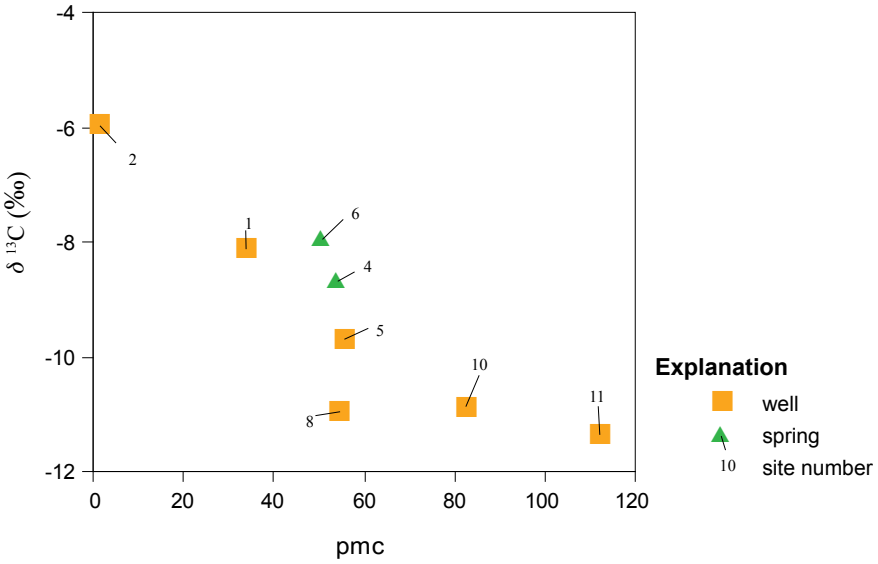

Figure 21. *Plot of percent modern carbon (pmc) versus $\delta^{13}C$ for sites in the Cove Fort area. See text for details. Lower pmc values correlate with higher $\delta^{13}C$ values (relatively enriched) and longer residence time in the principal aquifer. Sites 10 and 11 are considered indicative of groundwater in recharge zones of the prinicipal aquifer. Data are presented in table 2.*

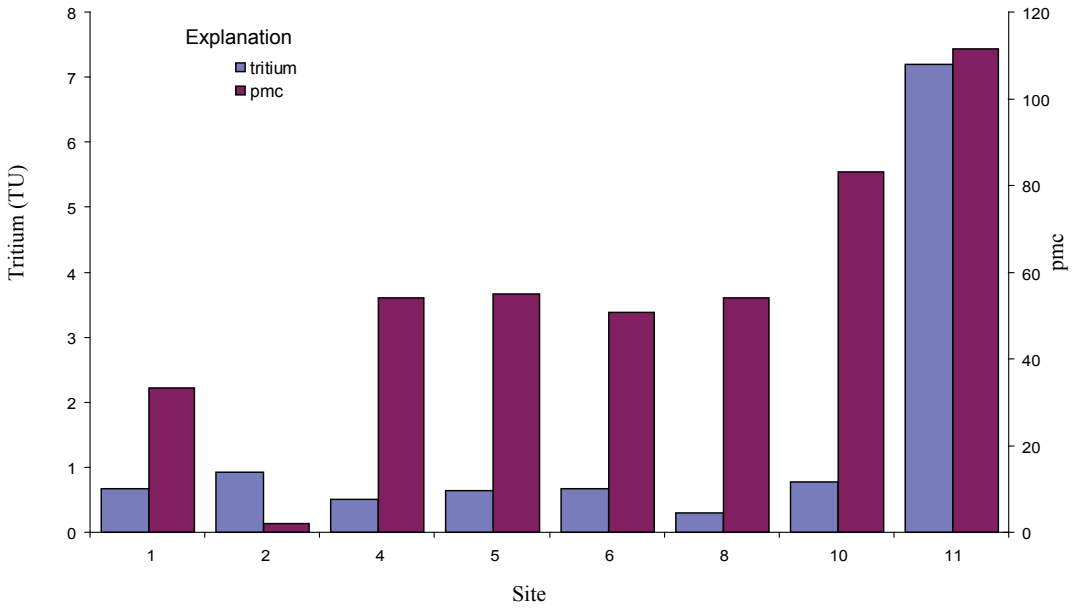

Figure 22. *Summary of tritium and percent modern carbon (pmc) data. Sites 10 and 11 are in upgradient portions of the principal aquifer where most recharge likely occurs. All other sites represent downgradient areas dominated by groundwater discharge. Data are presented in table 2.*

basin geometry and spatial extent of the principal aquifer, much of the groundwater can be assumed to reside in the basin-fill aquifer.

Change in storage represents water either stored in or removed from the principal aquifer on an annual basis and usually results in water-level changes in the principal aquifer (Freeze and Cherry, 1979). Measured long-term fluctuations in water level discussed in previous sections and shown on figure 12 are relatively small, generally less than plus or minus 5 feet (2 m) and spatially isolated. Most of the study area lacks relevant long-term water-level measurements. Therefore, the water balance in the principal aquifer may be assumed to be temporally static and no measure of relative change in storage at the basin scale is presented in subsequent sections of this report. Large-scale reduction in storage has been documented in the upper basin-fill aquifer near Milford (Mason, 1998). This reduction in storage may affect a part of the basin-fill aquifer south of Black Rock near Milford but is not considered in subsequent water-budget calculations.

Recharge

Introduction

Groundwater recharge may occur from direct infiltration of precipitation or surface water, or may result from subsurface inflow (Freeze and Cherry, 1979). Subsurface inflow of groundwater into the study area is unlikely because of a combination of relatively impermeable rock units (figure 3) and a potentiometric surface (figure 9) that generally slopes away from areas of contiguous permeable units that straddle basin boundaries. Therefore, all recharge to the principal aquifer likely occurs either from direct infiltration of precipitation or surface water.

Infiltration of surface water along perennial streams draining the Tushar Mountains may provide significant recharge to the principal aquifer in the eastern part of the study area. To the west, recharge of surface water historically occurred along the perennial Beaver River channel prior to construction of the Minersville dam and a series of irrigation canals south of the study area near Milford in the early 1900s (Mower and Cordova, 1974; Mason, 1998). Currently water flows in the lower Beaver River channel only in rare years of high precipitation (most recently, two years in the 1980s) and little if any recharge occurs along its course (Mason, 1998; U.S. Geological Survey, 2007). Stream courses in the remainder of the study area are ephemeral and may contribute recharge only during brief runoff events (Mower and Cordova, 1974). Away from the few perennial stream courses in the study area, nearly all recharge to the principal aquifer occurs as direct infiltration of precipitation. However, subsequent estimates of recharge do not constrain the relative contributions of infiltration of precipitation or infiltration of surface water to total recharge in the principal aquifer.

Many factors, including soil and rock characteristics, climate, vegetation, and depth to the water table control the amount and rate of recharge in semiarid environments (Scanlon and others, 2002, 2006). Among these variables, precipitation likely asserts the greatest control over the total amount of recharge (Scanlon and others, 2006). Basin-scale recharge may be estimated by a variety of techniques that most commonly include empirical estimates based on precipitation, numerical groundwater modeling, and various methods that indirectly quantify recharge at various scales (Scanlon and others, 2006). This study presents two types of estimates of recharge to the principal aquifer: (1) simple empirical estimate, and (2) a more robust indirect estimate based on spring flow and various known hydrogeologic characteristics of the principal aquifer.

Empirical Estimates of Recharge

Recharge in the study area is first estimated using modeled annual precipitation data (PRISM Climate Group [PRISM], 2006) for the study area and a simple approximation of the empirical methodology first presented by Maxey and Eakin (1949). The Maxey-Eakin methodology has been widely applied in the Basin and Range Province and may be considered a baseline estimate for comparison with other estimates of recharge (Avon and Durbin, 1994; Scanlon and others, 2006). This method uses assumed recharge rate coefficients, determined by trial-and-error balancing of recharge with assumed discharge for basins in central Nevada. The original Maxey-Eakin recharge rate coefficients vary stepwise for varying annual rates of precipitation (Maxey and Eakin, 1949; Eakin and others, 1951). These recharge rates were then applied to a unique spatially integrated precipitation data set, the Hardman map, to yield recharge amounts (Maxey and Eakin, 1949; Eakin and others, 1951). More recent precipitation data, such as the PRISM (2006) data, show much greater precipitation amounts than the original Hardman map over comparable areas. This precipitation discrepancy may therefore result in overestimation of recharge when the original Maxey-Eakin recharge coefficients are applied to the PRISM data (Scanlon and others, 2006). A limited curve approximation to the Maxey-Eakin method, presented below, may reduce the potential error produced by applying the Maxey-Eakin method to the PRISM (2006) precipitation.

This study uses a limited best-fit exponential regression of the original Maxey-Eakin step function. The resulting curve was limited to 25 percent recharge for all areas of precipitation greater than 20 inches (51 cm) per year, and no recharge for all areas of precipitation less than

3 inches (8 cm) per year. The calculated exponential regression for recharge rate is applied to recent modeled average annual precipitation data (PRISM, 2006) to yield estimates of annual recharge from precipitation (table 3). Estimated recharge for the Cove Creek, Mineral, and San Francisco basins is 29,200, 8800, and 5700 acre-feet (36, 11, and 7 hm^3) per year, respectively, and the total estimated recharge from precipitation for the entire study area is 43,700 acre-feet (54 hm^3) per year.

Quantitative Estimates of Recharge

Simple equations of fluid flow may be used to directly calculate unknown aquifer parameters including recharge rates and physical aquifer characteristics (Manga, 2001). Using measured parameters from large springs, including temperature and discharge, it is possible to constrain recharge rate and other parameters of groundwater flow in the principal aquifer in the Cove Creek basin.

Conservation of (water) mass places the most basic constraint on groundwater flow (Domenico and Schwartz, 1997) and yields a simple equation for discharge dependent on recharge rate and the area over which recharge occurs (Manga, 1997, 1998, 2001; James and others, 2000):

$$D = R \times A \quad (2)$$

where:

D = discharge (measured at springs)

R = recharge rate

A = area of recharge

Solving the equation for recharge rate and comparing a range of possible values for the area of recharge yields a range of recharge rates that are permissible based on the existing data and directly applicable to the study area. Permissible estimates of the area of recharge for the Black Rock springs are calculated in ArcGIS for four scenarios. Each possible recharge area is based on the potentiometric surface and varying extents of the basin that drain to the Black Rock springs (figure 23). Estimated area of recharge ranges from 21,250 to 83,230 acres (8600–33,680 ha) and is calculated at 21,250, 36,900, 56,050, and 83,230 acres (8600, 14,930, 22,680, and 33,680 ha) for recharge areas a, b, c, and d shown on figure 23.

For these calculations the large springs at Black Rock, that together discharge 2180 acre-feet (3 hm^3) per year, are used as the point of discharge. The flow rate is assumed to be constant for these springs because of a lack of detailed long-term spring-flow data. Subsequent discussions of discharge present a possible variation in flow of plus or minus 10 percent based on available data.

Based on the four possible recharge areas (figure 23) and assumed constant discharge of the Black Rock springs, equation 2 yields recharge rates ranging between 0.1 feet (30 mm) and 0.03 feet (9 mm) per year (figure 24). Because of the simplicity of this calculation these values are assumed to bracket reasonable estimates of recharge in the Cove Creek basin and are used to rule out unreasonable rates of recharge calculated using equation 3 (which is introduced in the following section).

Recharge Rates from Water Temperature

Water temperature measured at springs and wells can provide an additional constraint on aquifer properties and recharge rate (Manga, 2001; Anderson, 2005). Groundwater flow transports heat (advection) and can change the subsurface distribution of heat (Cartwright, 1970; Kilty and Chapman, 1980; Smith and Chapman, 1983). Advection dominates in areas of moderate permeability, significant topographic gradients, and moderate to high recharge rates (Forster and Smith, 1989). In mountainous areas and zones of high background heat flux, changes in temperature along flow paths can provide basic data about groundwater flow patterns in the subsurface (Forster and Smith, 1989). Change in groundwater temperature along a flow path is therefore a useful tracer and provides an additional independent measure of recharge rates and large-scale aquifer properties (Cartwright, 1970; Manga, 1998, 2001; James and others, 2000; Anderson, 2005). The conductive properties of most aquifer materials and depth of the water table generally limit significant heat loss from flowing groundwater (Manga, 2001). Increase in groundwater temperature can therefore be the result of background heat flux and time of residence in the aquifer. Conversely, decreases in groundwater temperature primarily result from the addition of cool, recently recharged groundwater (Forster and Smith, 1989). The following equation (Manga, 2001) relates change in temperature for a spring system to recharge rate and several other aquifer parameters:

$$\Delta T = \frac{Q}{\rho C R} \quad (3)$$

where:

ΔT= change in temperature from recharge to discharge

Q = average heat flux across the base of the aquifer

R = recharge rate

ρ = density of water

C = heat capacity of water

Solving this equation for recharge rate yields a second independent estimate of recharge based on measured groundwater temperatures and assumed average heat flux across the base of the aquifer. Change in temperature is 3.1°C (5°F), and is the difference between the as-

sumed recharge temperature of 9.7°C (50°F), measured at site 11, and the temperature at the main point of spring discharge (site 4) 12.8°C (55°F) measured during sampling. Because of a lack of data these temperatures are considered temporally constant. Average heat flux is assumed to range between new and compiled values presented by Henrikson and Chapman (2002) for the Basin and Range portion of Utah, 39 to 303 mW/m^2 with an average of 92 mW/m^2. Heat flow measured in known geothermal areas such as Cove Fort and Roosevelt Hot Springs can be much larger than these values but may not be indicative of background levels of heat flow elsewhere (Henrikson and Chapman, 2002). Minimum estimates of heat flux give a lower bound on recharge rate of 0.04 feet (12 mm) per year whereas high estimates of heat flux yield a recharge rate of 0.16 feet (49 mm) per year.

Comparison of Quantitative Recharge Rates

Each of the ranges of recharge presented above is internally valid based on the equation used to calculate them. Recharge rates calculated from maximum estimates of heat flux using equation 3 are greater than the reasonable range of recharge (0.1 to 0.03 feet per year) based on the simple recharge-area–discharge relationship (equation 2) and are therefore considered unreasonable. Minimum recharge rates are further constrained by heat flux (equation 3) at 0.04 feet (12 mm) per year. Recharge rates that satisfy all equations considered are therefore between 0.04 and 0.1 feet (12 and 30 mm) per year. Lacking any other data the middle of this range, 0.07 feet (21 mm) per year, is taken as the preferred rate of recharge with a possible range of plus or minus 0.03 feet (9 mm) per year.

Table 3. *Summary of water-budget components for the three basins. All water-budget components are in acre-feet per year. See text for further explanation of water-budget components.*

Water-budget Component	**Basin**			
	Cove Creek	Mineral	San Francisco	Study area
Basin acreage	199,080	90,770	125,230	415,080
Recharge components				
Modified Maxey-Eakin	29,200	8800	5700	43,700
Low Quantitative	7970	3630	5020	16,620
High Quantitative	19,910	9070	12,520	41,500
Best Quantitative	13,940	6350	8770	29,050
Discharge components				
Spring discharge	2375	—	—	2375
Total well withdrawal	1376	—	—	1376
Low ET	3640	6130	4700	14,470
High ET	4440	7490	5750	17,680
Best ET	4040	6810	5240	16,080
Minimum discharge	7390	6130	4700	18,220
Maximum discharge	8190	7490	5750	21,430
Best Discharge	7790	6810	5240	19,840
Potential subsurface outflow				
Minimum subsurface outflow	-220	-3230	-740	-4810
Maximum subsurface outflow	12,520	2940	7820	23,280
Best subsurface outflow	6150	-460	3530	9210

These estimates of recharge are temporally and spatially averaged values and not indicative of local rates of recharge. Because these rates are calculated from a large recharge area that includes varying zones of precipitation they likely provide valid quantitative estimates of recharge across the Cove Creek basin and hence may be considered the best available estimates of recharge to the principal aquifer. These quantitative rates can also be applied to each basin and directly compared to empirical estimates of recharge based on the modified Maxey-Eakin methodology presented above.

Recharge is calculated for each of the basins separately by applying the preferred recharge rate, 0.07 ± 0.03 feet (21 ± 9 mm) per year, to the area of each basin. For the Cove Creek, Mineral, and San Francisco basins preferred calculated recharge is 13,940 ± 5970, 6350 ± 2720, and 8770 ± 3750 acre-feet (17 ± 7, 8 ± 3, and 11 ± 5 hm^3) per year, respectively (table 3). Accounting for the uncertainty yields high and low recharge values that are meant to bracket possible recharge values for the study area.

Discharge

Introduction

Groundwater discharge represents the total volume of water lost from the regional groundwater system (Freeze and Cherry, 1979). The principal mechanisms of groundwater discharge include spring flow, evapotranspiration, well withdrawals, and subsurface outflow. For this water budget direct estimates of spring flow, evapotranspiration, and well withdrawals are made, and subsurface outflow is estimated as the residual component

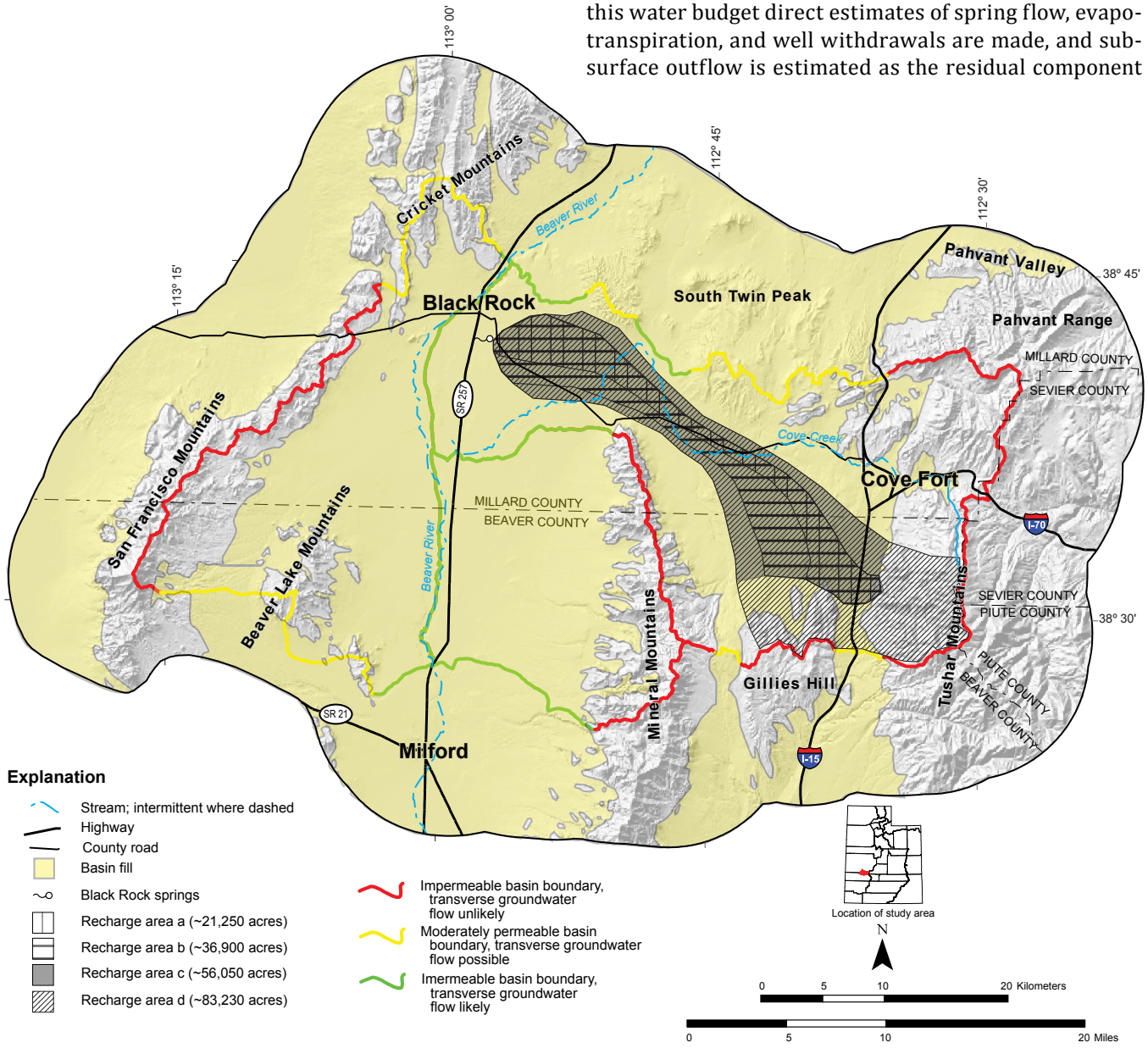

Figure 23. *Recharge areas for the Black Rock springs. Four potential recharge areas are presented based on the water-table surface shown on figure 9 and rate of spring discharge. Recharge areas are partially overlapping. See text for further discussion.*

when all other sources of discharge are balanced against estimates of recharge.

Springs

Groundwater discharges at springs and seeps at discrete sites across the study area. Total volume of groundwater discharged at selected springs was measured directly during fieldwork in the spring of 2006. Elsewhere spring discharge, or lack thereof, is taken from previously published data (Mason, 1998).

Groundwater may leave the study area to the north (figure 3), consequently spring discharge from several springs north of the study area are included in this water budget. Upland springs occur at several locations along Gillies Hill and in the Tushar Mountains to the east. These springs, however, lie in areas of recharge and water from these springs likely ultimately recharges basin-fill aquifers at lower elevations and are therefore not considered in the water budget. Water discharged at lowland springs in many cases does not directly recharge the larger groundwater system and is instead lost to evapotranspiration or is used for irrigation or stock watering.

The largest spring system in the study area is located just west of Black Rock and has an annual flow of 2180 acre-feet (3 hm^3) from several major springs (figure 24). Discharge at the Black Rock springs has been monitored for more than 10 years at a flume installed below the largest springhead. Monthly variation of discharge during this period was less than plus or minus 10 percent (John Kaufman, verbal communication, 2007) and flow from these springs is therefore considered temporally

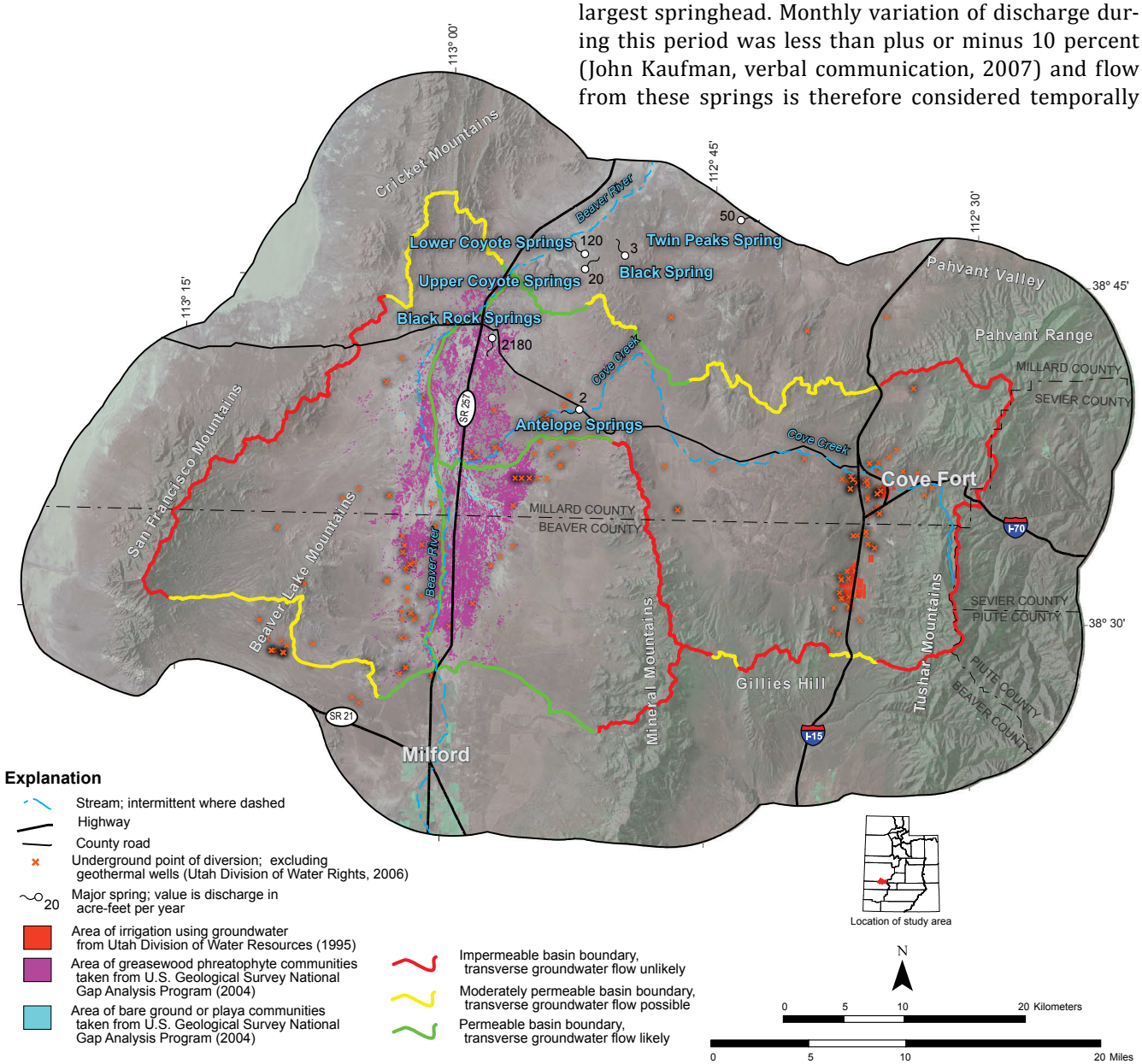

Figure 24. *Discharge summary for the principal aquifer. Most areas of evapotranspiration from the principal aquifer lie along the Beaver River drainage (U.S. Geological Survey National Gap Analysis Program, 2004). Irrigation using groundwater occurs primarily near Cove Fort (Utah Division of Water Resources, 1995). See text for further discussion.*

constant. All other springs lack long-term data but are assumed to have constant flow for this water budget. To the southeast of the Black Rock springs, minor discharge of 2 acre-feet (0.004 hm^3) per year was measured at Antelope Springs. Other springs north of the study area likely connected to the Cove Creek basin include upper and lower Coyote Springs, Black Spring, and Twin Peaks Spring. Annual discharge at these springs is 20, 120, 3, and 50 acre-feet (0.03, 0.15, 0.004, and 0.06 hm^3), respectively. Total groundwater discharged from springs within and potentially connected with the Cove Creek basin is 2375 acre-feet (3 hm^3) per year (table 3). The Mineral and San Francisco basins lack significant lowland spring discharge and do not contribute to the combined estimate of spring flow (Mower and Cordova, 1974; Mason, 1998). Other small springs or seeps in low-elevation portions of the study area are generally of limited extent and not included in water budget calculations. Total annual spring discharge for the entire study area is therefore 2375 acre-feet (3 hm^3).

Evapotranspiration

Direct evapotranspiration from regional groundwater systems in the Great Basin commonly occurs in low-elevation areas of phreatophytes and adjoining playa or bare-ground areas (Nichols, 1993, 1994, 2000). In the western part of the study area, north of Milford, much of the valley floor is covered by phreatophytes and has been assumed to account for significant evapotranspiration (White, 1932; Mower and Cordova, 1974; Mason, 1998) (figure 24). Evapotranspiration is estimated for this study using land-cover data (U.S. Geological Survey National Gap Analysis Program [GAP], 2004) and measured rates of groundwater discharge for the primary land-cover types in areas of evapotranspiration (Moreo and others, 2007; Smith and others, 2007).

The GAP land-cover dataset is a field-correlated, modeled dataset that defines the spatial extent of various plant communities. Of the plant communities mapped in the GAP data set, it is assumed that the intermountain greasewood flat and intermountain playa communities directly correspond with the actual extent of evapotranspiration units. Total area covered by greasewood communities is 13,010, 21,820, and 16,840 acres (5265, 8830, and 6815 ha) for the Cove Creek, Mineral, and San Francisco basins, respectively, and the total area covered by playa communities is 40, 270, and 40 acres (16, 109, 16 ha) for these same basins. Total area covered by greasewood and playa communities in the study area is 52,020 acres (21,050 ha).

Evapotranspiration rates for this study are taken from an aggregate of recent measured evapotranspiration rates for the principal bare-ground and greasewood communities obtained by modern micrometeorological methods to the west of the study area (Moreo and others, 2007). For subsequent calculations it is assumed that mapped greasewood and bare-ground communities have annual groundwater evaporation rates of 0.31 and 0.15 feet (95 and 46 mm), respectively (Moreo and others, 2007). Based on these rates and the area of phreatophyte communities, evapotranspiration for the Cove Creek, Mineral, and San Francisco basins is 4040, 6810, and 5230 acre-feet (5, 8, and 7 hm^3) per year, respectively (table 3). Total evapotranspiration is 16,080 acre-feet (20 hm^3) per year and represents the largest component of discharge for the study area.

The area covered by phreatophyte communities may change through time as land use and groundwater levels fluctuate. A comparison of preexisting estimates of the extent of phreatophytes (White, 1932; Mower and Cordova, 1974; Mason, 1998) with the 2004 land-cover dataset shows little change in area of mapped phreatophyte communities. Field investigation of phreatophyte communities, and discussions with local landowners, also revealed no evidence of recent changes in phreatophyte extent. Therefore, evapotranspiration from groundwater is considered steady through time. Error in these estimates is not directly quantified, but previous statistical analysis of similar evapotranspiration estimates found error to be generally 10 percent or less (Zhu and others, 2007). Hence, annual evapotranspiration may range from 3640 to 4440 acre-feet (6–5 hm^3) for the Cove Creek basin, 6130 to 7490 acre-feet (8–9 hm^3) for the Mineral basin, and 4700 to 5750 acre-feet (6–7 hm^3) for the San Francisco basin (table 3). Evapotranspiration is the principal discharge component and its range of error controls the total maximum and minimum discharge.

Well Withdrawals

Groundwater in the study area is withdrawn from wells for irrigation, domestic use, and geothermal power generation. The unconsumed portion of this water returns to the principal aquifer as recharge. Groundwater extracted for geothermal power production is reinjected and therefore is not considered in the well-withdrawal calculations (Moore and others, 2000). The estimates of consumptive well withdrawal presented below use existing data for domestic and irrigation use in the study area.

Nearly all irrigated land in the study area uses water withdrawn from the principal aquifer via wells. Irrigation water that is lost to evapotranspiration and not recharged is considered consumptive well withdrawal. Water removed from the principal aquifer for irrigation is estimated as the product of the total acreage of irrigated crops multiplied by an estimate of consumptive crop water use. Irrigated acreage is limited to about 890 acres (360 ha) in the Cove Creek basin based on Utah Division of Water Resources (1995) land-use data and

review of 2004 aerial photography (1:20,000-scale) (figure 24). The crop type for most of the irrigated acreage is alfalfa or hay and consumptive use for these crops is assumed equal to the 1.5 feet (0.5 m) per year calculated for these crops near Milford (Susong, 1995). Total consumption from irrigation in the Cove Creek basin is 1360 acre-feet (2 hm^3) per year (table 3). Actual water consumption from irrigation may differ from this value and depends on yearly changes in crop and irrigation type and climate. Because of a lack of detailed yearly crop and water application data, yearly withdrawal of irrigation water is assumed to be constant through time.

Total discharge from private wells is the average per capita water use multiplied by the number of citizens using private wells as their principal source of culinary water. Average water use for rural parts of Utah is 204 gallons (772 L) per capita per day or 0.228 acre-feet (0.001 hm^3) per capita per year (Utah Division of Water Resources, 2001). Total population relying on domestic wells is estimated at approximately 70, all of which reside in the Cove Creek basin. Based on these estimates, total yearly withdrawal from domestic wells is 16 acre-feet (0.1 hm^3) per year.

Total Discharge

Total discharge is the sum of all discharge components. For the Mineral and San Francisco basins where discharge is limited to evapotranspiration, preferred values of total discharge are 6810 ± 680 and 5230 ± 530 acre-feet (8 ± 1 and 7 ± 1 hm^3) per year, respectively (table 3). Total discharge from the Cove Creek basin includes evapotranspiration, spring discharge, and consumptive use from irrigation and culinary wells. Preferred discharge for the Cove Creek basin is 7790 + 400 acre-feet (10 ± 0.5 hm^3) per year (table 3).

Subsurface Outflow

Subsurface outflow is the component of groundwater in a basin that may move beyond the boundary of the basin beneath the land surface. Subsurface outflow of groundwater, particularly to the north from the Cove Creek basin, is supported by previously presented potentiometric gradients, groundwater chemistry, and isotopic data. Direct constraint on the amount of subsurface outflow is lacking, and this component is estimated as the residual of the other water-budget components of recharge and discharge (table 3, figure 25).

Comparison of preferred values of recharge and discharge yield subsurface outflow of 6150, -460, and 3530 acre-feet (8, -1, and 4 hm^3) per year for the Cove Creek, Mineral, and San Francisco basins, respectively (table 3). Figure 25 shows the preferred values and ranges of values for recharge and discharge, as well as subsurface outflow for each of the basins in the study area. Negative values represent a net inflow of groundwater, while positive values represent a net outflow of groundwater. The preferred values of recharge and discharge suggest a net subsurface outflow of water from the Cove Creek and San Francisco basins and the study area as a whole. A negative subsurface outflow for the Mineral basin may indicate groundwater influx in the basin fill from adjoining portions of the Cove Creek and San Francisco basins. Figure 26 shows summary water-budget data for each of the basins within the study area and indicates potential amounts and directions of interbasin flow between the basins. Subtracting the highest estimated discharge from the lowest estimated recharge yields the minimum subsurface outflow for a basin. Based on this method, all basins have negative subsurface outflow values, and no subsurface outflow is required for any of the three basins assuming the minimum acceptable water budget estimates. Minimum subsurface outflow estimated by this method is a conservative estimate that satisfies all assumptions and data presented in this report.

DISCUSSION

Groundwater in the study area is controlled by a combination of geologic, geographic, and climatic characteristics. Most groundwater in the study area resides in the principal aquifer that consists of unconsolidated deposits, interbedded volcanic and variously lithified sedimentary deposits, forming a large, interconnected basin-fill aquifer across much of the Cove Creek basin and the adjoining Beaver River valley. Where the principal aquifer is contiguous across study area boundaries, such as along the Beaver River and along the northern boundary of the Cove Creek basin, it may allow for groundwater flow into adjoining basins. The upper part of the principal aquifer includes geologic units ranging from fractured basalts to unconsolidated sedimentary deposits. Within the Cove Creek basin fractured basalts may form efficient conduits and reservoirs for groundwater as evidenced by the major spring system at Black Rock. Elsewhere along the Beaver River drainage, sedimentary deposits of unconsolidated sand and gravel form the important water-bearing strata. Confining beds in the uppermost part of the principal aquifer may consist of clay layers but are likely limited to areas along the Beaver River drainage. Much of the uppermost part of the principal aquifer in the Cove Creek basin is apparently unconfined.

The distribution of permeable rock units places fundamental constraints on the possibility for groundwater flow and interaction across geographic boundaries. Thick sections of relatively impermeable quartzite in the San Francisco Mountains make westward movement of groundwater from the study area unlikely. This is con-

trary to the assumptions of Mason (1998) who assumed groundwater moves westward toward Sevier Lake. Mason (1998), however, did not consider the relative permeability of bedrock in the San Francisco Mountains. Mason's (1998) interpretation was also based on several wells and water levels west of the Beaver River that were not located during fieldwork for this study and for which data could not be found in the existing U.S. Geological Survey water-level database (U.S. Geological Survey, 2007).

Intrusive rocks form the core of the Mineral Mountains and may prevent groundwater from moving westward from the Cove Creek basin into the Mineral basin. The potential for interbasin flow beneath the Mineral Mountains, near Roosevelt Hot Springs, has been investigated by several previous workers (e.g., Smith, 1980; Faulder, 1991). Two-dimensional numerical flow models calibrated with reasonable hydrogeologic data suggest that unless horizontal permeability is much greater than vertical permeability in the intrusives of the Mineral Mountains, interbasin flow across the Mineral Mountains is unlikely (Smith, 1980; Faulder, 1991). Permeability in the Mineral Mountains and the associated geothermal reservoir at Roosevelt Hot Springs is likely controlled by steeply dipping joints and faults (Nielsen and others, 1978) that imply vertical permeability is at least equal to, and likely much greater than, horizontal permeability across the Mineral Mountains. Isotopic work by Bowman and Rohrs (1981) concluded that all of the thermal groundwater encountered in the Roosevelt Hot Springs KGRA could have been recharged from precipitation in the nearby Mineral Mountains and these waters need not be far-traveled. It is therefore unlikely and certainly

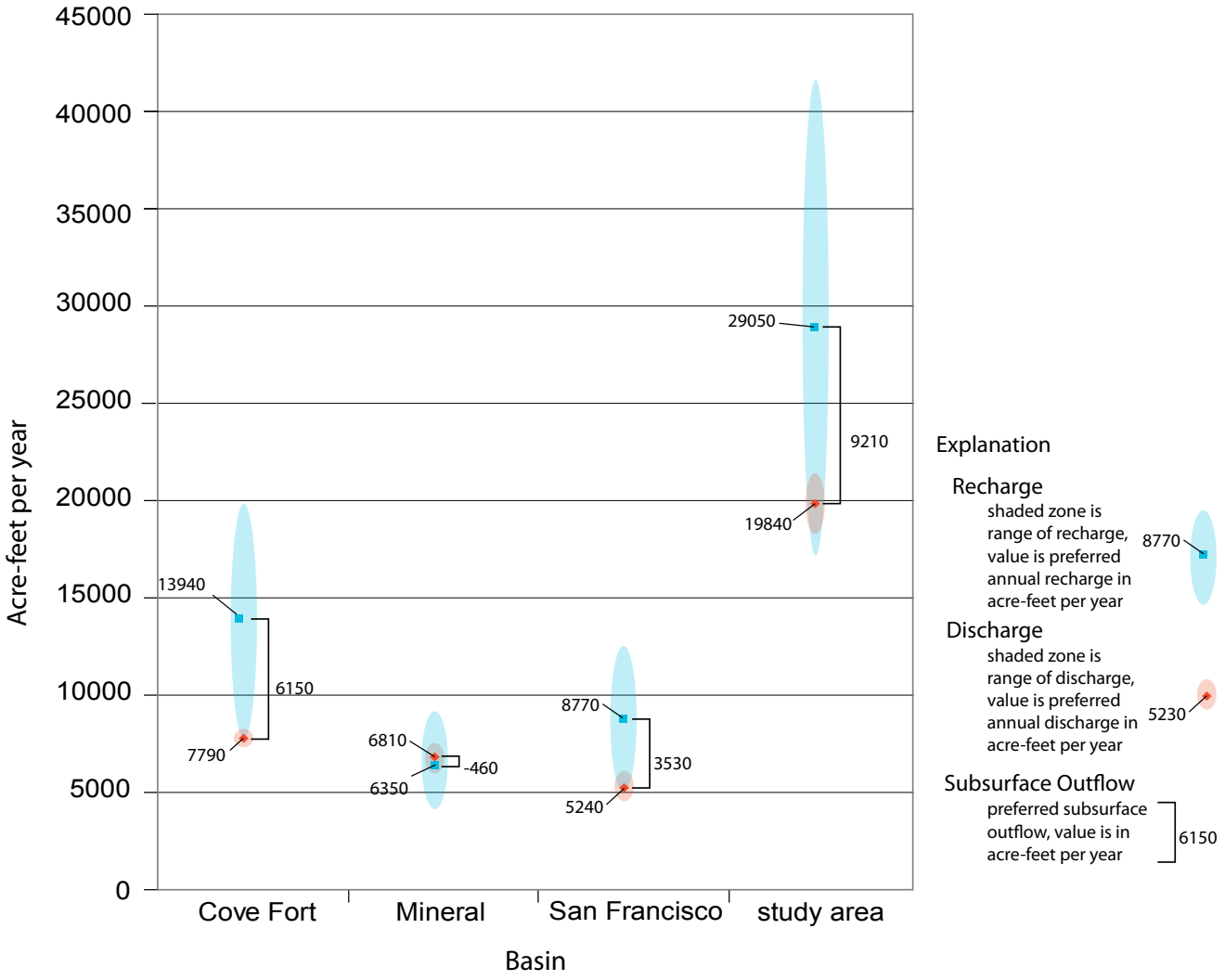

Figure 25. *Summary of recharge and discharge components and potential subsurface outflow. Potential subsurface outflow is the difference between preferred values of recharge and discharge, negative values indicate subsurface groundwater inflow. All basins have overlapping recharge and discharge estimates when a conservative range of recharge rates is considered and may therefore have little if any subsurface outflow. See text for further details and discussion.*

not required that significant volumes of groundwater move across the Mineral Mountains from the Cove Fort area.

The Paleozoic carbonate bedrock, where present, may be an important aquifer. These rocks may facilitate interbasin flow to the north and northwest in the southern Cricket Mountains. No groundwater level information is available for the Cricket Mountains, so the existence of such flow is uncertain at best.

Groundwater elevation in the basin fill is best constrained in the Cove Creek basin, and least constrained in the San Francisco and Mineral basins. In the Cove Creek basin groundwater flows from areas of recharge near the upper reaches of the interconnected basin fill between 6000 and 6250 feet (1830 and 1900 m) elevation, near Interstate 15 and to the west along the north flank of Gillies Hill, towards areas of discharge to the west along the Beaver River channel. Little evidence exists for significant recharge in lower elevation portions of the principal aquifer. Instead, most groundwater likely results from upland recharge along or near the interface of the basin fill and consolidated rocks of the bounding mountain ranges. Groundwater discharges from the principal aquifer in the Cove Creek basin as spring flow near Black Rock and several other springs, or as evapotranspiration, or leaves the basin to the north as subsurface outflow.

Large areas of shallow groundwater occur in the principal aquifer along the Beaver River and the lower reaches of the Cove Creek channel. To the east, across much of the Cove Creek basin depth to groundwater is much greater, generally more than 100 feet (30 m). Areas of shallow groundwater along the Beaver River correspond to sig-

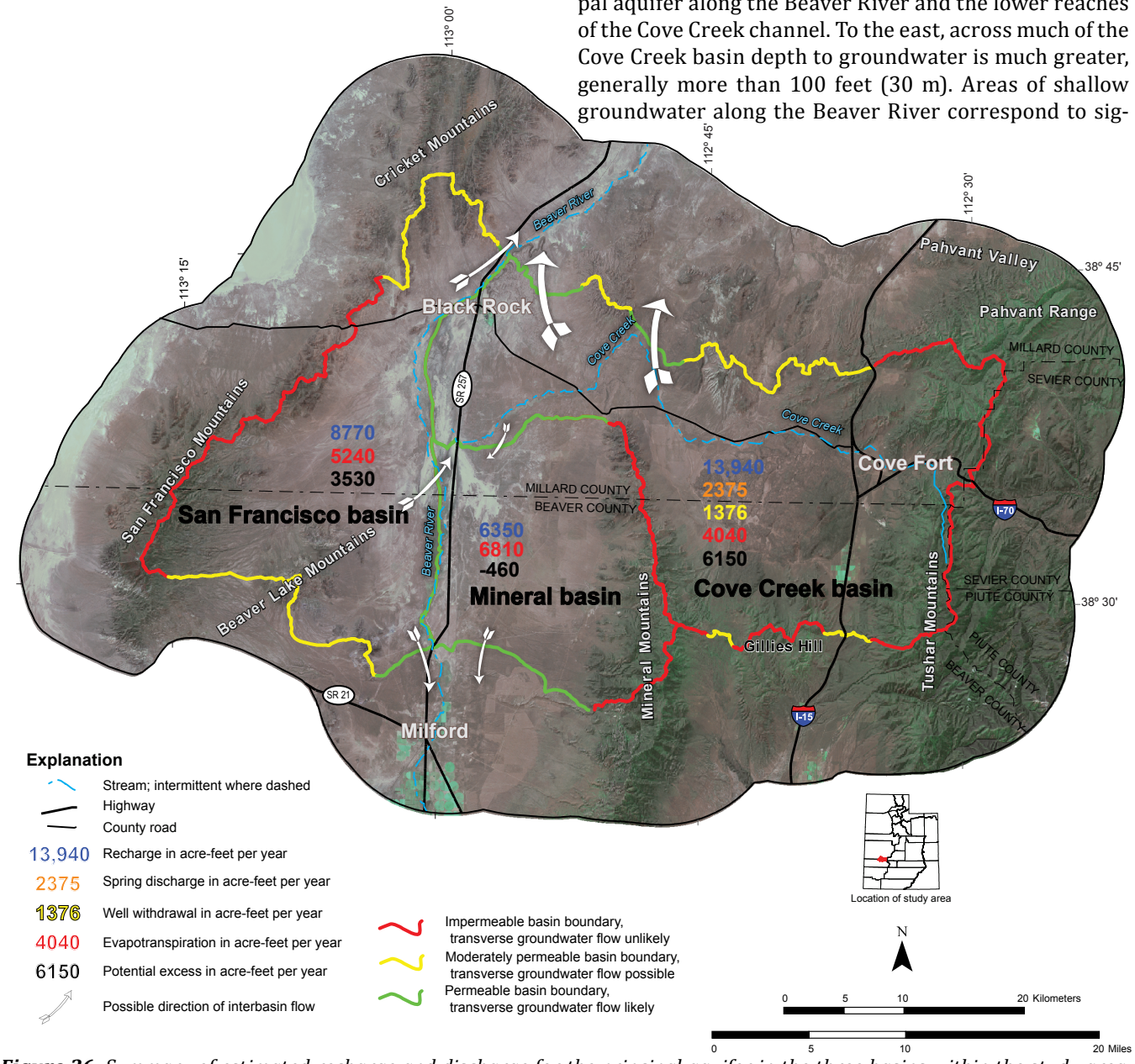

Figure 26. *Summary of estimated recharge and discharge for the principal aquifer in the three basins within the study area. Potential excess is the difference between preferred values of recharge and discharge for each basin listed in table 3. See text for further discussion.*

nificant areas of evapotranspiration. Deeper groundwater across much of the upper parts of the Cove Creek basin precludes direct evapotranspiration from the principal aquifer.

Groundwater chemistry is complex with a wide range of chemical compositions across the study area. Much of the groundwater sampled in the Cove Creek basin is of calcium or sodium bicarbonate type. Groundwater associated with the geothermal systems in the study area is commonly of sodium and chloride type. Available data indicate that much of the groundwater in the Cove Creek basin has low TDS concentrations and is likely to be of high quality. Lower quality, high-TDS water occurs as a broad plume extending northwestward away from the Roosevelt Hot Springs area. High TDS may also occur away from the known geothermal areas, possibly resulting from salt concentration in areas of significant evapotranspiration such as west of the Black Rock springs and along the Beaver River drainage, or dissolution of salts that have been deposited within the basin fill. Groundwater quality in the principal aquifer shows a positive correlation with measured groundwater temperature and generally is of higher quality with increasing distance from known geothermal areas and lower measured temperature.

Estimates of groundwater recharge in the study area vary significantly depending on the method used. Using simple mass balance and heat flux equations, recharge rates are quantified for the major springs at Black Rock and applied to the Cove Creek, Mineral, and San Francisco basins. A comparison of these rates of recharge with those calculated using a modified version of the widely used Maxey-Eakin empirical method shows that the recharge based on quantifiable data is lower than that calculated via empirical methods. Similar discrepancies are typical between early empirical estimates and more recent quantititative estimates of groundwater recharge (Manning and Solomon, 2004; Scanlon and others, 2006). Error associated with recharge estimates based on spring flow, are crudely known but do provide a working range for recharge that satisfies all of the equations. These equations are based on directly measured quantities and provide two separate simple relationships for recharge rate and are therefore considered to be robust relative to empirical estimates of recharge.

Most discharge of groundwater in the study area occurs as evapotranspiration. Extensive areas of greasewood exist in the western part of the study area along the Beaver River in lowland portions of the Cove Creek, Mineral, and San Francisco basins. Estimates of evapotranspiration are dependent on previously modeled land-cover data and measurements of direct groundwater use by a given plant community elsewhere in the Great Basin. Potential error associated with estimates of evapotranspiration is therefore poorly constrained and, because of the relative contribution of this component, is the single largest unknown in the water budget. Springs and irrigation and culinary wells also discharge groundwater from the principal aquifer in the Cove Creek basin. Subsurface outflow from each basin is considered to be the residual of discharge versus recharge. When error and range in reasonable recharge and discharge components is considered, subsurface outflow is not required for any of the three basins. Based on preferred estimates of recharge and discharge, subsurface outflow may occur from the Cove Creek and San Francisco basins. Preferred values yield a net inflow of groundwater into the Mineral basin. Inflow to the Mineral basin may occur either from a component of the potential outflow from adjoining portions of the principal aquifer in the Cove Creek or San Francisco basins or as deep underflow, not captured by the water budget discussed above, associated with the Roosevelt Hot Springs geothermal system beneath the Mineral Mountains. Most subsurface outflow from the Cove Creek basin likely leaves the study area to the north and enters southern Pahvant Valley in sections of contiguous basin fill. Subsurface outflow from the San Francisco basin that does not enter the adjoining Mineral basin may move to the southeast toward Milford or less likely to the northeast into Pahvant Valley along and near the Beaver River drainage.

CONCLUSIONS

The principal aquifer in the study area comprises a large and interconnected section of basin fill that includes interbedded volcanics and sedimentary deposits of various ages and degrees of lithification. The volcanics, particularly basaltic rocks, are most prominent in the Cove Creek basin. Along the Beaver River drainage the uppermost basin fill is dominated by unconsolidated sediments and generally exists in unconfined conditions. Paleozoic carbonate rocks may provide another important aquifer where they are present.

Impermeable intrusive rocks in the Mineral Mountains and quartzites in the San Francisco Mountains bound the principal aquifer and form important lateral boundaries to regional groundwater flow. Where basin fill is contiguous across hydrologic basin boundaries, such as along the northern and southern margins of the study area along the Beaver River valley and along the northern boundary of the Cove Creek basin, interbasin groundwater flow is possible.

Groundwater in the principal aquifer within the Mineral and San Francisco basins flows from areas of recharge along upper-elevation portions of the basin fill near adjoining bedrock highlands to areas of discharge in

major areas of phreatophytes along the Beaver River valley between Black Rock and Milford. In the Cove Creek basin groundwater flows from areas of recharge near the upper reaches of the interconnected basin fill between 6000 and 6250 feet (1830–1900 m) elevation near Interstate 15 and to the west along the north flank of Gillies Hill towards areas of discharge to the west along the Beaver River channel, at Black Rock Springs, and possibly north of the study area in Pahvant Valley. Increases in groundwater consumption in the upper parts of the basin-fill aquifer near Cove Fort may therefore affect groundwater levels to the west near Black Rock and possibly to the north in Pahvant Valley.

Groundwater recharge in the study area is directly estimated using spring discharge relationships. Calculations based on these data yield preferred recharge rates of 13,940 ± 5970, 6350 ± 2720, and 8770 ± 3750 acre-feet (17 ± 7, 8 ± 3, and 11 ± 5 hm^3) per year, for the Cove Creek, Mineral, and San Francisco basins, respectively. For the Mineral and San Francisco basins discharge is limited to evapotranspiration, and preferred values of total discharge are 6810 ± 680 and 5230 ± 530 acre-feet (8 ± 1 and 7 ± 1 hm^3) per year, respectively. Total discharge from the Cove Creek basin includes evapotranspiration, spring discharge, and consumptive use from irrigation and culinary wells. Preferred discharge for the Cove Creek basin is 7790 ± 400 acre-feet (10 ± 0.5 hm^3) per year.

In general recharge is balanced by discharge and most water is discharged via evapotranspiration in lowland areas. When error and the range of reasonable estimates are considered, subsurface outflow is not required for any of the three basins. Using preferred estimates for recharge and discharge does yield subsurface outflow from the Cove Creek basin (6150 acre-feet [8 hm^3] per year) and the San Francisco basin (3530 acre-feet [4 hm^3] per year). In the Mineral basin little if any groundwater may be available for subsurface outflow. To better constrain groundwater availability and the potential for subsurface outflow in the Cove Creek basin, further work should include numerical flow modeling of the basin-fill aquifer system across the area in conjunction with additional chemical, dissolved gas and isotopic sampling of groundwater in the principal aquifer.

ACKNOWLEDGMENTS

Dave Tingey at the Brigham Young University Department of Geology provided assistance with sampling methods and analyzed the solute, stable isotope, carbon isotope, and tritium samples. John Kaufman graciously provided long-term spring-flow data and allowed sampling at the Black Rock springs and an outlying well. Volunteers at the Cove Fort Historical Site, operated by the Church of Jesus Christ of Latter-day Saints, facilitated sampling of a supply well. The Yardley family also allowed sampling of their private well. Rich Emerson, Scott Horn, and Kim Nay assisted with creation of several of the figures and plates. Reviews by James Greer and Matt Lindon (Utah Division of Water Rights) greatly improved the content of this report. Dr. Alan Mayo of Brigham Young University also provided thoughtful review that greatly improved this manuscript. I also thank Rick Allis, Kimm Harty, Hugh Hurlow, Michael Hylland, Mike Lowe, and Mark Yidana (Utah Geological Survey) for helpful reviews of this report.

REFERENCES

Anderson, M.P., 2005, Heat as a groundwater tracer: Groundwater, v. 43, p. 951–968.

Anderson, P.B., Susong, D.D., Wold, S.R., Heilweil, V.M., and Baskin, R.L., 1994, Hydrogeology of recharge areas and water quality of the principal aquifers along the Wasatch Front and adjacent areas, Utah: U.S. Geological Survey Water-Resources Investigations Report 93-4221, 74 p., scale 1:100,000.

Anderson, R.E., and Bucknam, R.C., 1979, Map of fault scarps in unconsolidated sediments, Richfield 1° x 2° quadrangle, Utah: U.S. Geological Survey Open-File Report 79-1236, 15 p., 1 plate, scale 1:250,000.

Armstrong, R.L., 1968, Sevier orogenic belt in Nevada and Utah: Bulletin of the American Association of Petroleum Geologists, v. 79, p. 429–458.

Avon, L., and Durbin, T.J., 1994, Evaluation of the Maxey-Eakin method for estimating recharge to groundwater basins in Nevada: Water Resources Bulletin, v. 30, p. 99–111.

Bankey, V., Grauch, V.J.S., and Kucks, R.P., 1998, Utah aeromagnetic and gravity maps and data—a web site for distribution of data: Online, U.S. Geological Survey Open-File Report 98-761, http://pubs.usgs.gov/of/1998/ofr-98-0761/utah.html.

Barker, C.A., 1986, Upper-crustal structure of the Milford Valley and Roosevelt Hot Springs, Utah region, by seismic modeling: Logan, Utah State University, M.S. thesis, 101 p.

Best, M.G., McKee, E.H., and Damon, P.E., 1980, Space-time-composition patterns of late Cenozoic volcanism, southwestern Utah and adjoining areas: American Journal of Science, v. 280, p. 1035–1050.

Best, M.G., Lemmon, D.M., and Morris, H.T., 1989, Geologic map of the Milford quadrangle and east half of the Frisco quadrangle, Beaver County, Utah: U.S. Geological Survey Miscellaneous Investigations Series Map I-1904, scale 1:50,000.

Blackett, R.E., and Wakefield, S., 2004, Geothermal resources of Utah—2004—a digital atlas of Utah's geothermal resources: Utah Geological Survey Open-File Report 431, CD.

Bowen, G.J., and Revenaugh, J., 2003, Interpolating the isotopic composition of modern meteoric precipitation: Water Resources Research, v. 39, p. 9–13.

Bowman, J.R., and Rohrs, D.T., 1981, Light-stable-isotope studies of spring and thermal waters from the Roosevelt Hot Springs and Cove Fort/Sulphurdale Thermal Areas and of clay minerals from the Roosevelt Hot Springs Thermal Area: Topical Report, U.S. Department of Energy/Division of Geothermal Energy, contract number DE-AC07-80ID12079, 40 p.

Carrier, D.L., and Chapman, D.S., 1981, Gravity and thermal models for the Twin Peaks silicic center, southeastern Utah: Journal of Geophysical Research, v. 86, p. 10287–10302.

Cartwright, K., 1970, Groundwater discharge in the Illinois basin as suggested by temperature: Water Resources Research, v. 6, p. 912–918.

Clark, I., and Fritz, P., 1997, Environmental isotopes in hydrogeology: New York, Lewis Publishers, 328 p.

Coleman, D.S., 1991, Geology of the Mineral Mountains batholith, Utah: Lawrence, University of Kansas, unpublished Ph.D. thesis, 219 p., scale 1:12,000.

Coleman, D.S., Bartley, J.M., Walker, J.D., Price, D.E., and Friedrich, A.M., 1997, Extensional faulting, footwall deformation and plutonism in the Mineral Mountains, southern Sevier Desert, *in* Link, P.K., and Kowalis, B.J., editors, Mesozoic to recent geology of Utah: Brigham Young University Geology Studies, v. 42, part 2, p. 203–233.

Coplen, T.B., 1996, New guidelines for reporting stable hydrogen, carbon, and oxygen isotope-ratio data: Geochimica et Cosmochimica Acta, v. 60, p. 3359–3360.

Craig, H., 1961, Isotopic variations in meteoric waters: Science, v. 133, p. 1833–1834.

Dansgaard, W., 1964, Stable isotopes in precipitation: Tellus, v. 16, p. 435–468.

Davis, R.L., 1983, Geology of the Dog Valley-Red Ridge area, southern Pahvant Mountains, Millard County, Utah: Brigham Young University Geology Studies, v. 30, part 1, p. 19–36, scale 1:24,000.

DeCelles, P.G., and Coogan, J.C., 2006, Regional structure and kinematic history of the Sevier fold-and-thrust belt, central Utah: Geological Society of America Bulletin, v. 118, p. 841–864.

Domenico, P.A., and Schwartz, F.W., 1997, Physical and chemical hydrogeology: New York, John Wiley and Sons, 506 p.

Eakin, T.E., Maxey, G.B., Robinson, T.W., Fredericks, J.C., and Loeltz, O.J., 1951, Contributions to the hydrology of eastern Nevada: State of Nevada Office of the State Engineer, Water Resources Bulletin No. 12, 171 p.

Faulder, D.D., 1991, Conceptual geologic model and native state model of the Roosevelt Hot Springs hydrothermal system, *in* Ramey, H.J. Jr., Horne, R.N., Kruger, P., Miller, F.G., Brigham, W.E., Cook, J.W., editors, Proceedings of the Sixteenth Workshop on Geothermal Reservoir Engineering: Stanford, California, Stanford University, p. 131–142.

Fishman, M.J., 1993, Methods of analysis by the U.S. Geological Survey National Water Quality Laboratory—determination of inorganic and organic constituents in water and fluvial sediments: U.S. Geological Survey Open-File Report 93-125, 217 p.

Fishman, M.J., and Friedman, L.C., 1989, Methods for determination of inorganic substances in water and fluvial sediments: U.S. Geological Survey Techniques of Water-Resource Investigation 05-A1, 545 p.

Forster, C., and Smith, L., 1989, The influence of groundwater flow on thermal regimes in mountainous terrain—a model study: Journal of Geophysical Research, v. 94, p. 9439–9451.

Freeze, R.A., and Cherry, J.A., 1979, Groundwater: Englewood Cliffs, New Jersey, Prentice Hall, 604 p.

Friedman, I., Smith, G.I., Johnson, C.A., and Moscati, R.J., 2002, Stable isotopic compositions of waters in the Great Basin, United States—2. Modern precipitation: Journal of Geophysical Research, v. 107 (doi:10.1029/2001JD000566).

George, S.E., 1985, Geology of the Fillmore and Kanosh quadrangles, Millard County, Utah: Brigham Young University Geology Studies, v. 32, part 1, p. 39–62, scale 1:24,000.

Hart, R., Nelson, S.T., Parks, E., Mayo, A., and Tingey, D., 2008, Preliminary evaluation of del^{13}C and CO_2 concentration in soil gas in Utah based on constraining environmental variables for a more accurate and precise input parameter for groundwater model ages [abs.]: Online, Geological Society of America, Rocky Mountain Section Meeting, paper no. 26-5, gsa.confex.com/gsa/2008CD/finalprogram/abstract_135657.htm.

Henrikson, A., and Chapman, D.S., 2002, Terrestrial heat flow in Utah: Online, unpublished report, University of Utah Department of Geology and Geophysics, 46 p., http://geology.utah.gov/emp/geothermal/pdf/terrestrialhf.pdf.

Hintze, L.H., 1984, Geology of the Cricket Mountains, Millard County, Utah: U.S. Geological Survey Open-File Report 84-683, 9 plates, scale 1:24,000.

Hintze, L.H., and Davis F.D., 2002, Geologic map of the

Wah Wah Mountains North 30′ x 60′ quadrangle and part of the Garrison 30′ x 60′ quadrangle, southwest Millard County and part of Beaver County, Utah: Utah Geological Survey Map 182, 2 plates, scale 1:100,000.

Hintze, L.H., and Davis, F.D., 2003, The geology of Millard County, Utah: Utah Geological Survey Bulletin 133, 305 p.

Hintze, L.H., Davis, F.D., Rowley, P.D., Cunningham, C.G., Steven, T.A., and Willis, G.C., 2003, Geologic map of the Richfield 30′ x 60′ quadrangle, southeast Millard County, and parts of Beaver, Piute, and Sevier Counties, Utah: Utah Geological Survey Map 195, 2 plates, scale 1:100,000.

Hintze, L.F., and Kowallis, B.J., 2009, Geologic history of Utah: Brigham Young University Geology Studies, Special Publication 9, 225 p.

Holmes, W.F., and Thiros, S.A., 1991, Groundwater hydrology of Pahvant Valley and adjacent areas, Utah: State of Utah Department of Natural Resources Technical Publication No. 98, 64 p.

Intermountain Region Digital Image Archive Center, 2007, Intermountain image archive: Online, http://earth.gis.usu.edu/, accessed February 12, 2007.

James, E.R., Manga, M., Rose, T.P., and Hudson, G.B., 2000, The use of temperature and the isotopes of O, H, C, and noble gases to determine the pattern and spatial extent of groundwater flow: Journal of Hydrology, v. 237, p. 100–112.

Kilty, K. and Chapman, D.S., 1980, Convective heat transfer in selected geologic situations: Groundwater, v. 18, p. 386–394.

Lipman, P.W., Rowley, P.D., Mehnert, H.H., Evans, S.H., Jr., Nash, W.P., Brown, F.H., Izett, G.A., Naeser, C.W., and Friedman, Irving, 1978, Pleistocene rhyolite of the Mineral Mountains—Utah geothermal and archeological significance: U.S. Geological Survey Journal of Research, v. 6, no. 1, p. 133–147, scale 1:80,000.

Mabey, D.R., and Budding, K.E., 1987, High temperature geothermal resources of Utah: Utah Geological and Mineral Survey Bulletin 123, 64 p.

Machette, M.N., Steven, T.A., Cunningham, C.G., and Anderson, J.J., 1984, Geologic map of the Beaver quadrangle, Beaver and Piute Counties, Utah: U.S. Geological Survey Miscellaneous Investigations Series Map I-1520, scale 1:50,000.

Manga, M., 1997, Model for discharge in spring-dominated streams and implications for the transmissivity and recharge of Quarternary volcanics in the Oregon Cascades: Water Resources Research, v. 33, p. 1813–1822.

Manga, M., 1998, Advective heat transport by low-temperature discharge in the Oregon Cascades: Geology, v. 26, p. 799–802.

Manga, M., 2001, Using springs to study groundwater flow and active geologic processes: Annual Review of Earth and Planetary Science, v. 29, p. 201–228.

Manning, A.H., and Solomon, D.K., 2004, Constraining mountain-block recharge to the eastern Salt Lake Valley, Utah with dissolved noble gas and tritium data, *in* Hogan, J.F., Phillips, F.M., and Scanlon, B.R., editors, Groundwater recharge in a desert environment—the southwestern United States: American Geophysical Union, Washington, D.C., p. 139–158.

Mason, J.L., 1998, Groundwater hydrology and simulated effects of development in the Milford area, an arid basin in southwestern Utah: U.S. Geological Survey Professional Paper 1409-G, 69 p.

Maxey, G.B., and Eakin, T.E., 1949, Groundwater in White River Valley, White Pine, Nye, and Lincoln Counties, Nevada: Nevada State Engineer Water-Resources Bulletin No. 8, 59 p.

Moore, J.N., Adams, M.C., Sperry, T.L., Bloomfield, K.K., and Kunzman, R., 2000, Preliminary results of geochemical monitoring and tracer tests at the Cove Fort-Sulphurdale Geothermal System, Utah, *in* Twenty-fifth Workshop of Geothermal Reservoir Engineering, January 24–26, 2000, Proceedings: Stanford, California, p. 1–6.

Moore, J.N., and Nielsen, D.L., 1994, An overview of geology and geochemistry of the Roosevelt Hot Springs geothermal area, *in* Blackett, R.E., and Moore, J.N., editors, Cenozoic geology and geothermal systems of southwestern Utah: Utah Geological Association Publication 23, p. 25–36.

Moreo, M.T., Laczniak, R.J., and Stannard, D.I., 2007, Evapotranspiration rate measurements of vegetation typical of groundwater discharge areas in the Basin and Range carbonate-rock aquifer system, Nevada and Utah, September 2005—August 2006: U.S. Geological Survey Scientific Investigations Report 2007-5078, 34 p. + appendix.

Mower, R.W., 1965, Groundwater resources of Pahvant Valley, Utah: U.S. Geological Survey Water-Supply Paper 1794, 78 p.

Mower, R.W., 1978, Hydrology of the Beaver Valley area, Beaver County, Utah, with emphasis on groundwater: State of Utah Department of Natural Resources Technical Publication No. 63, 90 p.

Mower, R.W., and Cordova, R.M., 1974, Water resources of the Milford area, Utah, with emphasis on groundwater: State of Utah Department of Natural Resources Technical Publication No. 43, 106 p.

Nash, W.P., 1981, Geologic map of the South Twin Peak–Cove Creek area, west-central Utah: Unpublished report, University of Utah Department of Geology

and Geophysics, 12 p., scale 1:24,000.

Natural Resources Conservation Service, 2007, Utah SNOTEL sites: Online, www.wcc.nrcs.usda.gov/snotel/Utah/utah.html, accessed March 2007.

Nelson, S.T., 2000, A simple, practical methodology for routine VSMOW/SLAP normalization of water samples analyzed by continuous flow methods: Rapid Communications in Mass Spectrometry, v. 14, p. 1044–1046.

Nichols, W.D., 1993, Estimating discharge of shallow groundwater by transpiration from greasewood in the northern Great Basin: Water Resources Research, v. 29, p. 2771–2778.

Nichols, W.D., 1994, Groundwater discharge by phreatophyte shrubs in the Great Basin as related to depth to groundwater: Water Resources Research, v. 30, p. 3265–3274.

Nichols, W.D., 2000, Regional groundwater evapotranspiration and groundwater budgets, Great Basin, Nevada: U.S. Geological Survey Professional Paper 1628, variously paginated.

Nielson, D.L., Evans, S.H., and Sibbett, B.S., 1986, Magmatic, structural, and hydrothermal evolution of the Mineral Mountains intrusive complex, Utah: Geological Society of America Bulletin, v. 97, p. 765–777.

Nielson, D.L., Sibbett, R.S., McKinney, D.B., Hulen, J.R., Moore, S.N., and Samberg, S.M., 1978, The geology of the Roosevelt Hot Springs KGRA, Beaver County, Utah: University of Utah Research Institute Earth Science Laboratory Report, DOE Contract EG-78-C-07-1701, 120 p.

Oviatt, C.G., 1991, Quaternary geology of the Black Rock Desert, Millard County, Utah: Utah Geological and Mineral Survey Special Study 73, 23 p., 1 plate, scale 1:100,000.

Parkhurst, D.L., 1997, Geochemical mole-balance modeling with uncertain data: Water Resources Research, v. 33, p. 1957–1970.

Plummer, L.N., Busby, J.F., Lee, R.W., and Hanshaw, B.B., 1990, Geochemical modeling of the Madison aquifer in parts of Montana, Wyoming, and South Dakota: Water Resources Research, v. 26, p. 1981–2014.

Plummer, L.N., Prestemon, E.C., and Parkhurst, D.L., 1994, An interactive code (NETPATH) for modeling NET geochemical reactions along a flow path, version 2.0: U.S. Geological Survey Water-Resources Investigations Report 94-4169, 130 p.

PRISM Climate Group, 2006, United States average monthly or annual precipitation, 1971—2000: Online, Oregon State University, www.prismclimate.org, accessed February 22, 2007.

Rowley, P.D., Cunningham, C.G., Steven, T.A., Workman, J.B., Anderson, J.J., and Theissen, K.M., 2002, Geologic map of the central Marysvale volcanic field, southwestern Utah: U.S. Geological Survey Geologic Investigations Series I-2645-A, scale 1:100,000.

Rowley, P.D., Vice, G.E., McDonald, R.E., Anderson, J.J., Machette, M.N., Maxwell, D.J., Ekren, E.B., Cunningham, C.G., Steven, T.A., and Wardlaw, B.R., 2005, Interim geologic map of the Beaver 30′ x 60′ quadrangle, Beaver, Piute, Iron, and Garfield Counties, Utah: Utah Geological Survey Open-File Report 454, 27 p., 1 plate, scale 1:100,000.

Saltus, R.W., and Jachens, R.C., 1995, Gravity and basin-depth maps of the Basin and Range Province, western United States: U.S. Geological Survey Map GP-1012, scale 1:2,500,000.

Scanlon, B.R., Healy, R.W., and Cook, P.G., 2002, Choosing appropriate techniques for quantifying groundwater recharge: Hydrogeology Journal, v. 10, p. 18–39.

Scanlon, B.R., Keese, K.K., Flint, A.L., Flint, L.E., Gaye, C.B., Edmunds, W.M., and Simmers, I., 2006, Global synthesis of groundwater recharge in semiarid and arid regions: Hydrological Processes, v. 20, p. 3335–3370.

Sibbett, B.S., and Nielson, D.L., 1980, Geology of the central Mineral Mountains, Beaver County, Utah: Salt Lake City University of Utah Earth Science Laboratory Report, DOE contract DE-AC07ET28392, 42 p., 4 plates, scale 1:24,000.

Simpson, R.W., Jachens, R.C., and Blakely, R.J., 1986, A new isostatic residual gravity map of the conterminous United States with a discussion on the significance of isostatic residual anomalies: Journal of Geophysical Research, v. 91, p. 8348–8372.

Smith, J.L., 1980, A model study of the regional hydrogeologic regime, Roosevelt Hot Springs, Utah: Salt Lake City, University of Utah Department of Geology and Geophysics, U.S. Department of Energy Report IDO/78-28392.a.10, 30 p.

Smith, J.L., Laczniak, R.J., Moreo, M.T., and Welborn, T.L., 2007, Mapping evapotranspiration units in the Basin and Range carbonate-rock aquifer system, White Pine County, Nevada, and adjacent areas in Nevada and Utah: U.S. Geological Survey Scientific Investigations Report 2007-5087, 20 p.

Smith, L., and Chapman, D.S., 1983, On the thermal effects of groundwater flow—1. regional scale systems: Journal of Geophysical Research, v. 88, p. 593–608.

Smith, R.B., and Bruhn, R.L., 1984, Intraplate extensional tectonics of the western U.S. Cordillera—inferences on structural style from seismic-reflection data, regional tectonics and thermal-mechanical models of brittle-ductile deformation: Journal of Geophysical Research, v. 89, no. B7, p. 5733–5762.

Smith, R.B., Nagy, W.C., Julander, K.A., Viveiros, J.J., Barker,

C.A., and Gants, D.G., 1989, Geophysical and tectonic framework of the eastern Basin and Range–Colorado Plateau–Rocky Mountain transition, *in* Pakiser, L.C., and Mooney, W.D., editors, Geophysical framework of the continental United States: Geological Society of America Memoir 172, p. 205–233.

Steven, T.A., and Morris, H.T., 1983, Geologic map of the Cove Fort quadrangle, west-central Utah: U.S. Geological Survey Miscellaneous Investigations Series Map I-1481, scale 1:24,000.

Susong, D.D., 1995, Water budget and simulation of one-dimensional unsaturated flow for a flood- and sprinkler-irrigated field near Milford, Utah: Utah Department of Natural Resources Technical Publication No. 109, 32 p.

Thangsuphanich, I., 1976, Regional gravity survey over the southern Mineral Mountains, Beaver County, Utah: Salt Lake City, University of Utah, M.S. thesis, 37 p.

U.S. Geological Survey, 2007, National Water Information System database: Online, http://waterdata.usgs.gov/nwis, accessed February 2007.

U.S. Geological Survey National Gap Analysis Program, 2004, Provisional digital land cover map for the southwestern United States, version 1.0: Online, RS/GIS Laboratory, College of Natural Resources, Utah State University, http://earth.gis.usu.edu/swgap/, accessed October 2006.

Utah Division of Oil, Gas, and Mining, 2006, Oil and gas well database: Online, http://oilgas.ogm.utah.gov/Data_Center/LiveData_Search/main_menu.htm, accessed October 2006.

Utah Division of Water Resources, 1995, Utah state water plan—Cedar/Beaver Basin: Salt Lake City, Utah Department of Natural Resources, variously paginated.

Utah Division of Water Resources, 2001, Utah's water resources planning for the future: Salt Lake City, Utah Department of Natural Resources, 72 p.

Utah Division of Water Rights, 2006, Well-drilling database: Online, http://nrwrt4.waterrights.utah.gov/download/wrpod.exe, Utah Division of Water Rights, accessed February 2006.

Vuataz, F.D., and Goff, F., 1987, Water geochemistry and hydrogeology of the shallow aquifer at Roosevelt Hot Springs, southern Utah—a hot dry rock prospect: Los Alamos National Laboratory, contract report LA-11160-HDR, 63 p.

Wannamaker, P.E., Bartley, J.M., Sheehan, A.F., Jones, C.H., Lowry, A.R., Dumitru, T.A., Ehlers, T.A., Holbrook, W.S., Farmer, G.L., Unsworth, M.J., Hall, D.B., Chapman, D.S., Okaya, D.A., John, B.E., and Wolfe, J.A., 2001, Great Basin-Colorado Plateau transition in central Utah—an interface between active extension and stable interior, *in* Erskine, M.C., Faulds, J.E., Bartley, J.M., and Rowley, P.D., editors, The geologic transition, high plateaus to great basin—a symposium and field guide: Utah Geological Association Publication 30, p. 1–38.

Western Regional Climate Center, 2007, Climate summary–Utah: Online, http://www.wrcc.dri.edu/cgi-bin/cliMAIN.pl?utblan, accessed March 2007.

White, W.N., 1932, A method of estimating groundwater supplies based on discharge by plants and evaporation from soil: U.S. Geological Survey Water-Supply Paper 659-A, 96 p.

Wilde, F.D., Radtke, D.B., Gibs, J., and Iwatsubo, R.T., editors, 1998, National field manual for the collection of water-quality data: U.S. Geological Survey, Techniques of Water-Resources Investigations book 9, chapter A4, 103 p.

Zhu, C., and Murphy, W.M., 2002, On radiocarbon dating of groundwater: Groundwater, v. 38, p. 802–804.

Zhu, J., Young, M.H., and Cablk, M.E., 2007, Uncertainty analysis of estimates of groundwater discharge by evapotranspiration for the BARCAS study area: Reno, Nevada, Desert Research Institute Publication No. 41234, 28 p.

Zoback, M.L., and Anderson, R.E., 1983, Style of Basin-Range faulting as inferred from seismic reflection data in the Great Basin, Nevada and Utah, *in* Eaton, G., editor, The role of heat in the development of energy and mineral resources in the northern basin and range province: Geothermal Resources Council Special Report 13, p. 363–381.

APPENDICES

APPENDIX A

Well Log and Water Chemisty Data

Table A.1. *Summary of water-well logs shown on figures 6 and 7. Elevation, depths, and thicknesses are in feet. Dashed fields indicate no data. Logs are available from the Utah Division of Water Rights (2006).*

ID[1]	East[2]	North[2]	PLS Location[3]	Elevation[4]	Total depth[5]	Basin fill thickness	Bottom lithology[6]	Depth to water[7]	Screen interval	Depth to clay[8]	Recharge type[9]	Date[10]
1	365122	4281811	N1200 W2000 SE 32 24S 6W SL	5968	440	190	p	247	240-300	no clay	1	1/13/1998
2	363271	4280920	S2000 E2500 NW 06 25S 6W SL	5758	900	195	p	752	800-860	2-26	2	6/17/1999
3	323417	4273317	N1275 E160 SW 31 25S 10W SL	4882	100	100+	q	48	60-100	60-100	1	4/27/2002
4	324827	4264945	N450 E140 SW 29 26S 10W SL	4911	199	199+	q	13	--	79-115	3	7/28/1967
5	360653	4270127	S600 E350 NW 12 26S 7W SL	6063	100	100+	v	--	--	no clay	1	9/10/1977
6	359216	4264349	N1350 E1310 SW 26 26S 7W SL	6171	433	433+	q	250	250-433	no clay	1	4/29/1968
7	359231	4264060	N400 E1360 SW 26 26S 7W SL	6184	538	538+	v	280	--	no clay	1	11/11/1977
8	333221	4269279	S500 E830 NW 18 26S 9W SL	5036	248	248+	l	76	120-248	no clay	1	4/28/1975
9	360102	4273840	S1645 W1950 E4 26 25S 7W SL	5955	425	425+	l	62	157-425	no clay	1	1/20/1964
10	361478	4273049	S1630 W50 N4 36 25S 7W SL	5968	246	246+	v	90	95-246	no clay	1	9/15/1961
11	360645	4274356	N50 W170 E4 26 25S 7W SL	5935	385	385+	l	105	110-375	no clay	1	3/3/2006
12	335157	4274663	N1335 W3961 SE 29 25S 9W SL	5026	456	456+	q	95	100-456	no clay	1	2/24/1983
13	333422	4274694	N1311 W4368 SE 30 25S 9W SL	4964	399	399+	q	21	99-399	9-31	2	2/26/1983
14	333943	4274699	N1326 W2660 SE 30 25S 9W SL	4987	450	450+	q	35	150-450	1-28	2	1/24/1983
15	334550	4274700	N1330 W669 SE 30 25S 9W SL	5000	401	401+	l	40	101-401	no clay	1	12/15/1982
16	359308	4265140	S1345 E1520 NW 26 26S 7W SL	6122	600	600+	v	215	235-600	10-70	2	3/1/1977
17	360006	4264457	N1750 E1275 S4 26 26S 7W SL	6184	400	400+	q	295	340-380	no clay	1	11/10/1978
18	345333	4275603	0 W2450 SE 20 25S 8W SL	5489	297	297+	v	245	--	no clay	1	8/1/1979
19	327071	4270925	S1050 E1640 NW 09 26S 10W SL	4888	205	205+	q	--	30-205	0-21	2	6/1/1981
20	321012	4253897	N1225 W886 NE 02 28S 11W SL	5151	304	304+	q	--	224-304	87-119	2	7/13/1988
21	362240	4273459	S250 W225 NE 36 25S 7W SL	6017	253	253+	v	95	108-238	no clay	1	8/27/1991
22	362252	4275612	N1497 W310 SE 24 25S 7W SL	6112	350	350+	v	--	110-150, 260-360	no clay	1	--
23	360442	4265350	S525 W30 NE 26 26S 7W SL	6168	428	428+	v	--	170-420	180-270	2	5/25/1992
24	317331	4261515	S711 W406 N4 09 27S 11W SL	5305	200	28	l	88	135-165	no clay	1	12/14/2000
25	324467	4270090	N1500 W1435 SE 07 26S 10W SL	4888	100	100+	q	16	60-100	39-100	3	4/28/2002
26	321602	4260058	N100 E500 SW 12 27S 11W SL	5023	500	500+	q	104	220-500	no clay	1	8/5/1997
27	336298	4276601	S300 W400 E4 20 25S 9W SL	5059	178	178+	q	93	145-165	no clay	1	3/13/2002
28	363783	4276921	N650 W700 SE 18 25S 6W SL	6663	790	40	p	--	--	no clay	1	5/11/1999
29	320873	4253975	N1480 W1385 SE 35 27S 11W SL	5151	500	300	i	--	250-500	no clay	1	10/12/1981
30	359401	4266603	N838 E1774 W4 23 26S 7W SL	6079	406	406+	v	223	346-406	3-59	2	9/23/2003
31	361629	4275871	N2315 E326 S4 24 25S 7W SL	5955	353	353+	v	195	315-355	no clay	1	8/30/2004
32	356029	4254073	S620 E2200 NW 33 27S 7W SL	6243	320	320+	q	80	0-60	15-81	2	12/2/2006
33	355103	4254460	N650 W840 SE 29 27S 7W SL	6247	340	128	i	800	110-330	no clay	1	12/1/1979

Table A.1. *continued*

ID[1]	East[2]	North[2]	PLS Location[3]	Elevation[4]	Total depth[5]	Basin fill thickness	Bottom lithology[6]	Depth to water[7]	Screen interval	Depth to clay[8]	Recharge type[9]	Date[10]
34	356029	4254073	S620 E2200 NW 33 27S 7W SL	6243	495	345+	q	63	200-495	25-62	2	12/2/2006
35	321255	4253208	S1035 W90 NE 02 28S 11W SL	5121	453	453+	q	290	213-453	150-243	2	6/17/1999
36	326841	4259004	S230 E1830 W4 16 27S 10W SL	4977	405	405+	q	34	365-405	200-290	1	6/19/2000
37	313675	4261933	N460 W4435 SE 06 27S 11W SL	5909	500	60	p	60	--	0-60	2	11/23/2005
38	340361	4300267	N400 E600 SW 02 23S 9W	4872	395	395+	q	--	--	42-244	2	12/3/1997
39	342555	4298483	N150 W2640 SE 12 23S 9W	4836	800	800+	q	35	--	no clay	1	2/15/1952
40	343030	4300126	N200 W1120 SE1 23S 9W	4852	147	147+	q	21	48-55	no clay	1	7/1/1938
41	336344	4277843	N1100 W300 SE 17 25S 9W	5066	129	41	l	76	111-129	no clay	1	12/14/1940
42	315146	4293989	S500 W2200 NE 31 23S 11W	4528	705	705+	q	10	--	12-260	3	8/27/1978
43	315329	4293958	S600 W1600 NE 31 23S 11W	4531	920	920+	q	32	--	32-480	2	8/28/1978
44	356723	4286457	S48 E1857 NW 21 24S 7W	5548	500	500+	l	405	425-500	no clay	1	11/18/1956
45	355271	4282143	N1620 W2700 SE 32 24S 7W	6040	807	807+	l	777	--	no clay	1	4/11/1968
46	363465	4289555	E 2640 NW 7 24S 6W	5000	203	203+	q	100	--	no clay	1	9/15/1958
47	328037	4287357	S35 W1742 NE21 24S 10W	4852	250	250+	q	14	50-84	91-250	1	4/7/1969
48	323203	4282347	S1000 W1320 NE 1 25S 11W	4852	40	40+	q	20	--	0-20	2	10/10/1989
49	317884	4278661	--	4997	329	230	i	--	155-176	no clay	1	6/23/1947
50	347226	4277068	S488 E3680 NW 21 25S 8W	5568	320	320+	l	260	--	no clay	1	3/9/1936
51	356436	4276252	S1922 E1656 NW 21 25S 7W	5866	600	600+	v	360	400-600	no clay	1	10/12/1983
52	357225	4275624	S1260 W940 E4 21 25S 7W	5902	129	129+	q	--	--	no clay	1	5/3/1984
53	359218	4262198	S1500 72 W S4 35 26S 7W	6316	585	585+	v	295	--	no clay	1	12/28/1977
54	359761	4263878	S100 W2150 NE 35 26S 7W	6257	522	522+	v	261	--	no clay	1	7/15/1978
55	346534	4272032	S1105 E1250 NW 4 26S 8W	5591	360	360+	v	318	--	no clay	1	9/2/1944
56	333221	4269278	S503 E830 NW 18 26S 9W	5036	120	120+	q	68	--	no clay	1	9/17/1939
57	333221	4269278	S500 E830 NW 18 26S 9W	5036	248	248+	l	46	120-248	no clay	1	4/28/1975
58	333351	4265105	N1600 E1600 SW 30 26S 9W	5217	300	300+	l	191	210-300	no clay	1	3/2/1976
59	330041	4265186	N1350 E1300 SW 26 26S 10W	4980	140	140+	q	60	68-75, 89-110	no clay	1	9/21/1950
60	330047	4265087	N1320 E1320 SW 26 26S 10W	4984	385	385+	q	54	80-120, 160-200, 345-385	no clay	1	2/16/1979
61	325416	4263678	S1020 E2150 W4 32 26S 10W	4925	332	332+	q	31	248-254	144-164, 182-202, 282-332	3	9/15/1949

[1]ID corresponds to wells shown on figure 6,[2]easting and northing coordinates are in NAD 83 UTM zone 12 N, [3]Public Land Survey location from Utah Division of Water Rights (2006) database, [4]land surface elevation, in feet, at well site, [5]total depth of well, [6]lithology at the bottom of the hole; q = unconsolidated basin fill, l = lithified basin fill, v = volcanics that are part of the basin fill, p =Paleozoic carbonates, i = igneous rocks not part of the basin fill, [7]depth to water at the time of completion, [8]clay layer depth below the surface,[9]recharge type; 1 = primary recharge, 2 = secondary recharge, 3 = discharge, and [10]date of completion.

Table A.2. *Summary of oil-well logs shown on figure 6, and plates 1 and 2. Elevation, depth, and thickness are in feet.*

ID[1]	East[2]	North[2]	Elevation[3]	Name	Source[4]	Basin fill thickness	Total depth	Bottom lithology[5]
a	330319	4264971	4993	McCulloch Acord	Hintze and Davis, 2003	8320	12,650	i
b	334579	4274134	5000	#1	4302720293	3500+	3500	l
c	334077	4276255	5000	#2	4302720298	1545+	1545	l
d	335724	4277372	5056	Walter James 1	4302710080	3478+	3478	l
e	335444	4277735	5049	James 1	4302720296	3682+	3682	l
f	361859	4269650	6181	Cove Fort Sulphurdale	Hintze and Davis, 2003	60	7735	i
g	366642	4273156	6568	Cove Fort	Hintze and Davis, 2003	50	5207	p
h	363385	4283867	5942	Caroline Hunt	Hintze and Davis, 2003	0	8021	p

[1]ID corresponds to shown on figure 8, [2]easting and northing coordinates are in NAD 83 UTM zone 12 N, [3]land surface elevation, in feet, at well site, [4]numbers are API numbers, well logs available from the Utah Division of Oil, Gas, and Mining (2006), all other logs are taken from Hintze and Davis (2003), [5]lithology at the bottom of the hole; l = lithified basin fill, p =Paleozoic carbonates, i = igneous rocks not part of the basin fill.

Table A.3. *Summary of new and compiled groundwater chemistry data for the Cove Fort area. Samples 1 through 14 were collected for this study, samples 15 through 34 are from the USGS NWIS database (U.S. Geological Survey, 2007), and samples 34 through 40 are from Vuataz and Goff (1987). Dashed fields indicate no data. See text for further description.*

Site ID[1]	Site name	Sample date	East[2]	North[2]	Temp (°C)	pH	TDS (mg/L)	Water type[3]	Ca[4]	Na	Mg	K	Br	HCO_3	Cl	F	SO_4	NO_3	SiO_2	Sum anion[5]	Sum cation	Error %[6]
1	South Twin Well	06/04/07	345818	4287504	16.5	7.8	408	Ca-Mg-Na-HCO3	28.3	22.7	14.7	3.8	0.1	184.7	16.9	1.9	22.5	0.8	--	4.08	3.71	4.79
2	Cedars of Lebanon Well	06/04/07	354970	4290929	21.3	7.6	1097	Na-Mg-Cl-HCO3	37.4	167.5	36.3	40.6	1.0	353.9	222.3	1.2	99.8	0.12	--	14.22	13.17	3.83
3	Black Spring	06/05/07	340822	4292778	18.1	7.5	976	Na-Ca-Cl	73.6	187.7	16.1	9.3	1.7	142.2	318.6	2.6	109.8	2.71	--	13.79	13.4	1.45
4	Kaufman Spring	06/06/07	330111	4285809	12.8	7.9	388	Na-Ca-HCO3-SO4-Cl	29.7	35.2	9.0	7.0	0.8	122.4	31.4	0.6	42.9	1.05	--	3.85	3.93	-1.04
5	Kaufman Windmill	06/06/07	345302	4275597	16.3	8.1	389	Ca-Na-Mg-HCO3-Cl-SO4	34.2	30.2	11.3	6.9	0.3	120.5	46.4	0.4	44.2	1.22	--	4.25	4.13	1.41
6	Upper Coyote Spring	06/06/07	337524	4292021	18.6	7.7	528	Na-Ca-Cl-HCO3	40.1	64.0	13.5	4.4	0.6	122.5	113.1	3.2	47.6	0.74	--	6.37	6	2.99
7	Lower Coyote Spring	06/06/07	337351	4292972	13.6	7.5	776	Na-Ca-Cl-HCO3	64.4	105.1	20.0	6.7	0.2	216.5	181.3	3.5	84.1	0	--	10.6	9.6	4.95
8	Black Rock Well	06/06/07	328085	4287177	13.1	7.6	3407	Na-Cl-SO4	103.7	882.1	65.9	97.6	6.2	295.1	1358.8	5.7	509.2	0.76	--	54.18	51.46	2.58
9	Antelope Springs	06/06/07	337217	4280141	15.4	7.5	422	Ca-Na-HCO3-Cl	38.6	31.0	10.7	4.8	0.3	141.4	51.5	0.5	38.7	0.55	--	4.61	4.27	3.78
10	Cove Fort Well 1	06/07/07	360651	4274372	16.3	7.8	446	Ca-Mg-HCO3-Cl	63.2	19.9	17.1	4.9	0.5	200.7	55.1	0.3	20.3	1.91	--	5.31	5.55	-2.21
11	Yardley Well	06/07/07	360000	4264474	9.7	7.5	359	Ca-Mg-HCO3	44.3	11.4	10.7	2.2	0.1	168.8	25.4	0.3	9.0	0.4	--	3.69	3.64	0.68
12	Fourmile Spring	06/07/07	354500	4259567	7.3	7.0	238	Ca-HCO3-Cl	42.8	11.6	8.3	1.7	0.4	102.8	54.1	0.1	15.5	0.54	--	3.55	3.37	2.16
13	Twin Peak Spring	06/07/07	350754	4295304	27.9	7.3	4515	Na-Cl	145.0	1408.0	45.6	16.5	0.0	227.8	2170.9	5.0	388.5	0	--	73.32	72.66	0.46
14	Cove Creek	06/07/07	365366	4273925	16.8	8.1	860	Ca-Mg-Cl-HCO3	143.6	52.8	31.1	2.4	1.0	327.8	223.0	0.3	78.0	0	--	13.32	12.08	4.85
15	382259112565601	05/20/71	329765	4249903	20.5	8.0	313	Ca-Na-HCO3-Cl	33.0	29.0	5.7	2.2	0.0	130.0	33.0	1.0	25.0	--	27	3.63	3.43	2.85
16	382331113004301	12/02/55	324283	4251020	25.6	8.2	371	Na-HCO3-SO4	13.0	62.0	5.8	2.8	0.0	160.0	16.0	1.0	40.0	--	35	3.96	3.89	0.83
17	382349113021101	10/01/71	322165	4251615	20	7.9	671	Ca-Na-Mg-HCO3-SO4-Cl	64.0	72.0	23.0	4.9	0.0	200.0	86.0	1.0	130.0	--	45	8.49	8.34	0.85
18	382420112593001	07/16/81	326100	4252500	20.5	7.8	479	Na-Ca-Mg-Cl-HCO3	47.0	63.0	19.0	3.0	0.0	87.0	150.0	0.0	60.0	--	25	6.91	6.73	1.33
19	382919113004701	06/27/62	324361	4261948	13.3	8.2	801	Na-Cl-HCO3	25.0	203.8	15.0	0.0	0.0	250.0	240.0	1.2	20.0	--	22	11.53	11.35	0.81
20	383007112510101	09/11/57	338654	4262924	55	7.9	8107	Na-Cl	22.0	2500.0	0.0	488.0	0.0	156.0	4240.0	8.0	73.0	--	310	124.09	122.32	0.72
21	383101112365301	08/22/05	359161	4264407	15	8.1	521	Ca-HCO3-Cl	80.5	21.4	14.8	2.9	0.2	202.1	84.8	0.2	25.1	--	44.5	6.24	6.24	0.02
22	383105113140701	09/09/63	305056	4265662	17.8	8.4	905	Ca-Na-HCO3-Cl	110.0	84.0	25.0	1.7	1.0	364.0	150.0	0.4	51.0	--	53	11.71	11.24	2.02
23	383107112594301	09/09/63	326046	4265037	26.5	9.4	3445	Na-Cl	97.0	910.0	125.0	17.0	0.0	326.0	1900.0	1.0	14.0	--	24	59.28	56.27	2.6
24	383123113061201	09/07/63	316574	4265946	17.8	7.8	667	Na-Ca-Mg-Cl-HCO3	66.0	80.0	23.0	11.0	0.0	219.0	150.0	0.7	57.0	--	30	9.06	8.95	0.63
25	383138113063301	09/07/63	316076	4266420	15	7.8	547	Ca-Na-HCO3-Cl	56.0	64.0	14.0	6.7	0.0	240.0	78.0	0.4	40.0	--	24	7	6.9	0.71
26	383203113073701	09/07/63	314544	4267226	17.2	8.0	671	Na-Mg-Ca-Cl-HCO3	42.0	120.0	28.0	8.7	0.0	205.0	190.0	0.9	50.0	--	13	9.83	9.84	-0.06
27	383359113111701	09/07/63	309302	4270927	17.8	7.3	890	Ca-Mg-Na-Cl-HCO3	120.0	69.0	50.0	3.0	0.0	197.0	290.0	0.4	79.0	--	41	13.08	13.18	-0.37
28	383537113100701	09/07/63	311067	4273908	18	7.8	617	Na-Ca-Cl-HCO3	43.0	100.0	9.0	7.2	0.0	154.0	140.0	0.4	51.0	--	56	7.58	7.42	1.04
29	383545112352501	07/01/77	361444	4273124	13	7.8	1012	Ca-Mg-HCO3-Cl	180.0	50.0	37.0	2.7	0.0	370.0	180.0	0.2	130.0	--	31	13.86	14.27	-1.44
30	383617113140201	10/05/87	305412	4275278	13	7.6	572	Ca-Na-HCO3-Cl	64.0	64.0	17.0	7.9	0.0	263.6	86.0	0.4	39.0	--	15	7.58	7.58	0
31	383625112363201	11/11/77	359910	4274190	20	6.3	479	Ca-HCO3-Cl	62.0	20.0	12.0	6.0	0.0	196.0	43.0	0.0	42.0	--	49	5.3	5.1	1.88
32	383912112561201	09/03/87	331410	4280085	15	7.7	475	Ca-Na-Mg-HCO3-Cl	45.0	30.0	14.0	5.2	0.0	161.0	54.0	0.3	43.0	--	61	5.08	4.84	2.49
33	384306113112601	11/11/87	309543	4287693	23.5	7.9	593	Na-Mg-Ca-Cl-HCO3	38.0	86.0	24.0	9.0	0.0	134.0	150.0	0.0	70.0	--	41	7.89	7.84	0.27
34	385007112482201	03/05/87	343170	4300044	12	7.1	2013	Na-Ca-Mg-Cl	200.0	300.0	91.0	22.0	0.0	334.0	720.0	1.7	250.0	--	47	31.18	31.08	0.16
35	Bailey Spring	04/19/83	342448	4260377	6.1	7.2	252	Ca-Na-HCO3	32.0	15.0	5.6	2.3	0.0	127.0	14.2	0.8	9.3	--	23	2.72	2.77	-0.92
36	Shannon Spring	05/27/82	342200	4251319	7.3	7.7	58	Ca-Na-HCO3-Cl-SO4	4.0	3.0	1.0	0.6	0.0	10.0	3.8	0.7	5.0	--	15	0.41	0.42	-1.31
37	Well 26 9 18	04/20/83	333187	4269423	19.5	6.5	4017	Na-Ca-Cl-HCO3	318.0	910.0	15.6	62.0	1.2	860.0	1680.0	1.2	29.0	--	70	62.17	58.32	3.19
38	Willow Spring	05/27/82	346954	4261664	7.3	7.1	450	Ca-Na-HCO3	51.0	31.0	11.5	3.1	0.0	227.0	29.7	1.0	18.1	--	39	4.99	4.92	0.67
39	Wow 2	05/25/82	332777	4259793	32.3	7.2	2072	Na-Ca-Cl	151.0	494.0	33.0	19.0	0.2	229.0	1050.0	0.5	3.4	--	46	33.47	32.22	1.89
40	Wow 3	04/19/83	332534	4265687	23.5	8.3	4870	Na-Cl	77.0	1652.6	15.4	185.0	2.0	90.0	2840.0	0.9	3.2	--	2	81.72	81.72	0

[1]ID corresponds to site numbers shown on figures 13 and 14, [2]easting and northing coordinates are in NAD 83 UTM zone 12 N, [3]water type based on dominant ions, [4]concentrations of major anions and cations in mg/L, [5]meq/L sums of anions or cations, and [6]percent difference between the sum of anions and cations for a given sample.

APPENDIX B

Geologic Map Unit Descriptions (Plate 1)

Geologic map unit descriptions are taken from Best and others (1989), Hintze and Davis (2002), Hintze and others (2003), and Rowley and others (2005). See plates 1 and 2 for further explanation.

Quaternary

Qal_1 **Alluvium, late Holocene**—Youngest alluvium in the channels, floodplains, and low terraces of the Sevier River, Beaver River, Chalk Creek, Corn Creek, Cove Creek, and other large streams; includes overbank and marsh deposits in abandoned meanders of the Sevier River; consists of sand, silt, and clay with lenses of gravel; silt in lower Pahvant Valley; less than 100 feet (30 m) thick along Sevier River; mostly 0 to 20 feet (0–6 m) thick, but may be thicker locally.

Qal_2 **Alluvium, middle and early Holocene**—Sand, silt, and clay in the floodplain of Cove Creek, isolated remnants of older Chalk Creek and Corn Creek sand and gravel near Fillmore and Kanosh (respectively), along a stream near White Sage Flat, in the Pahvant Range along East Creek, and south of the Sevier River southwest of Elsinore; 0 to 30 feet (0–9 m) thick.

Qac **Alluvium and colluvium, undifferentiated**—Mixed alluvial and colluvial deposits that consist of fluvially reworked coarse-grained colluvium and/or alluvium with a significant colluvium component; also includes talus; generally 0 to 50 feet (0–15 m) thick, but may be thicker locally.

Qaf_1 **Younger alluvial-fan deposits**—Poorly sorted silt, sand, and pebble, cobble, and boulder gravel deposited by streams, sheetwash, debris flows, and flash floods on alluvial fans, and in canyons and mountain valleys; post-Bonneville shoreline in age; mostly 0 to 60 feet (0–18) thick, but may be up to 165 feet (50 m) thick along upper Sevier River.

Qaf_2 **Older alluvial-fan deposits**—Poorly sorted silt, sand, and pebble, cobble, and boulder gravel deposited by streams, debris flows, and flash floods on alluvial fans, and in canyons and mountain valleys above the Bonneville shoreline; includes colluvium in canyons and mountain valleys; Q – on flanks of Mineral Mountains is mostly pea-sized grus, locally including larger clasts and significant eolian silt; mostly pre-Lake Bonneville in age, but locally includes younger material; up to 200 feet (60 m), or more, in thickness.

Qat **Stream-terrace deposits**—Sand and gravel that form surfaces 5 to 40 feet (2–13 m) above the level of adjacent modern streams; maximum thickness about 10 feet (3 m).

Qat_1 **Younger stream-terrace deposits**—Sand and gravel that form dissected surfaces as much as 15 feet (5 m) above the level of adjacent modern streams; maximum thickness about 10 feet (3 m).

Qat_2 **Older stream-terrace deposits**—Sand and gravel that form well dissected surfaces 15 to 40 feet (5–13 m) above the level of adjacent modern streams; maximum thickness about 10 feet (3 m).

Qmu **Mass-movement deposits, undivided**—Masses of soil, sand, rock, and boulders that have moved downslope under the influence of gravity; includes soil creep, slopewash, talus, and fan alluvium, and locally slides and slumps; 0 to 100 feet (0–30 m) thick. Includes dissected older deposits on and near Bull Claim Hill southeast of Richfield.

Qms **Mass movement deposits, slides and slumps**—Masses of soil, sand, rock, and boulders that have moved downslope under the influence of gravity; includes slides and slumps; 0 to 100 feet (0–30 m) thick.

Qpm **Playa mud**—Laminated, silty, fine sand, silt, and clayey silt infused with various salts, gypsum, and calcium carbonate; thickness probably 20 feet (6 m) or less.

Qea **Eolian and alluvial deposits, mixed**—Interbedded and mixed windblown and alluvial sand and silt in the volcanic terrain west of Cove Fort; up to 20 feet (6 m) thick.

Qst **Spring travertine**—Cellular to dense and banded, spring-deposited travertine in southern Pahvant Valley and in White Sage Flat and siliceous spring deposits near Roosevelt Hot Springs in Beaver County; 0 to 90 feet (0–30 m) thick.

Qsa **Altered material**—White, porous aggregates of opaline silica, gypsum, native sulfur, and anhydrite, and remnant quartz and cristobalite produced by acid leaching; related to geothermal system; located near Cove Fort in Holocene(?) and likely Pleistocene alluvial fans and bedrock; only the largest area, exposed in a pit, is mapped; up to 105 feet (33 m) thick in this pit.

Qdg **Deltaic sand and gravel**—Silty, fine- to coarse-grained sand and gravel deposited by the Beaver River in

Lake Bonneville and then distributed by waves and currents; 0 to 24 feet (0–7 m) thick.

Qlg **Lacustrine gravel**—Silty, fine- to coarse-grained sand and gravel in shore zone deposits of Lake Bonneville; 0 to 30 feet (0–9 m) thick.

Qls **Lacustrine sand**—Fine- to coarse-grained sand, marly sand, and pebbly sand deposited in shore zone of Lake Bonneville as beaches, spits, and offshore bars; 0 to 30 feet (0–9 m) thick.

Qlf **Fine-grained lacustrine deposits**—Tan to light-gray, calcareous silts that are deep-water sediments of Lake Bonneville; locally includes younger alluvium; thickness probably 10 feet (3 m) or less.

Qlae **Mixed lacustrine, alluvial, and eolian deposits**—Mixed and reworked gravelly lacustrine and alluvial deposits on piedmont slopes; grades from pebbly sand and silt to sandy pebble gravel; lacustrine material was deposited in Escalante Bay of Lake Bonneville and perhaps of older Pleistocene lakes; maximum thickness about 20 feet (6 m).

Qrl **Lava flows**—Two compound lava flows of resistant, black to light-gray, flow-foliated, aphyric, high-silica rhyolite, most of which is devitrified but much of which is basal vitrophyre (obsidian); overlain by Qrt; the northern flow, the Bailey Ridge flow in Mag Wash, has been mined for perlite, whereas the southern flow, the Wildhorse Canyon flow, is famous for its implement-grade obsidian, artifacts of which have been found in archeological sites throughout the West; K-Ar age about 0.8 Ma (Lipman and others, 1978); maximum thickness of each flow is about 300 feet (100 m).

Qbc **Basalt of Cunningham Hill**—Resistant, dark-gray, scoriaceous to massive basalt lava flow that filled the ancestral valley of Cunningham Wash, in the west Beaver basin (Machette and others, 1984); K-Ar age 1.1 Ma (Best and others, 1980); maximum thickness about 30 feet (10 m).

Qbk **Basaltic andesite of Crater Knoll**—Resistant, dark-gray and black, blocky, vesicular, crystal-rich basaltic andesite lava flows and red and dark-gray cinder cone of ash and scoria, northwest Beaver basin; has a K-Ar age of 1.0 Ma (Best and others, 1980) but interpreted to overlie Qrt by Machette and others (1984) and more likely is closer to 0.5 Ma, the age of the lithologically similar basaltic andesite of Cove Fort just to the north of the map area (Steven and Morris, 1983; Hintze and others, 2003); maximum thickness about 100 feet (30 m).

Qll **Lacustrine lagoon deposits**—Sand, silt, clay, and silty marl that accumulated in lagoons behind (landward from) gravel barrier beaches of Lake Bonneville; present west of Milford, Utah and east of Twin Peaks; locally includes younger alluvium; generally less than 10 feet (3 m) thick.

Qlm **Lacustrine marl**—Fine-grained, thinly bedded to laminated, white to light-gray, offshore to deep-water marl deposited in Lake Bonneville; ostracodes are abundant throughout marl and, locally, gastropods are present at top and base of marl; 0 to 30 feet (0–9 m) thick. A layer of basaltic ash of Pahvant Butte is interbedded in the upper part of Qlm and is commonly 1 to 6 inches (2.5–15 cm) thick. This gray to black basaltic ash was blown into the atmosphere during a hydrovolcanic eruption when Lake Bonneville was near its highest level about 15,500 yr B.P.

Qla **Lacustrine and alluvial deposits, undifferentiated**—Mixed and reworked gravelly lacustrine and alluvial deposits on piedmont slopes; grades from pebbly sand and silt to sandy pebble gravel; generally 0 to 12 feet (0–4 m) thick, but may be thicker locally.

Qvb_4 **Basalt of Beaver Ridge**—Consists of older flow series, dated at 0.9 Ma, of diabasic basalts about 80 feet (24 m) thick, and younger series, dated at 0.5 Ma, of similar composition but fine-grained to glassy, and about 120 feet (37 m) thick.

Qcg **Basaltic andesite of Cedar Grove**—Dark-gray to black, porphyritic basaltic andesite with phenocrysts of plagioclase, clinopyroxene, hypersthene, magnetite, and olivine in a felted matrix; maximum thickness about 200 feet (60 m); age about 0.3 Ma.

Qcf **Basaltic andesite of Cove Fort**—Dark-gray to black, vesicular to dense basaltic andesite containing small phenocrysts of plagioclase, pyroxene, magnetite, olivine, and sparse corroded quartz in a felted to glassy matrix; age about 0.5 Ma; maximum thickness about 800 feet (250 m).

Qvrd **Rhyolite of Mineral Mountains, dome**—Tan perlitic glassy dome, commonly pumiceous and brecciated and containing scattered black obsidian fragments; northernmost of several similar domes in the Mineral Mountains; age 0.54 Ma.

Qvrt **Rhyolite of Mineral Mountains, tuff**—White to tan, poorly consolidated tuff vented from nearby rhyolite

dome in Mineral Mountains; less than 100 feet (30 m) thick; probably same age as nearby rhyolite dome (Qvrd).

Qrk **Basaltic andesite of Red Knoll**—Dark-gray to black, dense to vesicular, porphyritic basaltic andesite to latite lava flow with a blocky scoriaceous surface; contains 30 to 45% phenocrysts, mostly labradorite and pyroxene, in glassy to finely crystalline matrix; located southwest of Cove Fort and overlies basaltic andesite of Crater Knoll; vent lies a mile (1.6 km) south of map area; maximum thickness less than 200 feet (60 m).

Qck **Basaltic andesite of Crater Knoll**—Dark-gray to black, porphyritic basaltic andesite lava flows similar to Qrk; 40 to 45% phenocrysts, mostly labradorite and pyroxene; glassy to finely crystalline matrix, containing microlites of plagioclase, pyroxene, olivine(?), and opaque minerals; vent is 2 miles (3 km) south of map area southwest of Cove Fort; age 1.0 Ma; thickness in map area less than 100 feet (30 m).

Qvb_5 **Basalt of Black Rock**—Dark-gray, vesicular basalt composed of about 40% small zoned plagioclase phenocrysts, with lesser phenocrysts of clinopyroxene, olivine, and Fe-Ti oxides; age about 1.0–1.3 Ma; maximum thickness about 200 feet (60 m).

Quaternary-Tertiary

QTlf **Fine-grained lacustrine deposits of Sevier Desert**—Brown and light olive-gray, calcareous, lacustrine silt and silty clay with minor sand; offshore to deep-water sediments that are Pliocene to middle Pleistocene in age; 0 to 870 or more feet (0–270+ m) thick.

QTln **Near-shore lacustrine limestone of Sevier Desert**—Light-gray limestone and conglomeratic limestone that comprise the shoreline facies of QTlf; up to 90 feet (27 m) thick.

QTaf **Quaternary-Tertiary alluvial-fan deposits**—Poorly sorted silt, sand, and gravel, including boulders, in Dog Valley, upper Cove Creek, and in northeast corner of map area; locally has a calcic soil with a stage IV carbonate morphology (so early Pleistocene age) near the top of the deposit; 0 to 300 feet (0–90 m), or more, thick.

QTs **Basin-fill sedimentary rocks**—Poorly to moderately consolidated, tan and gray, tuffaceous sandstone and subordinate mudstone, siltstone, and conglomerate deposited in basins of different ages (Pliocene to late Miocene) and origins; deposits generally consist of fanglomerate near the present basin margins, piedmont slope deposits farther toward the centers of the basins, and lacustrine deposits near the centers of the basins; thickness of QTs at least 2000 feet (600 m).

Tertiary

Thb **Basalt of High Rock**—Brown-weathering, black, fine-grained flow rock containing small phenocrysts in a partly glassy matrix; Pliocene(?); maximum thickness 150 feet (50 m).

Tbm **Basaltic andesite of Burnt Mountain**—Black to medium-gray, fine to medium-grained, porphyritic, crystal-rich basaltic andesite with phenocrysts of labradorite, olivine, orthopyroxene, and clinopyroxene; map unit includes vent cone; age about 2.1 Ma; maximum thickness about 500 feet (150 m).

Trt **Rhyolite of North Twin Peak, South Twin Peak, and Mid-Dome**—Light-brownish-gray rocks from these three rhyolite domes are of similar, but not identical, composition; phenocryst content from 3 to 30% and includes plagioclase, quartz, sanidine, and biotite; groundmass is microcrystalline quartz, feldspar, Fe-Ti oxides, apatite, sphene, and zircon; age 2.35 to 2.5 Ma; thickness (exposed height) up to 1000 feet (300 m).

Tcc **Basalt of Cove Creek**—Dark-gray, olivine-tholeiite flow rock; map unit includes cone; age about 2.55 Ma; maximum thickness about 400 feet (120 m).

Tcr **Rhyolite of Cudahy Mine**—Interbedded black obsidian and light-gray felsite; felsite is devitrified and shows relict flow-layering, spherulites, and lithophysae; obsidian commonly shows "snowflake" clusters; age about 2.2 to 2.6 Ma; maximum thickness about 500 feet (150 m).

Toc **Oak City Formation**—Sandy, bouldery gravel; poorly to well cemented; forms dissected alluvial apron on west side of Pahvant Range; bed of Cudahy Mine pumice, K-Ar dated as 2.6 Ma, is within upper Oak City Formation in map area, so late Pliocene and Miocene(?) age; base of formation not exposed; estimated thickness

as much as 2000 feet (600 m).

Tse **Sevier River Formation**—In northeast corner of map area in Sevier County, light-gray, yellowish- or greenish-gray, poorly to moderately sorted mudstone, sandstone, conglomerate, and carbonaceous mudstone that is probably more than 600 feet (180 m) thick. South of Richfield in Sevier County, mostly moderately indurated, pale brownish- or reddish-gray sandstone, pebble to boulder conglomerate, mudstone, and siltstone of fluvial and, locally, lacustrine origin; volcanic clasts are common in south, decreasing northward; local interbedded tuffs and intertongued basalts yield K-Ar ages of 5.6 to 13.6 Ma; exposed thickness at least 330 feet (100 m), but total thickness may be up to 1000 feet (300 m).

Try **Young rhyolite lava flows**—Small, resistant, mostly gray, flow-banded, crystal-poor, high-silica rhyolite volcanic domes and subordinate pyroclastic material, although the dome of Phonolite Hill has relief of more than 1000 feet (300 m), in most other places the maximum thickness of the rhyolites is less than 200 feet (60 m).

Tir **Rhyolite porphyry**—Resistant, mostly small, gray, tan, and pink, hydrothermally altered dikes, sills, plugs, and a laccolith(?); phenocrysts of K-feldspar, quartz, plagioclase, and biotite; mostly high-silica rhyolite and fine-grained granite in the Mineral Mountains (Sibbett and Nielson, 1980) that intrudes rocks as young as the main granitic batholith of the Mineral Mountains (Tig); most bodies too small to be mapped at this scale but those shown on the map are as much as several hundred feet (100 m) across and more than a mile (1.6 km) long.

Tb **Basalt flows in northern Tushar Mountains**—Dark-gray, black, and red, locally vesicular and amygdaloidal olivine basalt and basaltic andesite lava flows, flow breccia, and cinder cones, scoria, and ash; not isotopically dated within map area, but similar basalts K-Ar dated as at least 10.9 to 12.9 Ma, and other basalts are as young as 7.4 Ma; maximum thickness about 425 feet (130 m).

Trg **Rhyolite of Gillies Hill**—Lava flows and domes of light-gray to white, flow-layered, dense to vesicular rhyolite; aphyric to porphyritic, with phenocrysts of plagioclase and biotite; located south-southwest of Cove Fort; age about 9 Ma; more than 1000 feet (300 m) high.

Tgp **Gabbro porphyry of Cedar Grove**—Dark-gray, strongly porphyritic gabbro with phenocrysts of labradorite and clinopyroxene in a felted matrix of plagioclase microlites and Fe-Ti-oxide grains; cuts and alters Bullion Canyon Volcanics (Tbc) southwest of Cove Fort.

Trd **Rhyolite porphyry dikes**—Speckled gray rock with about 10% phenocrysts each of K-feldspar and quartz, and a trace to 3% biotite in a matrix of granophyric intergrowths; age about 11–12 Ma; dikes cut granodiorite stock (Tgm) and quartz monzonite (Tqm) in Mineral Mountains.

TpCg **Intrusion and gneiss complex**—Tertiary dikes and other intrusive bodies interleaved with Neoproterozoic(?) gneisses; individual units cannot be shown at map scale; age of youngest dikes (Trd) 11 Ma; exposed on west side of Mineral Mountains.

Tdd **Microdiorite dikes**—Thin, resistant, dark-green to black dikes with subdiabasic texture; contain plagioclase (andesine), hornblende, actinolite, and biotite, with minor K-feldspar, and 1 to 3% each sphene, Fe-Ti oxides, apatite, orthopyroxene, and alteration minerals; cut granite dikes (Tgd) and quartz monzonite (Tqm) in Mineral Mountains, so less than 18 Ma.

Tgd **Granite dikes**—Includes fine-grained, leucocratic, and biotite-rich varieties, listed youngest first from intrusive relations; contain about 54% K-feldspar, 27% quartz, 9 to 16% plagioclase, and 3 to 7% biotite; biotite-granite dikes are medium grained and older than the syenite (Tsm); dikes intrude Tqm in Mineral Mountains, so less than 18 Ma.

Tsm **Syenite of Mineral Mountains**—Light-gray, coarse- to medium-grained syenite stock; weathers to grus; contains microcline, lesser plagioclase and quartz, minor biotite and sphene, and accessory Fe-Ti oxides, apatite, hornblende, and zircon; cut by most granite dikes, intrudes unit Tqm in Mineral Mountains, so less than 18 Ma.

Tqm **Quartz monzonite of Mineral Mountains**—Speckled gray, biotite-rich, coarse-grained quartz monzonite that forms massive light-brownish gray stock exposed extensively in the central Mineral Mountains south of the Millard County line; age about 18 Ma.

Tqmr **Quartz monzonite**—Gray to pinkish gray, medium graine intrusive bodies with hypidiomorphic-granular texture; consists principally of K-feldspar and andesine, with quartz, biotite, and augite; mapped west and

southwest of Milford; various K-Ar ages for this unit range from 21.3 ± 0.6 Ma to 30.0 ± 1.0 Ma (Best and others, 1989).

Tdm **Diorite of Mineral Mountains**—Medium-grained, equigranular, biotite hornblende diorite; contains small apatite and sphene crystals; exposed on northwest flank of Mineral Mountains; age between 18 and 25 Ma based on intrusive relationships with Tqm and Tgm.

Tmj **Joe Lott Tuff Member, Mount Belknap Volcanics**—Light-gray or brownish-gray, crystal-poor, slightly to moderately welded, alkali rhyolite ash-flow tuff containing 1 to 2% phenocrysts of quartz, sodic plagioclase, sanidine, and a trace of biotite; outflow from Mount Belknap caldera, mostly south of map area; age about 19 Ma; thickness about 200 feet (60 m) near Cove Fort and as much as 400 feet (120 m) to east in Sevier County.

Tmv **Volcaniclastic rocks**—Soft to moderately resistant, light-gray and white, mostly intracaldera volcanic mudflow breccia derived from, and deposited within, the Mount Belknap caldera; includes landslide debris and fluvial sandstone and conglomerate; thickness about 800 feet (240 m).

Tmb **Mount Baldy Rhyolite Member, Mount Belknap Volcanics**—Resistant, light-gray, flow-foliated, crystal-poor, rhyolite lava flows and dikes; consist mostly of fine-grained mosaic of quartz and alkali feldspar, with minor plagioclase, biotite, and hematite; deposited mostly within Mount Belknap caldera; age uncertain; maximum exposed thickness of about 2600 feet (800 m) is in caldera that is mostly south of map area.

Tmm **Middle tuff member**—Light-gray and tan, poorly welded, crystal poor, intracaldera rhyolite ash-flow tuff; lithologically similar to, and locally continuous across Mount Belknap caldera margin into upper part of Joe Lott Tuff Member (19 Ma; Tmj); thickness to south up to about 1640 feet (500 m), but thinner in map area.

Tmbl **Blue Lake Rhyolite Member and lower tuff member**—Lower parts of the intracaldera fill of the Mount Belknap caldera, consisting of (1) the Blue Lake Member, a moderately resistant, gray, flow-foliated, crystal-poor lava flow about 1100 feet (340 m) thick; and (2) the underlying lower tuff member, lithologically similar to Tmm and Tmj and at least 1500 feet (460 m) thick, with its base not exposed.

To **Osiris Tuff, outflow facies**—Resistant light-gray and reddish-brown, moderately crystal-rich, densely welded, rhyodacitic ash-flow tuff with drawn-out pumice fragments; contains one or two cooling units, commonly with basal black vitrophyres; outflow from Monroe Peak caldera in southeast part of map area; age 23 Ma; maximum thickness about 200 feet (60 m).

Tig **Granitic intrusive rocks**—Mostly resistant, mostly gray, high-alkali and mostly high-silica (bimodal igneous episode that is synchronous with basin-range extension) granite and related rocks; includes small, fine-grained intracaldera stocks within the Mount Belknap caldera in the Tushar Mountains (Rowley and others, 2002); to the west, in the Mineral Mountains, includes the main mass of the Mineral Mountains batholith, the largest exposed batholith in Utah, which is made up of individual stocks and sheeted dike-like masses of fine- to coarse-grained or porphyritic, nonfoliated, mostly granite (classification of intrusive rocks from International Union of Geological Sciences) but locally monzonite and syenite (Sibbett and Nielson, 1980; Nielson and others, 1978, 1986; Coleman, 1991) interpreted on the basis of U-Pb zircon and $^{40}Ar/^{39}Ar$ dates that the main granitic batholith in the Mineral Mountains has an age of about 17 to 18 Ma.

Tisg **Syenite of Cedar Grove**—Medium to coarse-grained, porphyritic to equigranular rock containing mostly orthoclase and plagioclase, lesser hornblende and pyroxene, and sparse biotite; age 23 Ma.

Tgm **Granodiorite of Mineral Mountains**—Speckled gray, medium-grained, equigranular, locally foliated rock composed of plagioclase, K-feldspar, quartz, hornblende, biotite, and trace minerals; stock weathers to gray, sandy grus; age about 25 Ma.

Tzt **Zeolite tuff**—Soft, white, partially welded, crystal-poor, rhyolitic ash-flow tuff; contains 10 to 30% lithic fragments; matrix altered to the zeolite mineral clinoptilolite; may correlate with 24.6 Ma (corrected) Leach Canyon Formation; exposed near Cove Fort where it overlies the tuff of Albinus Canyon and intertongues with Bullion Canyon Volcanics; about 400 feet (120 m) thick.

Tba **Basaltic andesite lava flows**—Resistant, dark-gray and black, locally vesicular and amygdaloidal, crystal-poor, basaltic andesite lava flows; exposed in southeast Pahvant Range; intertongued with Antimony Tuff and tuff of Albinus Canyon; maximum thickness about 500 feet (150 m).

Tac **Tuff of Albinus Canyon**—Red to gray, crystal-poor, densely welded, trachytic ash-flow tuff; contains few phenocrysts; flow structures and lineate vesicles are characteristic; has several thin cooling units, locally separated by thin beds of volcanic mudflow breccia, conglomerate, and sandstone in map area; lithologically

similar to overlying Antimony Tuff Member of the Mount Dutton Formation; age 25.3 Ma; maximum thickness about 650 feet (200 m).

Ti **Isom Tuff**—Multiple trachydacite ash-flow tuffs; exposed in Tunnel Spring Mountains, where it is about 20 feet (6 m) thick; also exposed near Brown Knoll and on the east flank of the San Francisco Mountains, where it is 33 to 50 feet (10–15 m) thick; K-Ar age 25.7 Ma.

Tigd **Granodiorite of Beaver Lake Mountains**—Light- to medium-gray, medium-grained, holocrystalline intrusive rocks; mostly granodiorite, but includes one small quartz-monzonite stock, granite border zones, dike-like bodies of quartz diorite and monzonite, and local aplite dikes; K-Ar ages 27.7 and 29.1 Ma.

Tbc **Bullion Canyon Volcanics**—Widely distributed, heterogeneous, varicolored, volcanic mudflow breccia, lava flows, flow breccia, ash-flow tuff, and fluvial volcanic conglomerate and sandstone; erupted and eroded from several clustered stratovolcanoes; lava flows are mostly crystal-rich dacite with some fine-grained, crystal-poor, black andesite, as well as rhyodacite and quartz latite lava flows; age at least 30 to 22 Ma; maximum thickness at least 5000 feet (1500 m) in Sevier County.

Tm **Marble**—Contact-metamorphosed Paleozoic carbonate rocks; light gray to white, locally blotchy or streaked; locally brecciated; in Beaver Lake Mountains, parent carbonates were probably Devonian and Mississippian limestone.

Tic **Calc-alkaline intrusives, undivided**—Moderately resistant, gray, tan, pink, and brown, crystal-rich monzonite, low-silica granite, granodiorite, and monzodiorite; the calc-alkaline sources of Tbc and several other volcanic units, and the calc-alkaline early products of the Mineral Mountains batholith.

Tbct **Three Creeks Tuff Member**—Resistant, light-gray and tan, moderately welded, crystal-rich, dacitic ash-flow tuff; derived from the Three Creeks caldera in the south Pahvant Range; K-Ar age is 27 Ma; the most voluminous ash-flow tuff in the Marysvale volcanic field and formerly was included within the Needles Range Group; maximum thickness about 700 feet (220 m).

Tbci **Monzonitic/latitic intrusions in Bullion Canyon Volcanics**—Dark- to light-gray, tan, and brown, crystal-rich monzonite and quartz monzonite and strongly porphyritic latite and quartz latite in small plutons and plugs; probably solidified magma sources of other rocks in the Bullion Canyon Volcanics; ages cluster about 23 Ma; near Cove Fort intrusions cut Three Creeks Tuff (27 Ma) and are unconformably overlain by Osiris Tuff (23 Ma).

Tj **Jasperoid**—Irregular masses of light- to dark-brown, fine-grained, silicified rock within marble bodies in Beaver Lake Mountains; produced by hydrothermal alteration and emanations from nearby igneous intrusions; largest mass about 100 feet (30 m) thick.

Tnu **Upper Needles Range Group**—Crystal-rich, dacitic ash-flow tuffs of the Lund Formation, Wah Wah Springs Tuff, and the Cottonwood Wash Tuff; Lund Formation only present in Halfway Hills; thickness up to 2300 feet (700 m); ages about 28, 30.5, and 31 Ma, respectively.

Tbr **Breccia of Cat Canyon**—Coarse, recemented breccia of gray, Cambrian carbonate rocks in Cricket Mountains; likely an indurated talus or rubble, rather than of tectonic origin; as much as 165 feet (50 m) thick.

Tw **Volcanic rocks of Wales Canyon**—Moderately resistant, red, moderately crystal-rich, intermediate-composition lava flows and densely welded ash-flow tuff; exposed near Cove Fort; overlies volcanic rocks of Dog Valley and locally intertongues with Three Creeks Tuff on north margin of Marysvale volcanic field; about 440 feet (135 m) thick. Locally resembles Wah Wah Springs Formation.

Tdt **Tuff of Dog Valley**—Mostly resistant, gray, tan and pink, crystal-rich, moderately welded, dacitic, ash-flow tuff; exposed near Cove Fort and on the north flank of the Marysvale volcanic field; locally interlayered with volcanic rocks of Dog Valley; looks like tuff of Wah Wah Springs Formation and Three Creeks Tuff; Ar/Ar age 33.6 Ma; maximum thickness about 400 feet (120 m).

Tsr **Skull Rock Pass Conglomerate**—Unconsolidated, boulder and cobble conglomerate of Paleozoic clasts that lies above Tunnel Spring Tuff and beneath tuffs of the Needles Range Group; lies beneath the Windous Butte Tuff in the Burbank Hills; overlies Horn Silver Andesite in Iron Mine Pass quadrangle; sand and silt matrix is locally tuffaceous; contains rare igneous rock clasts; as much as 350 feet (107 m) thick.

Tdv **Volcanic rocks of Dog Valley**—Heterogeneous assemblage of andesitic to dacitic rocks including lava flows, volcanic mudflow breccias, and minor moderately welded ash-flow tuff similar to some in the Needles Range Group, but here recognized as tuff of Dog Valley; age about 33 Ma; maximum thickness up to 1200 feet (370

m).

Ths **Horn Silver Andesite**—Heterogeneous unit of varicolored andesitic, dacitic, and latitic rocks in the northern San Francisco and Beaver Lake Mountains; rock types include agglomerate, tuff, and volcanic conglomerate and sandstone, as well as dark-colored, medium to fine-grained andesitic lava flows that increase in thickness and number to the south; total thickness up to about 2000 feet (600 m); K-Ar ages about 31.6 and 35.0 Ma.

Thr **Conglomerate of High Rock Pass**—Unconsolidated, bouldery conglomerate with gray, tuffaceous matrix; restricted to the High Rock quadrangle in the San Francisco Mountains where it may be as much as 300 feet (90 m) thick; age uncertain, appears to underlie Horn Silver Andesite.

Tau **Aurora Formation**—Mostly poorly resistant, pale-gray, reddish, and yellowish-gray, bentonitic siltstone and claystone, with beds of thin to medium-bedded, medium-gray limestone, fine-grained sandstone, and pebble to cobble conglomerate; contains upwardly increasing amounts of fine-grained rhyolitic ash and reworked volcanic detritus; coarsens to southwest; 38 to 40 Ma age implies volcanic source in west-central Utah; maximum thickness about 1200 feet (360 m) southeast of Kanosh thinning to 550 feet (170 m) near Richfield, and to less than 200 feet (60 m) near Cove Fort.

Tf **Flagstaff Formation**—White to very-light-gray, locally vuggy, thin to thick-bedded limestone that locally contains small bivalves and high-spired gastropods; limestone is interbedded with pebble and cobble conglomerate with a red sandstone or mudstone matrix; mottled purple limestone and yellow limy mudstone present here are also found in Claron Formation of southern Utah and Flagstaff Formation in central Utah; up to 585 feet (180 m) thick.

Tg **Green River Formation**—Yellowish-gray to pale-brown, cherty, algal, and oolitic limestone and dolomite, calcareous, fine-grained sandstone, and greenish-gray shale; about 800 feet (245 m) partial thickness exposed in northeast map area and thins to absence southwest of Richfield.

Tertiary-Cretaceous

TKbr **Tectonic breccia**—Includes breccia in Neoproterozoic rocks in the San Francisco Mountains, age uncertain; breccias are as much as 0.35 miles (0.56 km) wide and several miles long.

Cretaceous

Kcg **Conglomerate of Mineral Mountains**—Pebble-cobble conglomerate of limestone, quartzite, sandstone, and chert clasts in a sandy limestone matrix where it rests on Cambrian rocks; similar conglomerate present beneath overthrust Cambrian quartzite; may be Tertiary where it rests on other Cambrian rocks; about 110 feet (33 m) thick.

Kc **Canyon Range Conglomerate**—Massive, reddish-gray conglomerate with interbedded sandstone lenses; present locally beneath North Horn Formation in the central Pahvant Range and southwest of Kanosh; rests unconformably on Paleozoic strata; maximum exposed thickness about 850 feet (260 m).

Jurassic

Jn **Navajo Sandstone**—Reddish-brown, fine-grained, cross-bedded, cliff-forming sandstone; exposed thickness about 2000 feet (600 m).

Triassic

Trcu **Chinle Formation, upper member**—Interbedded, varicolored sandstone, siltstone, mudstone, and shale; prone to slump; thickness 69 to 274 feet (21–83 m).

Trcs **Chinle Formation, Shinarump Conglomerate Member**—Interbedded quartzite, pebble conglomerate, and

white to brown, coarse sandstone that contains petrified wood; thickness 177 to 566 feet (54–172 m).

Trm **Moenkopi Formation**—Interbedded brownish-red sandstone, siltstone, shale, and gray limestone; minor cross-beds, mud cracks, and ripplemarks are common; fossil brachiopods and ammonoids abundant locally; maximum thickness 1876 feet (572 m).

Permian

Ppt **Plympton, Kaibab, and Toroweap Formations, undivided**—Mapped only north of Minersville; maximum thickness several hundred feet (30–90 m).

Ppk **Plympton and Kaibab Formations, undivided**—Mapped only east and north of Minersville. Plympton Formation – Moderately resistant, gray and tan, thin-bedded, ledgy, chert-bearing, marine dolomite and limestone; maximum thickness about 200 feet (60 m).

Pk **Kaibab Formation**—Resistant, light- to dark-gray, medium-grained, thin- to thick-bedded, fossiliferous marine limestone characterized by cliffs and ledges and by abundant dark-brown chert concretions and beds; maximum thickness about 550 feet (170 m).

Pp **Pakoon Dolomite**—Alternating soft and resistant, light- to dark-gray and pink, ledgy and cliffy, medium-grained, thick-bedded, locally chert-bearing, marine dolomite and subordinate to minor sandstone; thickness about 800 feet (240 m).

Pq **Queantoweap Sandstone**—Pinkish- or light-brownish-gray, fine-grained, cross-bedded sandstone; locally poorly cemented; thickness 817 feet (249 m).

Pt **Toroweap Formation**—Generally resistant, light- to dark-gray, black, and tan, fine-grained, mostly thin-bedded, ledgy, locally cherty and fossiliferous, marine limestone and subordinate sandstone; maximum thickness is about 300 feet (100 m).

Pennsylvanian

lPc **Callville Limestone**—Medium- to light-gray, fine- to medium-bedded, medium- to thick-bedded, cherty limestone and dolomite with a few thin pinkish-gray sandstone beds; thickness 538 feet (164 m).

Mississippian

Mr **Redwall Limestone**—Upper third is interbedded calcareous sandstone, limestone, and dolomite; middle part is gray, cherty, fossiliferous limestone; basal one-quarter is medium-gray interbedded dolomite and limestone; thickness 1545 feet (471 m).

Devonian

Dc **Cove Fort Quartzite**—Yellowish-gray, medium-grained quartzite with thin interbeds of dolomitic quartzite in middle third; forms prominent ledges; thickness 82 to 160 feet (25–49 m).

Dg **Guilmette Formation**—Dark-gray, medium-grained, medium-bedded dolomite with a few interbeds of brown-weathering quartzite; thickness 575 feet (175 m).

Dcs **Crystal Pass Formation undifferentiated**—Includes units from Simonson Dolomite and Sevy Dolomite, undivided – Mapped only along the west fault scarp of the south Mineral Mountains. Mostly soft, light-gray, thin- to medium-bedded, interbedded marine dolomite and sandstone; thickness about 600 feet (180 m).

Ds **Simonson Dolomite**—Light-brownish-gray, medium- to coarse-grained, thin-bedded dolomite; thickness 185 feet (56 m).

Dsy **Sevy Dolomite**—Very-light-gray, fine-grained, medium-bedded, clayey dolomite; rare fossil fish fragments found in Sevy strata in Dog Valley quadrangle; thickness 710 feet (217 m).

Silurian

Sl **Laketown Dolomite**—Banded dark- and light-brownish-gray, cherty, cliff-forming dolomite; locally tectonically brecciated in map area; silicified corals and brachiopods common in upper part; average apparent thickness about 1300 feet (400 m).

Silurian-Ordovican

SOu **Laketown and Fish Haven Dolomites, undivided**—Interbedded light-gray and medium dark-gray to brownish-gray, medium- to thick-bedded dolomite; brown chert bands in middle of exposed strata, so Laketown may or may not be exposed; incomplete thickness 200 feet (60 m).

Ordovician

Oe **Eureka Quartzite**—Light-colored, medium-bedded, vitreous quartzite with lower half thinner bedded quartzite, sandstone, and dark, fissile shale; 172 feet (52 m) thick.

Oes **Ely Springs Dolomite**—Dark-brownish-gray, cherty, unfossiliferous, ledge- and cliff-forming dolomite; commonly tectonically brecciated; average thickness about 500 feet (150 m).

Oew **Eureka–Crystal Peak–Watson Ranch Formations, undivided**—These formations are too thin to show individually at 1:100,000 scale; listed from the top downwards. Eureka Quartzite is light-gray, medium- to fine-grained quartzite that weathers reddish-brown; characteristically pitted with pock-marks about 0.5 inch (1 cm) across; forms orange cliffs conspicuous among the gray carbonate rocks; thickness as much as 600 feet (180 m). Crystal Peak Dolomite is interbedded, thin-bedded, light-olive-gray dolomite and bluish-gray, silty limestone; *Eofletcheria* coral fossils are common; thickness 90–164 feet (27–50 m). Watson Ranch Quartzite is interbedded orangish-brown, fucoidal quartzite and bluish-gray, silty limestone and dolomite; thickness 190 feet (60 m).

Opu **Upper Pogonip Group, undivided**—Consists of four formations too thin to show individually at 1:100,000 scale; listed from the top downwards; Lehman Formation, Kanosh Shale, Juab Limestone, and Wah Wah Limestone; up to 1100 feet (320 m) thick.

Op **Pogonip Group**—Fossiliferous, interbedded shale and limestone at top; underlain by medium-gray, thin- to medium-bedded limestone, with intraformational conglomerate and sparse chert, and thin shale interbeds; 1200+ feet (350+ m) thick.

Ok **Kanosh Shale**—Light-olive-gray, fissile shale with interbeds of thin-bedded, bioclastic limestone made up of brachiopod, ostracode, trilobite, and echinoderm fragments; up to 560 feet (170 m) thick.

Of **Fillmore Formation**—Medium-gray, thin- to medium-bedded limestone and intraformational, flat-pebble limestone conglomerate interbedded with light-olive and yellowish-gray shale; up to 1800 feet (550 m) thick.

Oh **House Limestone**—Medium-bluish-gray, thick-bedded to massive, cherty limestone; thickness 460 feet (140 m).

Ordovician-Cambrian

OCn **Notch Peak Formation**—Dark-brownish-gray dolomite and gray limestone that commonly contain stromatolites; some beds cherty; forms massive cliffs; about 1700 feet (520 m) thick.

Cambrian

Ca **Ajax Dolomite**—Dark-gray, massive dolomite with a few interbeds of light-gray dolomite and bluish-gray limestone with "algal" stromatolites; thickness about 700 feet (210 m).

Cou **Orr Formation, upper members, undivided**—In descending order, the following members constitute this combined unit: Sneakover Limestone Member, 100 feet (30 m) thick; Corset Spring Shale Member, 40 feet (12 m) thick; Johns Wash Limestone Member, 100 feet (30 m) thick; and Candland Shale Member, 165 feet (50 m) thick.

Cob **Orr Formation, Big Horse Limestone Member**—Pinkish- to dark-gray limestone with dolomitic "algal" stromatolites and boundstone in the middle; bioclastic beds contain *Crepicephalus* trilobites; thickness 656 feet (200 m).

Cwt **Wah Wah Summit Formation and Trippe Limestone, undivided**—Wah Wah Summit Formation includes a white dolomite and limestone and a dark-gray, ledge- and cliff-forming, carbonate sequence below. Trippe Limestone consists of alternating dark-gray, ledge-forming limestone, and light-gray, laminated, slope-forming, dolomitic boundstone, 660 to 760 feet (200–230 m) thick. Combined map unit about 1420 feet (433 m) thick; structurally thinned and identification uncertain in Mineral Mountains.

Ccm **Limestone of Cricket Mountains**—Interbedded, dark-gray limestone, brownish-gray dolomitic limestone, and light-gray, laminated, dolomitic boundstone; forms cliffs and ledges; thickness 1970 feet (600 m).

Cum **Upper and Middle Cambrian carbonate rocks, undivided**—ncludes Middle Cambrian strata above the Ophir southwest of Kanosh. These carbonate rocks are unfossiliferous and mostly dolomites that range from light- to dark-gray, laminated to massive; thickness up to 1200 feet (350 m).

Cw **Whirlwind Formation**—Light-olive-gray shale interbedded with thin-bedded, nodular limestone bearing coquinas of the trilobite *Ehmaniella*; forms recessive slopes; thickness 200 to 265 feet (60–80 m).

Cdh **Dome-Chisholm-Howell Formations, undivided**—Listed from top downward. Dome Limestone is gray, massive, forms cliffs, and is 230 to 330 feet (70–100 m) thick. Chisholm Formation consists of lower and upper shales, bearing the trilobite Glossopleura, separated by dark-gray, oncolitic limestone; 165 to 265 feet (50–80 m) thick. Howell Limestone forms cliffs that are light gray in the upper third and dark gray below; thickness about 300 to 360 feet (90–110 m).

Cop **Ophir Formation**—Upper part is medium- to thick-bedded limestone with some shale interbeds, uppermost of which bears *Ehmaniella* trilobites; basal third is phyllitic quartzite, shale, and thin-bedded limestone bearing *Glossopleura* trilobites; both parts form slope-ledge topography; thickness about 850 feet (260 m).

Cp **Pioche Formation**—Mostly interbedded dark-brown quartzite and dark-greenish-gray, phyllitic siltstone characterized by abundant trace fossils; upper tenth includes beds of orange-weathering dolomite; thickness about 800 feet (245 m).

Ct **Tintic Quartzite**—White to brownish-orange-weathering, vitreous quartzite, with a few quartzite pebble conglomerate beds; commonly sheared and fractured; estimated thickness 3300 feet (1000 m).

Cpm **Prospect Mountain Quartzite**—Grayish-pink, vitreous quartzite ranging from very fine- to coarse-grained with some thin, quartzite-pebble conglomerate beds; forms ledges and cliffs; at least 4000 feet (1200 m) thick.

Paleozoic

Pzu **Paleozoic carbonate rocks, undivided**—Mapped only in the Gillies Hill area and Mineral Mountains where intensely metamorphosed carbonate units cannot be distinguished.

Precambrian

pCm **Mutual Formation**—Reddish-purple quartzite and metaconglomerate with some interbeds of red and green phyllitic slate; about 2100 feet (635 m) thick in the San Francisco Mountains.

pCi **Inkom Formation**—Olive-gray, green, and reddish-brown, phyllitic slate that forms recessive topography and is commonly covered; lacks quartzite beds; about 500 feet (150 m) thick in the San Francisco Mountains.

pCc **Caddy Canyon Quartzite**—Light-pinkish or yellowish-gray quartzite with interbeds of conglomerate, siltstone, and argillite in the upper part; about 300 feet (90 m) thick in the San Francisco Mountains, probably

thicker elsewhere.

pCb **Blackrock Canyon Limestone**—Chiefly interbedded argillite and quartzite with about 10% interbeds of limestone and dolomite that are commonly silty or sandy; contains the only carbonate rock in the Neoproterozoic of western Utah; maximum thickness about 600 to 990 feet (180–300 m) in the San Francisco Mountains.

pCp **Pocatello Formation**—Light-gray, thick-bedded, medium- to coarse-grained quartzite with a few red slate beds near the top; exposed thickness 970 feet (300 m).

pCg **Banded gneiss**—Light bands are composed of quartz and K-feldspar with minor biotite and plagioclase; dark bands are mostly biotite, plagioclase, and quartz with minor hornblende and K-feldspar; accessory minerals are apatite and rounded zircon; present in Mineral Mountains; age 1750 Ma.